



National Library
of Canada

Acquisitions and
Bibliographic Services Branch

395 Wellington Street
Ottawa, Ontario
K1A 0N4

Bibliothèque nationale
du Canada

Direction des acquisitions et
des services bibliographiques

395, rue Wellington
Ottawa (Ontario)
K1A 0N4

Your file Votre référence

Our file Notre référence

NOTICE

The quality of this microform is heavily dependent upon the quality of the original thesis submitted for microfilming. Every effort has been made to ensure the highest quality of reproduction possible.

If pages are missing, contact the university which granted the degree.

Some pages may have indistinct print especially if the original pages were typed with a poor typewriter ribbon or if the university sent us an inferior photocopy.

Reproduction in full or in part of this microform is governed by the Canadian Copyright Act, R.S.C. 1970, c. C-30, and subsequent amendments.

AVIS

La qualité de cette microforme dépend grandement de la qualité de la thèse soumise au microfilmage. Nous avons tout fait pour assurer une qualité supérieure de reproduction.

S'il manque des pages, veuillez communiquer avec l'université qui a conféré le grade.

La qualité d'impression de certaines pages peut laisser à désirer, surtout si les pages originales ont été dactylographiées à l'aide d'un ruban usé ou si l'université nous a fait parvenir une photocopie de qualité inférieure.

La reproduction, même partielle, de cette microforme est soumise à la Loi canadienne sur le droit d'auteur, SRC 1970, c. C-30, et ses amendements subséquents.

Canada

UNIVERSITY OF ALBERTA

**ANALYTICAL MODELLING OF CYCLIC STEAM STIMULATION
INCLUDING FORMATION PARTING**

BY
MOHAMMAD TAMIM



A THESIS
SUBMITTED TO THE FACULTY OF GRADUATE STUDIES AND RESEARCH
IN PARTIAL FULFILLMENT OF THE REQUIREMENTS FOR THE DEGREE
OF DOCTOR OF PHILOSOPHY
IN
PETROLEUM ENGINEERING

DEPARTMENT OF MINING, METALLURGICAL AND PETROLEUM
ENGINEERING

EDMONTON, ALBERTA, CANADA

FALL, 1995



National Library
of Canada

Acquisitions and
Bibliographic Services Branch

395 Wellington Street
Ottawa, Ontario
K1A 0N4

Bibliothèque nationale
du Canada

Direction des acquisitions et
des services bibliographiques

395, rue Wellington
Ottawa (Ontario)
K1A 0N4

Your file Votre référence

Our file Notre référence

THE AUTHOR HAS GRANTED AN
IRREVOCABLE NON-EXCLUSIVE
LICENCE ALLOWING THE NATIONAL
LIBRARY OF CANADA TO
REPRODUCE, LOAN, DISTRIBUTE OR
SELL COPIES OF HIS/HER THESIS BY
ANY MEANS AND IN ANY FORM OR
FORMAT, MAKING THIS THESIS
AVAILABLE TO INTERESTED
PERSONS.

L'AUTEUR A ACCORDE UNE LICENCE
IRREVOCABLE ET NON EXCLUSIVE
PERMETTANT A LA BIBLIOTHEQUE
NATIONALE DU CANADA DE
REPRODUIRE, PRETER, DISTRIBUER
OU VENDRE DES COPIES DE SA
THESE DE QUELQUE MANIERE ET
SOUS QUELQUE FORME QUE CE SOIT
POUR METTRE DES EXEMPLAIRES DE
CETTE THESE A LA DISPOSITION DES
PERSONNE INTERESSEES.

THE AUTHOR RETAINS OWNERSHIP
OF THE COPYRIGHT IN HIS/HER
THESIS. NEITHER THE THESIS NOR
SUBSTANTIAL EXTRACTS FROM IT
MAY BE PRINTED OR OTHERWISE
REPRODUCED WITHOUT HIS/HER
PERMISSION.

L'AUTEUR CONSERVE LA PROPRIETE
DU DROIT D'AUTEUR QUI PROTEGE
SA THESE. NI LA THESE NI DES
EXTRAITS SUBSTANTIELS DE CELLE-
CI NE DOIVENT ETRE IMPRIMES OU
AUTREMENT REPRODUITS SANS SON
AUTORISATION.

ISBN 0-612-06301-1

Canada

UNIVERSITY OF ALBERTA
RELEASE FORM

NAME OF AUTHOR : Mohammad Tamim

TITLE OF THESIS: Analytical Modelling of Cyclic Steam Stimulation
Including Formation Parting

DEGREE FOR WHICH THESIS WAS GRANTED: Doctor of Philosophy

YEAR THIS DEGREE WAS GRANTED: 1995

Permission is hereby granted to the University of Alberta Library to reproduce single copies of this thesis and to lend or sell such copies for private, scholarly or scientific research purposes only.

The author reserves all other publication and other rights in association with the copyright in the thesis, and except as hereinbefore provided neither the thesis nor any substantial portion thereof may be printed or otherwise reproduced in any material form whatever without the author's prior written permission.




12/7 Iqbal Road
Block - A
Mohammadpur, Dhaka 1207
Bangladesh


DATED: Aug 24, '95

UNIVERSITY OF ALBERTA
FACULTY OF GRADUATE STUDIES AND RESEARCH

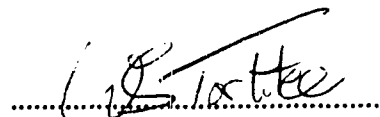
The undersigned certify that they have read and recommend to the Faculty of Graduate Studies and Research, for acceptance, a thesis entitled ANALYTICAL MODELLING OF CYCLIC STEAM STIMULATION INCLUDING FORMATION PARTING submitted by MOHAMMAD TAMIM in partial fulfillment of the requirements for the degree of DOCTOR OF PHILOSOPHY in PETROLEUM ENGINEERING.



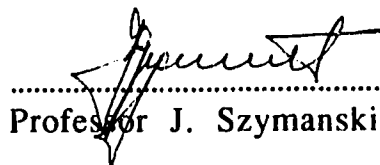
Professor S.M. Farouq Ali



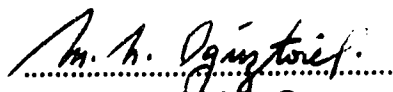
Professor R.G. Bentsen



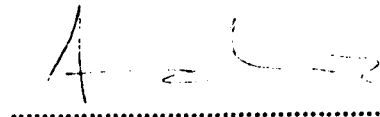
Professor W.S. Tortike



Professor J. Szymanski



Professor M.N. Oguztoreli



Professor A. Chakma

DATE Aug 21, 95

ABSTRACT

Cyclic steam stimulation (CSS) is the commercial oil recovery process of choice for the Cold Lake oil sands. Much of CSS is performed under fracture pressures and, as a result, performance predictions are difficult. This work presents a new mathematical model, involving analytical techniques, for CSS performance prediction. The model is based upon a fracture heating computation, coupled with fluid flow—both during steam injection and oil and water production. Thus two-phase flow is accounted for. Two situations, involving different flow geometries, bracketing actual flow in the field are considered. These consist of fracture flow, and flow in an elliptical geometry with a circular well in the centre.

A vertical fracture is assumed to be created during steam injection. Fracture half length is calculated either from an analytical formula or provided by the user. No mechanistic approach is taken to do any stress analysis. An investigation for a completely closed fracture during production is performed. Based on the results from this investigation, existence of a partially open fracture during production is suggested.

An improved average temperature calculation technique and a new method of evaluating the effect of spatial oil viscosity distribution have been incorporated into the new model.

The model is used to simulate previously reported results showing an excellent match. A sensitivity study for the variation of different parameters produces a reliable response from the model. It is capable of predicting various production performance parameters (i.e. calendar day oil rate, oil-steam ratio, water-oil ratio, oil recovery etc.) of the CSS process. The water-oil ratio prediction is restricted to the first five cycles only. The model can serve as a valuable adjunct to numerical simulation or physical modelling.

ACKNOWLEDGEMENTS

The author wishes to express sincere gratitude and appreciation to Dr. S.M. Farouq Ali, for his encouragement, support and supervision throughout this research. His trust, patience and generosity made this sometimes frustrating work pleasant and successful.

A special thanks is extended to the author's wife, Minu, for her love, understanding and tolerance of the long night works; and to his daughter, Malika, whose birth brought much joy and happiness.

The author is grateful to Mr. John Arthur of Essien Consulting Engineers, Calgary, for his valuable advice and help in the early stage of this research. Dr. K. Miller of AEC Oil and Gas, Calgary, is also thanked for his critical comments and suggestions.

The Canadian International Development Agency (CIDA) is thanked for supporting this project. Mr. Bob Schimdt and Ms. Lori Constantine, CIDA Project Managers at the University of Alberta are thanked for their numerous help, often beyond their call of duty.

To Amma and Abba who set me free with their love and trust

TABLE OF CONTENTS

	Page
Chapter I: Introduction	1
Chapter II: Review of the Literature	3
2.1 Analytical Models	4
2.1.1 Pressure Drawdown.....	4
2.1.2 Gravity Drainage.....	8
2.1.3 Rock Expansion	10
2.2 Semi-Analytical Models	11
2.3 Steam Zone Growth Calculation	13
2.3.1 Frontal Advance Models.....	13
2.3.2 Override Models	15
2.4 Heat Transfer and Temperature Distribution	15
2.4.1 Unfractured Well	16
2.4.2 Fractured Well	17
2.5 Elliptical Flow Regime	19
2.5.1 Homogeneous Reservoir	19
2.5.2 Composite Reservoir.....	20
Chapter III: Statement of the Problem.....	22
3.1 Statement of the Problem.....	22
Chapter IV: Model Development.....	23
4.1 Flow Equations.....	24
4.1.1 Flow into a Wellbore at the Centre of an Elliptical Drainage Boundary	24
4.1.2 Flow From a Finite Line Source into a Well	27
4.1.3 Gravity Drainage.....	27

4.1.4 Outer Warm Zone.....	28
4.2 Pressure	28
4.3 Fracture Length.....	29
4.4 Initial Temperature Calculation	30
4.5 Heat Loss Equation	32
4.6 Average Soak and Production Temperature.....	33
4.7 Saturation	35
4.8 Average Viscosity Calculation	36
4.9 Flow Reduction Factor	37
4.9.1 Vertical Steam Sweep Efficiency	38
4.9.2 Fracture Parameters	38
4.9.2.1 Fracture Height.....	38
4.9.2.2 Fracture Length.....	39
4.10 Relative Permeability	40
Chapter V: Solution and Computer Implementation	41
5.1 Description of the Model	41
5.2 Description of the Subroutines	42
5.2.1 Initialization	42
5.2.2 Injection Period	43
5.2.3 Soak Period	44
5.2.4 Production Period	44
Chapter VI: Results and Discussion	47
6.1 Simulation Data.....	47
6.2 Elliptical Flow into a Well (EFW).....	49
6.2.1 EFW Approximate Solution	52
6.2.2 EFW Closed-form Solution	57
6.3 New Model	58

6.3.1 Saturation Schemes.....	59
6.3.2 Effect of Temperature on Relative Permeability.....	62
6.4 Effect of Viscosity	67
6.5 Conduction Between the Two Zones	74
6.5.1 Relative Error Compared to Erroneous Viscosity Calculation.....	83
6.6 Sensitivity Study	83
6.6.1 Hot Zone Boundary Temperature.....	85
6.6.2 Soak Time	88
6.6.3 Increasing Steam Volume.....	91
6.6.4 Slug Size.....	95
6.6.5 Time Step	101
6.6.6 Steam Temperature	105
6.6.7 Steam Quality	112
6.6.8 Initial Reservoir Temperature.....	117
6.6.9 Formation Thickness	121
Chapter VII: Conclusions	125
7.1 Suggestions for Future Studies.....	126
References	127
Appendix A: Correction of Sylvester and Chen (1988) Equation	138
Appendix B: Flow into a Well Located at the Centre of an Elliptical Drainage Boundary.....	140
Appendix C: Heat Loss Calculation to the Cap Rock.....	145
Appendix D: Average Zone Temperatures During Soak and Production.....	147
Appendix E: Saturations	152
Appendix F: Fluid Properties.....	153

LIST OF TABLES

	Page
Table 2.1 Comparison of Existing Models.....	6
Table 6.1 Simulation input data.....	50
Table 6.2 Water-oil relative permeability	51
Table 6.3 Operational data.....	51
Table 6.4 Average temperature change (°C) during soak with conduction.....	84
Table 6.5 Average temperature change (°C) during soak without conduction.....	84
Table 6.6 Slug sizes (m ³) for steaming schemes	96

LIST OF FIGURES

	Page
Figure 2.1 Review of the literature	5
Figure 4.1 Conceptual diagram of fluid flow and heat transfer for the proposed model	25
Figure 4.2 Different flow geometries	26
Figure 5.1 Computational flow diagram of the model	46
Figure 6.1 Overall scheme of the simulation runs conducted	48
Figure 6.2 Comparison of cycle oil production for closed fracture models	53
Figure 6.3 Comparison of cycle water production for closed fracture models	53
Figure 6.4 Comparison of cumulative oil production for closed fracture models	54
Figure 6.5 Comparison of cumulative water production for closed fracture models	54
Figure 6.6 Comparison of cycle oil-steam ratio for closed fracture models	55
Figure 6.7 Comparison of calendar day oil production rate for unfractured wellbore model	55
Figure 6.8 Comparison of cycle water-oil ratio for closed fracture models	56
Figure 6.9 Comparison of cycle oil production for fractured wellbore models	60
Figure 6.10 Comparison of cumulative oil production for fractured wellbore models	60
Figure 6.11 Comparison of cycle water production for fractured wellbore models.....	61

Figure 6.12	Comparison of cumulative water production for fractured wellbore models.....	61
Figure 6.13	Comparison of cycle oil-steam ratio for fractured wellbore models	63
Figure 6.14	Comparison of calendar day oil production rate for fractured wellbore models.....	63
Figure 6.15	Comparison of cycle water-oil ratio for fractured wellbore models.....	64
Figure 6.16	Adjusted relative permeability	65
Figure 6.17	Oil production at each cycle for model LGTB, with adjusted relative permeability due to temperature effect	66
Figure 6.18	Cumulative oil production for model LGTB, with adjusted relative permeability due to temperature effect	66
Figure 6.19	Water production at each cycle for model LGTB, with adjusted relative permeability due to temperature effect.....	68
Figure 6.20	Cumulative water production for model LGTB, with adjusted relative permeability due to temperature effect.....	68
Figure 6.21	Oil-steam ratio for model LGTB, with adjusted relative permeability due to temperature effect	69
Figure 6.22	Calendar day oil production rate for model LGTB, with adjusted relative permeability due to temperature effect.....	69
Figure 6.23	Water-oil ratio for model LGTB, with adjusted relative permeability due to temperature effect	70
Figure 6.24	Predicted oil recovery as a percentage of original oil in place.....	71
Figure 6.25	Comparison of area weighted average oil viscosity and direct values from the average temperature	73
Figure 6.26	Comparison of area weighted average water viscosity and direct values from the average temperatures.....	73

Figure 6.27	Effect of different methods of oil viscosity calculation on cumulative oil production	75
Figure 6.28	Effect of calculating oil viscosity without areal average temperature on oil produced at each cycle	75
Figure 6.29	Effect of calculating oil viscosity without areal average on cycle oil-steam ratios	76
Figure 6.30	Effect of calculating oil viscosity without areal average on cycle calendar day oil rates.....	76
Figure 6.31	Effect of calculating oil viscosity without areal average on cycle water-oil ratios	77
Figure 6.32	Effect of conduction heat loss on average hot zone temperature	79
Figure 6.33	Effect of conduction heat loss from the hot zone to the warm zone on cumulative oil production	80
Figure 6.34	Effect of conduction heat loss from the hot zone to the warm zone on cycle oil production.....	80
Figure 6.35	Effect of conduction heat loss from the hot zone to the warm zone on cumulative water production.....	81
Figure 6.36	Effect of conduction heat loss from the hot zone to the warm zone on cycle oil-steam ratios.....	81
Figure 6.37	Effect of conduction heat loss from the hot zone to the warm zone on cycle calendar day oil rates.....	82
Figure 6.38	Effect of conduction heat loss from the hot zone to the warm zone on cycle water-oil ratios.....	82
Figure 6.39	Oil produced at each cycle for various hot zone boundary temperature values.....	86
Figure 6.40	Cumulative oil production for various hot zone boundary values.....	86

Figure 6.41	Water production at each cycle for different hot zone boundary values.....	87
Figure 6.42	Cumulative water production for various hot zone boundary temperature values	87
Figure 6.43	Oil-steam ratio at each cycle for various hot zone boundary values.....	89
Figure 6.44	Calendar day oil production rate at each cycle for various hot zone boundary values.....	89
Figure 6.45	Water-oil ratio at each cycle for various hot zone boundary values.....	90
Figure 6.46	Oil production at each cycle for different soak periods.....	92
Figure 6.47	Cumulative oil production for different soak periods	92
Figure 6.48	Water production at each cycle for different soak periods	93
Figure 6.49	Cumulative water production for different soak periods	93
Figure 6.50	Oil production at each cycle for various steam injection rates	94
Figure 6.51	Cumulative oil production for different steam injection rates.....	94
Figure 6.52	Water production at each cycle for different steam injection rates.....	97
Figure 6.53	Cumulative water production for various steam injection rates.....	97
Figure 6.54	Oil-steam ratio at each cycle for various steam injection rates	98
Figure 6.55	Calendar day oil production rates for different steam injection rates.....	98
Figure 6.56	Water-oil ratio at each cycle for different steam injection rates	99
Figure 6.57	Oil production at each cycle for different slug sizes with constant total steam.....	100
Figure 6.58	Cumulative oil produced for different slug sizes with same total injected steam.....	100

Figure 6.59	Water production at each cycle for various slug sizes with constant total injected steam	102
Figure 6.60	Cumulative water production for various slug sizes with constant total injected steam	102
Figure 6.61	Cumulative water production for various slug sizes with constant total injected steam	103
Figure 6.62	Calendar day oil production rate at each cycle for various slug sizes with constant total injected steam	103
Figure 6.63	Water-oil ratio at each cycle for various slug sizes with constant total injected steam.....	104
Figure 6.64	Oil produced at each cycle for various production time-steps	104
Figure 6.65	Cumulative oil production for various production time-step sizes	106
Figure 6.66	Water production at each cycle for various production time-step sizes.....	106
Figure 6.67	Cumulative water production for various production time-step sizes.....	107
Figure 6.68	Oil production at each cycle for different steam temperatures	107
Figure 6.69	Effect of steam temperature on 1st cycle oil production rate	108
Figure 6.70	Effect of steam temperature on 1st cycle average hot zone temperature.....	109
Figure 6.71	Cumulative oil produced for different steam injection temperatures	109
Figure 6.72	Heat lost to fluid production at each cycle for varying steam injection temperature	110
Figure 6.73	Water production at each cycle for various steam injection temperatures.....	111
Figure 6.74	Cumulative water produced for different steam injection temperatures.....	111

Figure 6.75 Oil production at each cycle for various steam qualities.....	113
Figure 6.76 Cumulative oil production for various steam qualities.....	113
Figure 6.77 Water production at each cycle for various steam qualities	114
Figure 6.78 Cumulative water production for various steam qualities	114
Figure 6.79 Oil-steam ratios at each cycle for various steam qualities	115
Figure 6.80 Calendar day oil rate at each cycle for various steam qualities	115
Figure 6.81 Water-oil ratios at each cycle for various steam qualities.....	116
Figure 6.82 Effect of initial reservoir temperature on net heat injection.....	118
Figure 6.83 Oil production at each cycle for different initial reservoir temperatures.....	119
Figure 6.84 Effect of initial reservoir temperature on total oil production	119
Figure 6.85 Effect of initial reservoir temperature on hot zone propagation.....	120
Figure 6.86 Effect of initial reservoir temperature on total water production.....	120
Figure 6.87 Oil produced at each cycle for different pay thicknesses	122
Figure 6.88 Cumulative oil production for different pay thicknesses	122
Figure 6.89 Effect of formation thickness on heat loss to over/underburden	123
Figure 6.90 Water produced at each cycle for different pay thicknesses.....	124
Figure 6.91 Cumulative water production for different pay thicknesses.....	124

NOMENCLATURE

a	major axis of ellipse (m)
A	area (m^2)
b	width of fracture (m), minor axis of ellipse (m)
C	specific heat ($\text{kJ m}^{-3}\text{K}^{-1}$), fluid loss coefficient ($\text{m d}^{-1/2}$)
c	compressibility (kPa^{-1}), half length of the line source (m)
d	diffusivity length (m)
E_c	energy stored in the cap and base rock (kJ)
g	acceleration due to gravity (9.81 ms^{-2})
h	formation thickness (m), specific enthalpy (kJ kg^{-1})
h_{fg}	latent heat of vaporization (kJ kg^{-1})
H	dimensionless heat input
i	steam injection rate ($\text{m}^3 \text{ day}^{-1}$)
k	absolute permeability (m^2)
k_h	thermal conductivity ($\text{kJ m}^{-1} \text{ d}^{-1} \text{ K}^{-1}$)
K	hydraulic conductivity (ms^{-1})
K_{end}	number of total cycles
L	distance (m)
L_f	fracture half length (m)
L_v	latent heat of vaporization (kJ kg^{-1})
M	mobility ratio, volumetric heat capacity (kJ kg^{-1})
p	pressure (kPa)
P_I	pressure at time zero for the exponential decline curve
q	fluid flow rate ($\text{m}^3 \text{ day}^{-1}$)
\dot{q}_L	heat loss rate (kJ s^{-1})
Q	heat flow rate (kJ day^{-1})
r	radius (m)
R	radius in polar coordinates
S_{wir}	irreducible water saturation (fraction)
S_o	oil saturation (fraction)
S_{or}	residual oil saturation (fraction)
S_p	spurt loss quotient
S_{wi}	initial water saturation (fraction)
S_{wr}	residual water saturation (fraction)

t	time (day)
T	temperature ($^{\circ}\text{C}$)
\bar{T}	$(T - T_r) / (T_s - T_r)$
U	unit step function
ν	variable of integration
V	volume (m^3)
V_f	fluid leak-off velocity ($\text{m}^3 \text{s}^{-1}$)
x_i	steam quality
y_0	distance between the line source and the wellbore

Greek Symbols

α	thermal diffusivity ($\text{m}^2 \text{s}^{-1}$), effective fracture width (m)
β	1, thermal expansion coefficient (K^{-1})
λ	mobility ($\text{m}^2 \text{Pa}^{-1} \text{s}^{-1}$)
δ	fluid heat loss due to production (fraction)
ε	eccentricity of the ellipse (fraction)
Φ	potential
ϕ	porosity (fraction)
γ	density (kg m^{-3})
Γ	dimensionless x co-ordinate
η	dimensionless z co-ordinate, hydraulic diffusivity
μ	dynamic viscosity (Pa.s)
ξ	dimensionless y co-ordinate
ρ	density (kg m^{-3})
τ	dimensionless time
τ_s	dimensionless time for steam advancement in the fracture
τ_{sa}	dimensionless time for the steam to move into the formation
θ	dimensionless temperature, angle
ν	kinematic viscosity ($\text{m}^2 \text{s}^{-1}$)

subscript

0	interface between reservoir and the adjacent strata
1	hot
2	warm
b	bulk, interface
c	condensate
d	drainage
e	external
f	formation, fluid
h	hot, interface
i	initial, injected
o	oil
om	mobile oil
p	pore
r	radial
R	reservoir
s	steam
sc	standard condition
st	stock tank, steam
w	water, wellbore, warm
wc	connate water
wf	flowing wellbore
wm	mobile water
z	vertical

Abbreviations

CDOR	calendar day oil rate
CSS	cyclic steam stimulation
CWE	cold water equivalent
EFW	elliptic flow into a well
LGTB	linear gravity with total balance
LGWB	linear gravity with water balance
LSL	large-small-large

OSR
WOR

oil-steam ratio
water-oil ratio

Chapter I

INTRODUCTION

For reservoirs with medium to high viscosity oil, thermal methods of enhanced oil recovery are very effective. Steam was used for oil recovery as early as 1931 when it was injected into a sand at a depth of 380 ft. for an extended period in Woodson, Texas. After a relatively quiet period of 20 years with some smaller projects starting in California, the first large scale steam drive was employed in Tia Juana, Venezuela (Prats, 1986). Cyclic Steam Stimulation (CSS) or steam soak was discovered rather accidentally in the Mene Grande Tar Sands, Venezuela in 1959 (Adams and Khan, 1969). When steam broke through the overburden after injection into a non-productive primary well, the well was produced to relieve the pressure. To everyone's surprise, it produced a considerable amount of oil with little water. Since then, steam soak has been used widely all over the world. It is being used successfully in California where many reservoirs contain high viscosity crude oil. Success with this method has been reported also in Cold Lake, Alberta and Venezuela. For economy and high early cycle production rates, it has become routine to employ CSS for moderate to heavy oil reservoirs prior to a steamflood.

The extensive use of CSS by the oil industry points to the need for a simple performance prediction technique. The CSS process has complex mechanisms: the reversal of flow during the injection and production periods; saturation hysteresis; possible formation of fractures during injection and, in some cases, dilation and compaction. These factors make the solution of simulator equations difficult, expensive and time-consuming. Although, multiphase, multidimensional thermal simulators are appropriate and more accurate for the detailed analysis of the process, most of the simulators do not include all of these effects. Moreover, the lack of ability to handle sophisticated simulators precludes their widespread use in the field. The conventional simulators do not include the geomechanical aspects of the process. Absence of flow equations coupled with the stress field in the reservoir is the major obstacle for the success of the simulator predictions. The most prohibitive factors to use a numerical simulator are cost and time. It may take a few months and several hundred thousand dollars to do a comprehensive analysis.

Before going into a detailed and expensive simulator analysis, a simplistic initial assessment of the operation is quite important and valuable. Empirical and correlative

methods are mostly specific to a particular field and their predictive ability is also limited. Analytical models are capable of rough production estimates for various operating conditions. These constitute an excellent tool for process control and operation strategy. A reliable analytical model may be useful for the field engineer and can save considerable amounts of time and money. Often the lack of available data also makes the use of an analytical model imperative.

A number of analytical models have been proposed in the literature, but most of these models are not applicable to CSS in Cold Lake and other heavy oil reservoirs in Alberta, where formation parting takes place. McGee, Arthur and Best (1987) and Arthur, Best, Jha and Mourits (1991) considered the fracturing phenomenon during the injection period which often occurs in oil sands. This was ignored by others who also considered only radial flow, whereas the fluid flow from a fractured well is elliptic (Dietrich, 1986). Elliptic flow geometry has been investigated in different fields of petroleum engineering: hydraulic fracturing, water-flooding, well testing etc. The two extreme views regarding flow during production involve the opening and closing of the fracture. Arthur *et al.* (1991) assumed flow into a fracture during production. They introduced anisotropy to handle the opening and closure of the fracture but their flow equation was based on an elliptic coordinate system which inherently assumes an open fracture.

In a reservoir, where a considerable amount of primary production exists, the effect of temperature change of the incoming fluid from the cold outer zone may not be that significant. In the case of heavy oil, it is very important to calculate the heat exchange between the hot and cold zone through conduction and convection. Arthur *et al.* (1991) ignored the conduction heat transfer between the two zones. Seba and Perry (1969) also considered the calculation of the change of average temperature in the cold zone, but they kept the hot zone temperature at steam temperature for the whole project time.

The most important aspect of the flow calculation is the proper evaluation of oil viscosity. So far, there has not been any attempt to calculate an average viscosity based on its areal distribution during production. A direct calculation of viscosity from the average zone temperature would produce erroneous results.

Chapter II

REVIEW OF THE LITERATURE

Reduction in the viscosity of the viscous oil around an injecting well is the main reason for a higher production response in cyclic steam injection operations. Apart from this obvious factor, there are several aspects of the production mechanism which make the process complex and diverse. Generation of non-condensable gas, flashing of steam, different phase compressibilities, gas evolved from chemical reactions and enhanced solution-gas/oil expansion due to increased temperature may contribute to the driving force independently or in combination. Solution-gas drive and gravity drainage are two important forces in many reservoirs (Prats, 1986; Jones and Cawthon, 1990). Compaction has also been cited as the major driving force in Venezuela (de Haan and van Lookeren, 1969).

The performance of the cyclic steam stimulation process is sensitive to drive and drainage mechanisms, reservoir and fluid properties evaluation and operating variables. For any predictive model, reservoir temperature calculation and relative permeability approximation are particularly important. A small variation in relative permeability may significantly alter the production response. Most authors of the several analytical models presented in the literature assumed radial flow geometry. Both depletion and non-depletion type reservoirs were considered. Many of these works investigated the effect of gravity drainage. The role of compaction and solution-gas drive was also explored.

A few authors used a semi-analytic technique to overcome some of the limitations of a fully analytical model. Incorporation of relative permeability and gas phase, non-linear variation of fluid heights and transient effects are some of the reasons for taking such an approach.

Steam injection at a thermally efficient rate requires the injection pressure to be higher than the formation parting pressure in a variety of Canadian heavy oil and bitumen reservoirs. This is particularly true for the earlier cycles. For such cases, analysis of heat and fluid flow to and from the fracture are crucial. Although there are a number of papers in the literature dealing with heat transfer within the fracture, very few have considered the whole reservoir system.

It is also important to have a good estimation of the size and shape of the hot or steam zone. In many cases this calculation sets the limit of the drainage area. Assumption and estimation of the shape of the steam zone are critical for determining the drainage mechanism. A number of works in this area are also found in the steam-drive literature.

Due to the creation of a fracture in some of the heavy oil reservoirs, the flow geometry is quite different from that in a radial system. There is a general consensus in the literature that the flow geometry around a fractured well is elliptic. Elliptic flow geometry has been investigated in different fields of petroleum engineering: hydraulic fracturing, water-flooding and well testing. There is a considerable absence of interest regarding its application in the cyclic steam injection process. Figure 2.1 gives a schematic overview of the work which will be discussed in this Chapter. A quick look at the key features of the existing CSS analytical models is presented in Table 2.1.

2.1 Analytical Models

The physical models developed in the literature to calculate cyclic steam stimulation performance are based on various forces: pressure drawdown, gravity drainage and compaction. It is difficult to categorize them in a general fashion. The analytical models are reviewed here on the basis of drive and drainage systems.

2.1.1 Pressure Drawdown

This approach assumes that there is enough energy in the reservoir to produce some oil at the initial reservoir temperature. Apart from reducing oil viscosity in the heated zone, it assumes that no drive mechanism is enhanced by steam injection. Discussion of some of the major works follows.

Owens and Suter (1965), in one of the earliest analytical models, recognized the inverse proportionality of oil production to the change of viscosity. They assumed that the bottomhole temperature followed the harmonic decline trend of the surface temperature. They suggested making spot measurements of the bottomhole temperature to calculate the parameters of the harmonic equation. Values of temperature and production decline with time were presented in a graphical form. Generally, this very simplistic approach tends to overestimate the effect of CSS. In a typical case, production enhancement of 20 to 50 times

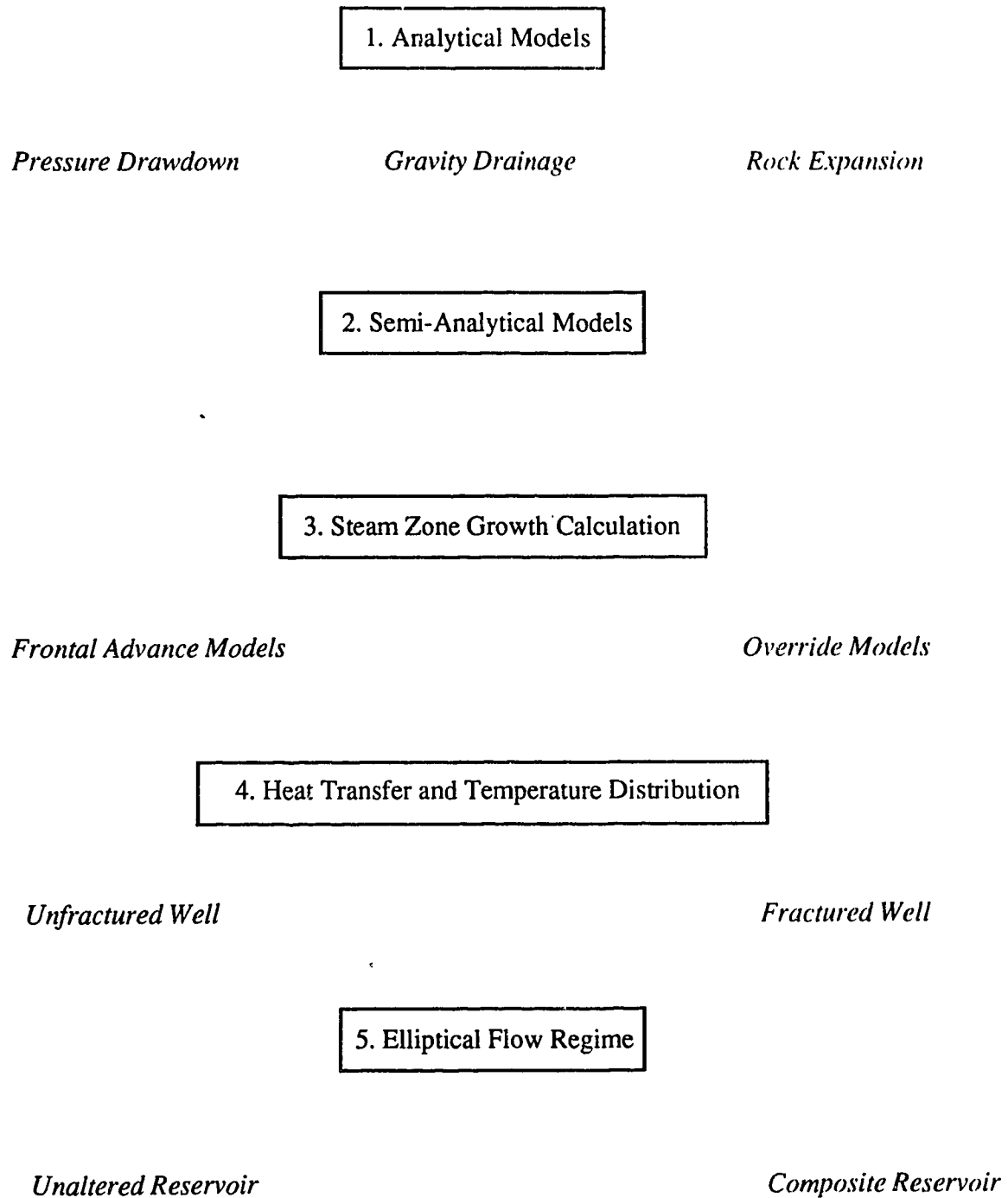


Figure 2.1—Review of the Literature

Table 2.1—Comparison of existing models.

	Geometry			Flow		Heat Calculation		Well Fracture		Inflow		Rel. Perm.	Area/Temp Ave Visc.
	Radial	Conical	Elliptic	Pressure Drawdown	Gravity Drainage	Hot Zone Temp Decline	Cold Zone Heating	No	Yes	No	Yes		
Owens & Suter (1965)	X			X		X		X		X			
Boberg & Lantz (1966)	X			X		X		X			X		
Martin (1967)	X			X		X		X		X			
Seba & Perry (1969)	X				X		X	X				X	
de Haan & van Lookeren (1969)	X			Compaction				X		X			
Kuo et al. (1970)	X				X				X	X		X	
Closmann et al. (1970)	X			X		X			X	X			
Jones (1977)	X				X	X			X			X	
Gonjijo & Aziz (1984)		X		X	X	X			X		X	X	
Sylvester & Chen (1988)	X			X		X			X		X		
Gozde et al. (1989)		X		X	X	X			X		X		
Arthur et al. (1991)			X	X		X	X	X		X		X	
Jones (1992)	X				X	X			X			X	
This Model			X		X	X	X	X		X		X	X

would be predicted compared to a model which actually calculates the average reservoir temperature.

Boberg and Lantz (1966) presented the first comprehensive analytical model to calculate the production rate of a thermally stimulated well. They found the average temperature of the heated zone using correction factors for vertical, radial heat conduction and fluid production heat losses. Their radial flow equations are accurate only for conventional reservoirs with primary production mainly from the cold zone. Pressure-depleted reservoirs, where the production is mainly from the hot zone itself, need a different treatment. The heat remaining in the reservoir at the end of each cycle was added to the heat injected in the next cycle. They assumed the same initial temperature for the interbedded shale, overburden and underburden at the beginning of each cycle. The neglect of low-level heating of the oil outside the hot zone and exclusion of any enhanced drive mechanism would generally result in an underestimate of their production response.

Closmann, Ratliff and Truitt (1970) studied the effect of stratification and cross-flow in a depletion-type reservoir. The effects of saturation change and viscosity distribution with temperature were considered. They neglected gravity and assumed only vertical heat loss with a constant heated zone. A Van Everdingen and Hurst (1949) type influx was used to calculate the radial flow volume. The way this model is formulated, makes it applicable to a first cycle calculation only.

Ershaghi, Al-Adawiya and Kogawan (1983) presented a graphical method of predicting cumulative production. They used the Boberg and Lantz method to generate cumulative production data using various parameters. These sets of data were plotted against cumulative steam injection on log-log coordinates. It was shown that the slopes of these plots were roughly equal to one. All the variables were lumped together into a response factor, which was the intercept. There was no rate calculation. Although they matched their results with field data, the proportionality of steam injection and oil production cannot be applied to many wells.

Another Boberg and Lantz based model was presented by Gros, Pope and Lake (1985). The mathematical formulation of Boberg and Lantz was modified to accommodate variable parameters in different layers. They also included temperature dependent relative permeability and time dependent average saturation, calculated from a simple material balance. No cross-flow between the layers was considered.

Because of the need to calculate the size and shape of the heated volume, McGee, Arthur and Best (1987) analyzed a vertically fractured reservoir in a steam stimulation process. They applied the principle of superposition with Wheeler's (1969) latent heat model to find the temperature distribution. A negative value during production and zero injection during soak were used. Their main objective was to find out the heated volume. For that, they supplied steam injection, volume of oil and water produced, cycle time, steam quality and reservoir properties data. The results were used to analyze well performance, to calculate well spacing and to determine an overall operating strategy.

Arthur, Best, Jha and Mourits (1991) extended the work of McGee *et al.* (1987) and presented a comprehensive CSS predictive model for a composite reservoir in elliptical flow geometry. They used Boltzman's transformation to solve the flow equations in an elliptical coordinate system. The rate equation was an exponential-integral solution for a fractured wellbore. They assumed the outer thermal boundary, which was one degree higher than the initial reservoir temperature, as their drainage area. They did not consider the periodic nature of the η coordinate in the elliptic system, thus committing an error in the production equations. A more detailed discussion of this work will be presented later.

2.1.2 Gravity Drainage

For heavy oil and depletion-type reservoirs, gravity drainage has been identified as a critical factor. At the injection period, the steam zone is depleted of oil to some residual oil saturation. During the production time, reservoir fluids start flowing into the steam zone and resaturate the area. Many authors have employed gravity drainage to calculate this flow rate in the heated zone. In heavy oil reservoirs, where it is difficult to move the oil, steam heats up the oil around the wellbore; during production, this mobile oil flows into the well under the force of gravity. Some of the more important models are discussed below.

In their study of a depletion-type reservoir, Matthews and Lefkovits (1956) observed that at the stripper stage the gas concentration was so low that gravity remained the only driving force. By using an average gas-oil free surface height and the pseudo steady-state radial flow equation, they derived a gravity drainage equation for a bounded reservoir. Later, this equation was widely used by several authors in cyclic steam stimulation applications.

Doscher (1966), in one of the earlier analyses on CSS process, discussed its importance and qualitatively described a model that involved an inner and an outer cylindrical segment. He emphasized the significance of the temperature increase calculation of the outer segment. It was argued that after the initial production a considerable amount of oil would be produced from this section. In his model the hot zone temperature remained at the steam temperature during the whole project life. This might create a large error in the flow calculation. He proposed using Muskat's infinite reservoir equation until the pressure transient reached the inner zone boundary, and then using the Matthews–Lefkovits (1956) bounded reservoir equation.

Towson and Boberg (1967) used the gravity flow equation derived by Matthews and Lefkovits for a bounded reservoir to develop their gravity drainage model. Their thermal model was an extension of the previously published Boberg–Lantz model. They compared the rate calculated by the gravity drainage equation with the steady-state radial flow equation and used the greater of the two values. A step-wise calculation procedure was used where the average fluid height of the hot zone was adjusted at each time step. Unlike the Boberg–Lantz model, this model gave more realistic results for reservoirs with no primary drive. The authors did not consider any effect of temperature on the cold zone which always remained at the initial reservoir temperature.

Seba and Perry (1969) implemented the concept of Doscher (1966) in a concentric double cylindrical reservoir with their gravity drainage model. Their model was restricted by several assumptions. The radius of the hot zone remained constant assuming no fluid displacement during the injection period. Although they calculated the change in temperature of the cold zone, they assumed the heated zone temperature remained constant at the injected steam temperature. This overestimates production. Their finding of a harmonic production decline may not be valid for other reservoirs.

Jones (1977) reported a depletion-type reservoir model with gravity drainage. He used the Boberg and Lantz physical model and the gravity drainage flow equation for his rate calculation. A linear water saturation profile with time was assumed. The cumulative effect of changing temperature, fluid levels, relative permeability, fluid viscosities and fluid saturations was integrated into his calculation. He used scaling factors to calculate water and oil flow rates. These factors were determined with significant uncertainty.

Gontijo and Aziz (1984) improved the Jones model by using a cone shaped steam zone. They used Butler, McNab and Lo's (1979) temperature–viscosity relationship for

horizontal wells to get the expression for the pseudo-steady state flow potential which was a combination of pressure drop and gravity force. A more rigorous heat balance and heat loss during soaking was incorporated into this model. They neglected flow from the cold zone.

Sylvester and Chen (1988) presented another model for a pressure depleted reservoir. A pseudo-steady state radial flow drainage equation for both water and oil was developed in their work. This was derived on the basis of an erroneous equation. A detailed discussion of this work is presented in Appendix A. The flow equation contained only the fluid height at the wellbore. They considered the steam remaining from the previous cycle when calculating the first water saturation value during production.

Gozde, Chhina and Best (1989) used Gontijo and Aziz's flow equations in their model. They also considered cold oil outflow/influx which depends on the pressure difference between the interface and the external (outer) boundary. They calculated the pressure variation with time at the interface using Ramey's (1970) unsteady-state flow equation for a composite radial reservoir. Superposition was imposed in the outer colder region in a stepwise calculation. Heat flow from the cap rock to the reservoir during production was also considered. A good match with field data was reported.

Jones (1992) discussed the reasons why cyclic steam stimulation analytical models had not been widely accepted by the industry. He argued that the division of the production rates of gravity drainage, radial flow models by a scaling factor of 2 to 4 was due to the assumption of the entire open wellbore receiving steam. Another factor which had been ignored by previous authors was the growth of an air zone at the top of the formation which he called the steam thief zone. By taking into account these two observations, he constructed a gravity drainage model using existing equations. He reported good history-matches with two California heavy-oil projects and also presented some economic analyses.

2.1.3 Rock Expansion

One model which used an effective fluid compressibility to account for rock expansion, which is the most dominant driving force, is reviewed here.

De Haan and van Lookeren (1969) simplified the combined effects of all the drive mechanisms by representing them by an effective compressibility. Vertical inflow due to steam override was treated by finding the effective well radius corresponding to the fracture in the steam zone radius at the top of the sand. Then an effective hot zone radius was calculated by averaging the steam zone radius and the effective well radius. The authors considered the transient effect by assuming semi-steady state flow. They showed that about 40 percent of the cumulative production in the Tia Juana heavy-oil field, the Bolivar Coast, Western Venezuela, was due to compaction drive.

2.2 Semi-Analytical Models

Many authors have combined numerical methods with some analytical calculations. Most of these semi-analytic approaches were taken to incorporate various complex phenomenon of CSS. These works have made considerable contributions to the development and understanding different aspects of the steam stimulation process.

As the temperature of the injected steam increases, it enhances the depletion mechanism by making the dissolved gas in the oil less soluble, thus promoting solution gas drive. Davidson, Miller and Mueller (1967) used a solution gas drive model to find the volumetric rate of oil and water production in the heated zone. They did not consider the fluid production heat loss to calculate the average temperature of the reservoir. They found that the reservoir response did not depend on the amount of solution gas available within their range of gas-oil ratio values. The effect of temperature on oil relative permeability was found to be negligible under 400°F, but was significant over 500°F. The limitation imposed by the solution gas-oil ratio makes the use of this model very restrictive.

Martin's (1967) model used only a single sand and is valid primarily for the prediction of the first cycle production. He neglected the heat loss through conduction during injection, which produced a larger steam zone radius. Radial flow equations for both a constant pressure boundary and a no-flow boundary were developed. The effect of temperature was incorporated with the inclusion of a temperature dependent oil formation volume factor. He solved the production rate and temperature equations numerically using an iterative procedure. Controlling the bottom hole pressure value, he analyzed the effect of flash steam production on the oil rate and concluded that the oil production almost doubled when there was no steam production.

Kuo, Shain and Pochas (1970) used a finite differences method to calculate the free surface for their gravity drainage model. The heated zone was maintained at a constant temperature and the effect of continuous conduction heating of the colder part of the reservoir was studied with the help of finite differences. It was concluded that a large amount of oil flowed from the area adjacent to the hot zone in the early life despite the formation near the outer boundary remaining cold. They presented the results for one cycle in terms of cumulative oil production only. The assumption of a constant hot zone temperature results in an overestimate of the oil production rate.

De Swaan (1972) predicted the unsteady three-dimensional temperature distribution analytically and used it with the fluid-flow equations for a numerical solution. His model could predict the production response of a depletion-type stratified reservoir or of a homogeneous gravity drainage reservoir. He noted the importance of radial heat conduction. It was concluded that a slight rise of the outer zone oil temperature increased the production significantly.

Williamson, Dake and Chappelaar (1976) used an isothermal simulator to do a fieldwide investigation of the steam-soak process. They used a semi-analytical approach to obtain fluid production rates from the wells by dividing the reservoir into cylindrical annuli. Using an average value of the saturation calculation and the flow rate equation, they used the Boberg and Lantz method to calculate the average temperature of the hot zone. This model was developed to circumvent the difficulties the authors faced when using a thermal simulator for a field-wide simulation.

Flow in the early stages of a CSS cycle is transient in nature. Bidner, Horclo and Vampa (1990) argued that Boberg and Lantz's (1966) assumption of steady-state flow from the start of production was not correct. They solved numerically the transient diffusivity equation in the cold outer zone. A steady-state equation was assumed for the hot inner zone. They combined the two equations at the interface through continuity in a stepwise manner. Average temperature was calculated according to Boberg and Lantz (1966). Three different boundary conditions at the outer drainage radius were considered: constant pressure, no-flow and infinite medium. After 95 days of production, no-flow and constant pressure conditions produced the minimum and maximum oil respectively, the infinite medium assumption gave a result in between these two values. They were not able to show any significant difference in cumulative oil production with their approach as compared to the Boberg and Lantz method, although early production varied for all three boundary conditions.

2.3 Steam Zone Growth Calculation

Production rate and ultimate recovery depend heavily on the size of the steam zone. Therefore, it is very important to have a good estimate of the steam or hot zone size. Steam zone growth models have been presented in the literature for both cyclic steam stimulation and steam-drive processes. They can be classified into one dimensional frontal advance models and two dimensional (r-z) steam override models.

2.3.1 Frontal Advance Models

In frontal advance models, the steam front is assumed to be vertical in a horizontal reservoir. No variation of saturation and temperature in the vertical plane is allowed. For horizontal reservoirs, where gravity plays a critical role, these models would overestimate the steam zone growth. Review of the principal works is presented below.

Marx and Langenheim (1959) introduced the first frontal advance steam zone growth theory which was widely used in later works on analytical CSS models. A step function approximation of the temperature profile for one dimensional radial flow was made. The heat balance equation, which considered only vertical heat loss, was solved by Laplace transform producing a solution involving the error function. Only latent heat transfer from the steam was assumed in their model.

Ramey (1959) showed that there was no geometric restriction to Marx and Langenheim's solution and it could be applied for the variable injection cases with the help of superposition, though Ramey's equation for variable rates was incorrect. In the summation term he considered only the superposition of the heat injection terms, ignoring the superposition of the time dependent error functions.

Hearn (1969) modified Marx and Langenheim's solution to include the sensible heat of the saturated steam for the heat loss calculation. He concluded that, at a later time for a step function temperature profile, enough heat would not be supplied from the latent heat part for a limited injection rate. This resulted in a smaller steam zone than previously predicted by the Marx–Langenheim solution.

Mandl and Volek (1969) examined Marx and Langenheim's limiting assumption of no heat flow across the condensing front and introduced the concept of critical time to the frontal advance theory. They argued that after the critical time, convective heat transfer across the front becomes dominant and cannot be neglected. They presented a steam zone growth rate equation after the critical time which depends on reservoir thickness, injection rate, temperature and steam quality.

Closmann (1967) developed the steam zone growth equation for multiple-layer reservoirs. The steam zones were assumed to be of equal thickness and heat loss to the impermeable layers was also included. In a later work (1968) he studied the growth of steam in a preheated reservoir. This was an extension of Marx and Langenheim's work which could be employed to calculate the steam zone for the second and later cycles. He assumed a linear variation of the initial temperature in the overburden and underburden rock.

Yortsos and Gavalas (1981a, 1981b) developed integral equations for the steam drive process and solved them with the help of upper bounds, approximate and asymptotic solutions. These methods produced better estimates of steam zones for intermediate and late time calculations. They also solved the steam zone growth problem for low quality steam and a low injection rate as encountered in the Mandl–Volek model which was valid for a convection dominant processes (high injection rate). Calculation of upper bounds on the basis of the latent heat ratio of the injected heat is also useful in processes which produce receding fronts (such as CSS). The general approach of their model can be used also for three-dimensional steam zone growth.

McGee *et al.* (1987) calculated the heated zone volume by determining the time at which the steam advanced to the formation. This was done by equating the heat injection rate and the heat dissipation rate from the fracture face to the formation. They used equations derived by Wheeler (1969). Their analysis did not include any flow model and needed prior knowledge of production quantities.

Gajdica, Brigham and Aziz (1990) developed one and two-dimensional semi-analytical steam drive models from Yortsos and Gavalas' integral equations. They reported a good match with thermal simulator results except when the length to height ratio was less than unity.

2.3.2 Override Models

Steam overlay, bypass or gravity override models consider the effect of gravity on the density differences of the fluids. Apart from gravity, reservoir layering can also cause an override. The relevant papers are presented here.

Neuman (1975, 1985) proposed a gravity override model where the frontal movement is vertically downward. Areal growth of the steam zone was calculated by making a heat balance of the heat injected, energy produced and steam condensation rate per unit area. This model is applicable only under some specific conditions where the horizontal pressure gradient in the steam zone is much less than the vertical pressure gradient caused by the difference between the densities of the steam and the liquids. He presented a method to calculate the oil displacement beneath the steam zone and the vertical sweep.

Van Lookeren (1983) studied the effect of gravity override on steam zone growth and presented a one-dimensional equation for variation of steam height. An expression for an average steam height was derived which could be used to calculate the vertical sweep. He indicated that for a very viscous oil (over 1000 mPa.s), viscous tonguing may cause considerable bypassing of oil by steam. Thus, his model seems to work well for low and medium viscosity oils. There was no attempt to find the volumetric rate of the oil production.

Vogel (1984) studied a descending steam zone model where steam frontal movement is vertically downward from the overlaying steam. He proposed a simplification of previous models by assuming instantaneous steam overlay for the whole project period. This enabled him to use the well known linear heat flow equation in an infinite plane. He showed that the error for such a simplification over a ten year period would be only 2.6 percent for the ultimate heat requirement.

2.4 Heat Transfer and Temperature Distribution

Heat transfer calculations are very important for the overall performance prediction of the stimulation process. Determination of the temperature distribution in the formation for different steam injection schemes at various stages of the process have been studied by several authors. These investigations can be classified into two categories—unfractured and fractured wells.

2.4.1 Unfractured Well

Because of the complexity of the heat and fluid flow, in most of the studies, many approximations and simplifying assumptions were made to find the temperature profile around an unfractured well. Several key papers are reviewed here.

Lauwerier (1955) is credited as being the first to give an approximate analytical solution for the temperature distribution in the reservoir and the surrounding formation. He assumed a linear one-dimensional reservoir with constant physical and fluid properties. The temperature distribution within the reservoir was independent of vertical position and heat flow within the reservoir was by convection only. He only considered vertical conduction heat loss.

Boberg and Lantz (1966) in their model considered temperature distribution during the production period. Heat loss was calculated for vertical and radial conduction and by production of hot fluid. The temperature was represented by a step function where the unheated zone remained at the initial reservoir temperature. They assumed the reservoir sand and adjacent rock heat capacities to be the same. An equation for average reservoir temperature was presented which used approximate correction factors for all three modes of heat loss. This simple, easy and fairly accurate method attracted several authors who used it in their steam stimulation analytical models.

Davidson *et al.* (1967) developed an equation for the average temperature in the heated region during the soaking period. For the production period they only considered vertical and radial heat loss. These quantities were approximated by some equivalent expressions and a dimensionless temperature distribution in differential form was presented.

De Haan and van Lookeren (1969) also assumed conduction heat losses in the vertical direction only and used Carslaw and Jaeger's (1959) simple analytical solution to calculate the average temperature of the steam zone.

Closmann *et al.* (1970) derived a simplified expression for the temperature distribution in the reservoir after steam injection by assuming only vertical conduction heat loss. They assumed the thermal properties of oil bearing sand and the adjacent cap and base rock to be equal.

2.4.2 Fractured Well

Thermal recovery in many heavy oil reservoirs requires high steam injectivity. In very viscous oil-bearing formations, it can be achieved only by parting the formation. Especially for CSS, heat transfer around a fractured well and calculation of the temperature profile during the injection and soaking period is critical for performance prediction. A review of the more important papers is presented here.

Dysart and Whitsitt (1967) first attempted to calculate the transient heat transfer from a vertical fracture by making an energy and mass balance of an elementary volume of the fracture. Heat flow to the overburden was neglected and only conduction heat transfer to the pay sand was assumed. In a subsequent paper (Whitsitt and Dysart, 1970) the authors improved the model by allowing fluid leak-off from the fracture face. They assumed a linear variation of the leak-off from zero at the wellbore to the maximum value at the fracture tip. This model was a representative of a fracture which used additives to minimize leak-off. Heat loss from the top and bottom of the element was neglected again. Despite the over-simplification of the model, it did serve the purpose of identifying some aspects of hydraulic fracturing.

Wheeler (1969) presented a comprehensive analytical investigation of heat transfer from a fracture. He studied three different models—hot water injection, steam injection and a latent heat model. The hot water model accounted for convection in the fracture, conduction and convection in the pay zone and conduction in the overburden. A steam injection model also considered condensation in the vertical fracture. He predicted the presence of a non-isothermal water zone in front of an isothermal steam zone in the fracture. This model is valid for a thick impermeable formation since heat losses to the adjacent formation are neglected. His latent heat model did not allow for a hot water front in the fracture but heat loss to the overburden was considered. Equating the injected heat rate to the energy transferred to the sand by conduction and convection, he neglected any energy accumulation in the fracture. This assumption creates a condensate advancing front from the fracture face instead of a steam advancing front. He argued that the error due to this limitation would probably be no worse than assuming a step function temperature distribution in the fracture. A constant injection rate was also assumed. Wheeler reported a close match of his steam injection model results with a more sophisticated numerical model.

Sinclair (1971) used Wheeler's latent heat model which assumed a constant leak-off velocity from the fracture face. He studied the effects of heat transfer in deep well fracturing.

Ben-Naceur and Stephenson (1985) reviewed different heat transfer mechanisms during fracture propagation for their numerical model. They considered temperature-dependent fluid properties in the model. They cited a cubic approximation for temperature penetration in the formation which matched fairly well with the results from the analytical and numerical methods.

Biot, Massé and Medlin (1987) determined that, during hydraulic fracture growth, the fracture fluid temperature linearly rises to the reservoir temperature until reaching the middle of the fracture and then remained constant beyond that point. They used two different methods to obtain the solution: the method of characteristics and the method of successive approximation.

Meyer (1987) presented an analytical solution which combined transient heat conduction and convection from the fracture with a convection boundary condition at the fracture face. His model also included a time-dependent fracture face temperature and energy storage. He coupled the energy and two different fracture propagation models (i.e. Geertsma-de Klerk and Perkins-Kern-Nordgren) to find a closed-form dimensionless integral solution. This model seems to be the most realistic in handling the actual heat and fluid flow mechanisms in the fracture.

Boone and Bharatha (1993) studied the temperature distribution along a propagating leak-off dominated fracture. They developed a temperature profile along a horizontal fracture assuming only conduction heat loss. Later they extended this to find two limiting bounded solutions which included convectional heat loss. Their solutions are based on the assumptions of Carter's (1957) leak-off dominated fracture and Marx-Langenheim's steam injection theory. They concluded that, in Cold Lake oil sands, effective permeability is the primary factor for the advancement of heat. The initial heat transfer is dominated by conduction and the effect of convection is felt by the later cycles only.

2.5 Elliptical Flow Regime

Flow around a fractured well and in anisotropic reservoirs has generated interest in elliptic flow equations. Studies of the elliptical flow regime have been made for homogeneous and composite reservoirs. A brief description of the key papers is presented below.

2.5.1 Homogeneous Reservoir

The earliest flow studies in the elliptic coordinate system were for homogeneous unaltered reservoirs. Some of these papers are reviewed here.

Coats, Tek and Katz (1959) investigated the unsteady state problem of water encroachment into elliptic shaped reservoirs. A numerical solution of the diffusivity equation in the elliptic coordinate system was presented. They showed that the water influx calculation was about 7% in error when an elliptic boundary was approximated by an equal area circle for short dimensionless time.

Prats (1961) and Prats, Hazebroek and Strickler (1962) considered the elliptic flow of incompressible and compressible fluid respectively in a reservoir with an infinite-conductivity vertical fracture. For an incompressible fluid, the choice of an elliptic boundary for a large area ($r_{ed} > 2$) has a negligible effect on the pressure transient response. In the later work it was shown that the effect on compressible fluid could also be ignored.

A closed-form solution for flow into a circular wellbore in an elliptic drainage system was proposed by van der Ploeg, Kirkham and Boast (1971). Their work was related to water flow in a confined elliptical aquifer. A free surface was assumed at the water head. Steady-state solutions were developed for various well locations using gravity flow. Results and flow nets were presented for several cases.

In 1974, Gringarten, Ramey and Raghavan studied the unsteady-state pressure distribution created by an infinite-conductivity vertical fracture. This study was done because of a lack of predictive models to analyze the performance of short-time pressure transients. They applied Green's function to obtain both early-time and long-time solutions. In comparison with a radial system, they concluded that the effective well radius for an

infinite conductivity vertical fracture in an infinite reservoir during the pseudoradial (long-time) period is exactly one-fourth of the fracture length.

Kucuk and Brigham (1979) reported a study where they tried to handle elliptical problems in a unified and consistent manner. They gave analytical closed-form solutions for constant pressure and constant rate wellbore conditions. A long time approximation was also presented. In their following work (1981) they applied the elliptic flow solution to a water influx problem. For a constant pressure interface they constructed tables and curves of dimensionless influx and rate for different a_e/b_e ratios. Using different effective radii for a closed-form solution, they concluded that for intermediate and long times, an effective radius based on elliptic flow gave the most accurate results.

Hale and Evers (1981) used a conformal transform to solve the steady-state elliptic problem for application in vertically fractured gas wells. By defining a radius of investigation which changes with time, they modified the steady-state solution to approximate the unsteady-state solution for both the constant pressure and the constant rate case.

Perkins and Gonzales (1985) investigated the effect of thermoelastic stress on injection well fracturing. They discussed the change of stress due to the temperature difference of injected fluid and the reservoir fluid. They used Marx and Langenheim's method to calculate the volume of the elliptic shaped flooded zone and derived an expression to find the major and minor axes of the ellipse.

2.5.2 Composite Reservoir

Water and steamflood processes (or any other drive method) create two distinctly different regions in the reservoir with different fluid properties. Investigations of these composite reservoirs are briefly discussed below.

Obut and Ertekin (1987) developed a transient flow equation for a composite system in elliptic coordinates. Assuming equal pressure and flux at the interface they gave solutions for both constant pressure and constant rate at the wellbore using separation of variables. The well is an infinite-conductivity vertical fracture. Their solution is a good approximation of the stated problem.

The same problem was addressed by Stanislav, Easwaran and Kokal (1987). They gave a solution that is strictly applicable for equal diffusivity in both regions, but they showed that even for a diffusivity ratio as high as four, they got fairly good results. They attributed this to the more robust stability properties of Mathieu's function with respect to changes in parameters. In the case of steam stimulation, where the value of diffusivity ratio may be much higher than four, their equation fails to produce any meaningful result.

One study on dual porosity reservoirs was reported which followed the same approach as that used for a composite reservoir. Okoye, Matese, Hayatdavoudi and Ghalambor (1988) gave a solution for an elliptical flow system in dual porosity reservoirs. They concluded that elliptic geometry could be more appropriate for natural and vertically fractured reservoirs where anisotropy creates an elliptical boundary.

Chapter III

STATEMENT OF THE PROBLEM

With the steady depletion of Canada's conventional oil resources, ever-increasing attention is being given to the heavy oil reservoirs. The largest commercial heavy oil operation is in Cold Lake, Alberta. Cyclic Steam Stimulation (CSS) is the principal mode of thermal operation currently employed in Cold Lake and other heavy oil reservoirs.

Analytical models are excellent tools to make a quick assessment of new projects as well as current operations before a large undertaking. Although the need for such tools is well recognized, few models adequately address the problems involved in Cold Lake CSS operations. The objective of this research is to explore heat and fluid flow around an open fracture, as well as after it closes, and develop an analytical model which incorporates the actual flow situation in the field. As oil viscosity is the single most important parameter in flow calculations, special attention is given to the proper evaluation of average temperature and oil viscosity.

3.1 Statement of the Problem

The object of this study is to develop an analytical model which includes formation fracturing. For realistic modelling, the following tasks have to be accomplished:

1. Examination and evaluation of flow patterns around a fracture.
2. Appropriate heat balance and flow calculations.
3. Proper evaluation of oil viscosity in reservoir.
4. Computer implementation of the solution.

After a program is written to implement the ideas, the model should be able to successfully predict Cold Lake and other heavy oil CSS performances. It should give proper flow patterns and accurate temperature (and oil viscosity) values. It is also expected to appropriately respond to changes in a wide variety of parameters.

Chapter IV

MODEL DEVELOPMENT

One of the most significant applications of the Cyclic Steam Stimulation (CSS) process is in very heavy oil reservoirs. There are a number of analytical models reported in the literature which deal with lighter oils. All of these models consider radial flow into a well.

In the case of heavy oil reservoirs like Cold Lake, Alberta, the flow conditions are quite different from conventional reservoirs. Steam injection rates under normal conditions are too low and injection pressures must be increased until parting occurs to achieve a high injection rate. Fluid flow, heat transfer and mass balance have to account for the presence of this fracture at the wellbore. There are very few works which deal with this process in the CSS literature. McGee *et al.* (1987) probed the importance of a fractured wellbore in a fieldwide CSS operation. Arthur *et al.* (1991) presented the only analytical predictive model.

The mechanisms of fluid and heat flow in CSS are complex and diverse. Several authors (Vittoratos, 1991; Denbina, Boberg and Rotter, 1991; Beattie, Boberg and McNab, 1991) have discussed different aspects of this complex process. Although chemical reaction, relative permeability hysteresis, compaction and fluid expansion with temperature are present in CSS to various extents, gravity drainage and depletion type reservoirs have generated the most interest for their significance in heavy, as well as light oil reservoirs.

Although the importance of gravity drainage into a fractured well has been recognized, so far no one has attempted to investigate it. Elliptic flow occurs in the area surrounding a vertical fracture in an anisotropic formation or in an aquifer with an elliptic inner boundary (Kucuk and Brigham, 1979). In the case of pressure drawdown, Arthur *et al.* (1991) assumed the existence of a vertical fracture in an isotropic formation during the injection period, yet they solved the flow equation assuming an anisotropic reservoir for elliptic flow. Although anisotropy was introduced for the fracturing phenomenon, directional permeability was not included in the flow equation. To close the fracture during production, Arthur *et al.* assumed an isotropic reservoir, essentially treating the reservoir as an elliptical system with an open fracture at the wellbore. In reality, the reservoir remains isotropic for most of the time. The effect of any directional permeability would be

significant during production and limited to an area close to the fracture face. The case of a closed fracture should also be examined as a part of an elliptic drainage system.

4.1 Flow Equations

Three different flow equations are considered in the present study. The vertical fracture is assumed to be of negligible width and is bounded by over- and underburden. A conceptual diagram of the fluid and heat flow is shown in Figure 4.1. The reservoir is divided into two concentric elliptical cylinders. The inner region is called the hot zone and the outer region is called the warm zone. All three geometric configurations for the flow equations are presented in Figure 4.2.

4.1.1 Flow into a Wellbore at the Centre of an Elliptical Drainage Boundary

It may be assumed that the fracture formed during injection is completely closed during production without leaving any residual permeability in the hot zone. Under this assumption, the flow geometry in the reservoir is an elliptical shaped confined hot zone with a well at the centre (Figure 4.2a). Van der Ploeg, Kirkham and Boast (1971) developed a closed-form solution for steady saturated flow into a fully penetrating well in an elliptical flow geometry. They considered several well locations for their study. The essence of their approach was to derive orthonormal functions for the problem. The coefficients A_{Nm} were evaluated for various cases. If one were concerned about flow at the wellbore only, a few values of A_{Nm} were needed for quick convergence. These were used to determine A_{N0} , which was the only coefficient required in the flow equation. A well located at the centre with reservoir thickness of h has a flow rate of,

$$q = \frac{-2\pi K h \Delta\Phi A_{N0}}{\ln\left(\frac{a}{r_w}\right)}, \quad (4.1)$$

where $\Delta\Phi$ is the difference in hydraulic head, K is the hydraulic conductivity of the reservoir, a is the major axis of the ellipse and r_w is the wellbore radius. A detailed description of the development and solution procedure of this equation is given in Appendix B.

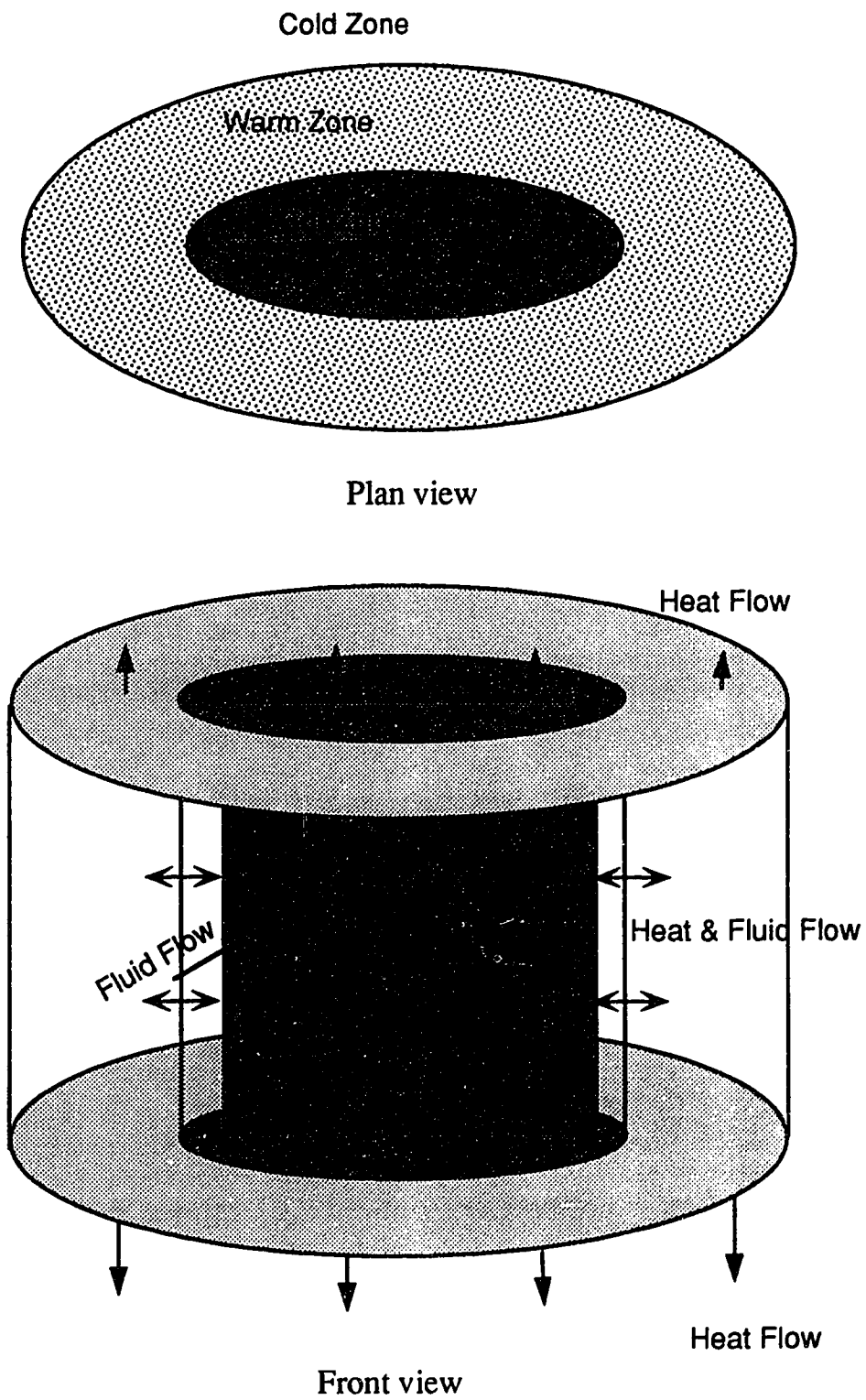
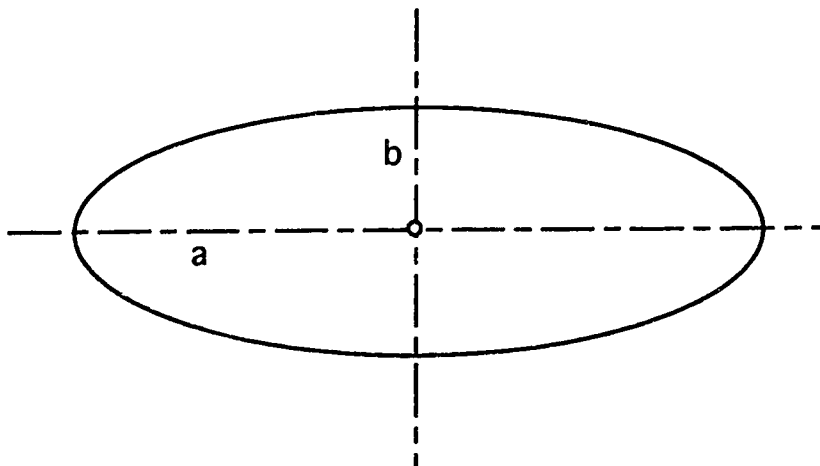
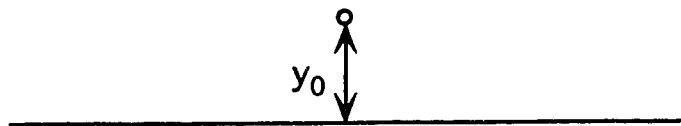


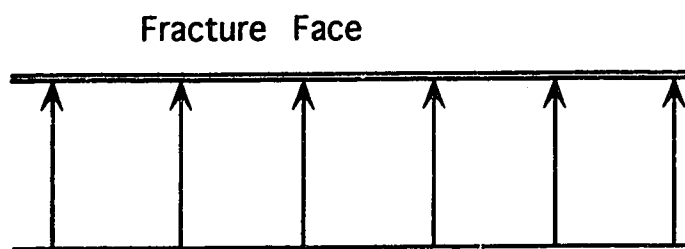
Figure 4.1— Conceptual diagram of fluid flow and heat transfer for the proposed model.



a. Circular well at the centre of an elliptical drainage system



b. Approximation of the elliptical drainage system with a well at the centre



c. Linear gravity flow approximation with a fractured wellbore

Figure 4.2—Plan views of different flow geometries.

4.1.2 Flow From a Finite Line Source into a Well

If an approximation of the above equation were to be made, one could imagine a long rectangular block producing oil from a well at the centre. As the system is symmetric, only one-half of it needs to be considered. Muskat's (1937) equation for flow from a finite line source can be used (Figure 4.2b). For a well, which is on the perpendicular bisector of the line source, the flow equation is,

$$q = \frac{2\pi kh(p_b - p_w)}{\mu \ln \left\{ \frac{2y_0}{r_w} \left(1 - \frac{y_0^2}{c^2} \right) \right\}}, \quad (4.2)$$

where y_0 is the distance between the well and the line source and $2c$ is the length of the line source. If $(y_0/c) \ll 1$, the above equation can be written as,

$$q = \frac{2\pi kh(p_b - p_w)}{\mu \ln \frac{2y_0}{r_w}}. \quad (4.3)$$

4.1.3 Gravity Drainage

From numerical simulation (Dietrich, 1986; Pethrick, Sennhauser and Harding, 1988) and observation wells (Duerksen, Cruikshank and Wasserman, 1984; Reis, 1990), it has been observed that the heated elliptic zone around the fracture is quite eccentric. An eccentricity (ϵ) value of zero represents a circle whereas unit eccentricity is a straight line. The perpendicular distance between the boundary of this zone and the fracture face at the steam injection point varies from 2 to 8 meters over the life of a well, whereas the fracture length could be several hundred meters. So, after injecting steam, essentially a very long rectangular block around the fracture with hot mobile oil would be created (Nzekwu, Hallam and Williams, 1990). Figure 4.2c shows this flow geometry. Due to the high permeability in the fractured zone, linear gravity flow of this hot oil into the fracture would take place. Gringarten *et al.* (1974) reported linear flow from a vertical fracture at early times. This occurs close to the fracture face.

Muskat (1937) described linear gravity flow in conjunction with his discussion of flow through dams. He presented a simple equation for the flux per unit length:

$$q = \frac{k\gamma g(h_b^2 - h_w^2)}{2\mu L}. \quad (4.4)$$

Forchheimer (1930) proposed this equation for a linear system based on the assumptions of Dupuit. This equation is known as the Dupuit–Forchheimer equation. Muskat showed that the assumptions made by Dupuit were in marked contradiction to those given by calculations with rigorous hydrodynamic theory. On the other hand, he showed that the same equation could be derived using an approximate potential theory. He found that the results were remarkably close approximations of the values of the flux determined using rigorous analytical or empirical methods.

The above equation is not an exact solution of the problem but is very much within the error bounds of the calculation of a rigorous solution.

4.1.4 Outer Warm Zone

Steady-state elliptical flow was assumed to be taking place in the outer warm zone at each time step. The equation (Muskat, 1937) for this situation can be written as

$$q = \frac{2\pi k h (p_e - p_b)}{\mu \ln \left(\frac{a_e + b_e}{a_b + b_b} \right)}. \quad (4.5)$$

4.2 Pressure

For an approximate solution to the flow from an elliptical drainage boundary into a well at the centre, an exponential decline curve was used in the present study to control the wellbore fluid height. The index of this equation was used as a history-matching parameter. In the proposed linear gravity models, the wellbore fluid heights were fixed for each cycle. These heights were allowed to decline at the rate of $1/(\text{total cycle production time})$ to achieve stability and an improved history-match. Average fluid heights at any time step n for the hot and warm zones were estimated from the following equations which were derived for the present study

$$\bar{h}_{hot}^n = \bar{h}_{hot}^{n-1} - (Q_{hot} - Q_{warm}) / \phi A_{hot}, \quad (4.6)$$

$$\bar{h}_{warm}^n = \bar{h}_{warm}^{n-1} - Q_{warm} / \phi A_{warm}, \quad (4.7)$$

where Q is the total fluid flow at each time step.

The interface fluid height was estimated from an area weighted average of fluid heights in the two zones. This height determined the pressure at the interface.

$$h_b = \frac{\bar{h}_{hot} A_{hot} + \bar{h}_{warm} A_{warm}}{A_{hot} + A_{warm}}. \quad (4.8)$$

Fluid height at the drainage boundary was taken to be constant and hence the pressure was assumed to be the initial reservoir pressure. Jones (1977) and Chen (1987) reported very little change in fluid height at the interface for a smaller radial system. Considering low flow rates and the huge size of the outer warm zone, this assumption would not produce any appreciable error. The change in the interface fluid height was monitored to track any gross error in this assumption.

4.3 Fracture Length

If no fluid flows from the fracture into the formation, it can be assumed that the fracture always extends beyond the calculated heat front in the fracture. For a constant leak-off velocity, a simple material balance will determine the maximum extent of the fracture in the formation (Wheeler, 1969). Assuming that only condensate flows into the formation and that there is no accumulation in the fracture, the fracture length is given by

$$L_f = \frac{i \rho_{st}}{4 V_f \rho_c}. \quad (4.9)$$

This equation, in effect, assumes that the fracture tip always propagates ahead of the heat front in the fracture. Although there would be a time when this condition will not be satisfied, that time is usually large. Wheeler reported achieving accurate results for injecting steam at 159 m³/day for 100 days.

The other option which has been included in the model is Carter's (1957) fracture propagation equation, which was derived as a function of time assuming constant width,

$$L = \frac{i(W + 2S_p)}{4\pi h C^2} \left[\frac{2\alpha}{\sqrt{\pi}} - 1 + e^{\alpha^2} \operatorname{erfc} \alpha \right], \quad (4.10)$$

where C is the fluid loss coefficient, α is effective fracture width and S_p is the spurt loss quotient. For large injection times, the above equation reduces to the familiar form of

$$L = \frac{1}{\pi} \frac{i\sqrt{t}}{hC} \quad (4.11)$$

For shorter injection time or small fluid leak-off, Carter's equation overestimates the fracture length. It gives a fair estimate of the fracture length for most of the cyclic steam stimulation projects. There is provision in the model to specify fracture length for each cycle.

4.4 Initial Temperature Calculation

Steam is injected into the formation to decrease the oil viscosity. Although there are several analytical models which deal with the temperature profile inside the fracture, very few include fracture and overburden together in the calculation. Wheeler (1969) presented the only comprehensive analytical calculations for heat transfer from a vertical fracture. He presented three models based on different states of fluids and modes of heat transfer. The following assumptions were made for the "latent heat" model.

1. Fracture height is equal to the sand height.
2. Two equal and symmetric fracture wings of negligible width are formed.
3. The pay sand is infinite horizontally and confined by impermeable overburden and underburden strata vertically.
4. Mode of heat transfer:
 - a. Fracture - convection and condensation.
 - b. Sand - conduction and convection.
 - c. Cap and base rock - conduction.
5. No energy accumulation in the fracture.
6. Temperature in the fracture is defined by a unit step function.
7. Leak-off is constant for the injection period.
8. Energy from the fracture into the formation is transferred by condensate.

Given the injection rate and total injection time, the following equation gives the temperature profile for any point in the reservoir including the fracture, pay sand and over- and underburden.

$$\begin{aligned} \bar{T}(\Gamma, \xi, \eta, \tau) = U(\tau - \tau_s) \frac{\xi}{\sqrt{\pi} \sqrt{\tau - \tau_s}} \int_0^1 \operatorname{erfc} \left\{ \frac{\sqrt{\beta} [v^2 (\tau - \tau_s)] + \frac{\eta}{2\beta}}{\sqrt{\gamma (\tau - \tau_s) (1 - v^2)}} \right\} \times \\ \exp \left\{ - \left[\frac{\xi}{2v \sqrt{\tau - \tau_s}} - \alpha v \sqrt{\tau - \tau_s} \right]^2 \right\} \frac{dv}{v^2}. \end{aligned} \quad (4.12)$$

This equation is used to determine how temperature is distributed in the hot and warm zones after the injection period. The dimensionless time for the steam front to reach any point in the fracture was estimated by

$$\Gamma = 2H \sqrt{\tau_s} \int_0^1 \operatorname{erfc} \left[v^2 \sqrt{\frac{\beta \tau_s}{\alpha (1 - v^2)}} \right] \operatorname{ierfc}(\alpha v \sqrt{\tau_s}) dv. \quad (4.13)$$

The temperature in the fracture maintained a step function profile. Initially only condensate flows into the formation. Once the energy supplied to the fracture exceeds the energy transferred into the formation, a steam zone will advance. The time for this process was calculated from the following equation,

$$\frac{1}{\alpha \sqrt{\tau_{sa}}} \operatorname{ierfc}(\alpha \sqrt{\tau_{sa}}) = \frac{2x_i h_{fg}}{C_f (T_i - T_f)} \quad (4.14)$$

Using these three equations presented by Wheeler (1969), an isotherm of 100°C was used as the hot zone boundary in the present study. The warm zone boundary was selected to be the isotherm at 0.01 degrees above the initial reservoir temperature. The choice of 100°C is based on the flowing mobility of the oil at Wolf Lake as reported by Pethrick *et al.* (1988). In general, this temperature may be defined on the basis of oil mobility for a particular reservoir. A sensitivity study of the choice of boundary temperature will be presented later.

The average temperature of the two zones was estimated using a linear polynomial approximation (trapezoidal).

4.5 Heat Loss Equation

Carslaw and Jaeger (1959) presented a transient solution for a heat dissipating semi-infinite slab inside an infinite medium. The slab had a unit initial temperature. They solved the one dimensional heat conduction equation in the vertical direction to obtain the solution which involved the error function. Boberg and Lantz (1966) used this solution as part of their heat loss calculation to determine the average steam zone temperature during production. Marx and Langenheim (1959) used a similar approach to find the steam zone growth during injection.

Souza, Pedrosa Jr. and Marchesin (1987) used an analytical-numerical method to determine the heat loss to the overburden and underburden. This method was developed for an easier treatment of the heat loss equation in the overburden. They employed an approximation to solve the heat conduction equation in a finite medium with variable temperature at the reservoir-overburden boundary. This eliminated the need for an additional grid system for the overlying strata and storage of temperature history of each grid block.

Vinsome and Westerveld (1980), with an aim to save computer storage and grid block calculation, adopted a simpler strategy. They argued that due to the uncertainty in the cap and base rock thermal properties, high accuracy in the solution of the heat loss calculation was not required. They proposed a much simpler semi-analytical solution of the linear one-dimensional conduction equation based on the results found from the more complex variational method (Weinstein, 1972, 1974; Chase and O'Dell, 1973). The assumptions for their solution were,

1. Temperature in the cap rock varies smoothly.
2. Horizontal heat conduction in the cap rock can usually be neglected.
3. The tail of the temperature distribution contains little energy and is relatively unimportant.

Based on the above assumptions, they gave a fitting function for the temperature profile which adequately met all the boundary conditions. Inserting this function into the one-dimensional heat conduction equation at the interface using a finite difference discretization of the time derivative, the following equation was found

$$\frac{T_0 - T_0^N}{\Delta t} = \alpha_h \left(\frac{T_0}{d^2} - \frac{2p}{d} + 2q \right), \quad (4.15)$$

where α_h is the thermal diffusivity, T_0 is the interface temperature, d is the diffusivity length and p and q are parameters. The parameter T_0^N is the interface temperature at the beginning of the time count. This ensured that the heat loss rate decreased from cycle to cycle in a CSS implementation of this method. This also eliminated the need of superposition. Heat loss rate and energy stored in the cap and base rock were given by,

$$\dot{q}_L = k_h \left(\frac{T_0}{d} - p \right) \quad (4.16)$$

$$E_c = \frac{k_h}{\alpha_h} d (T_0 + pd + 2qd^2) \quad (4.17)$$

where k_h is the thermal conductivity. This solution was used in the present model in order to calculate the heat loss to the over- and underburden as well as the heat conduction between the two zones. Appendix C presents the equations which were used in evaluating the average temperatures.

4.6 Average Soak and Production Temperature

Vogel (1984) presented a simple heat-loss equation for the over- and underburden assuming that the steam covered the entire heated area instantly. Several authors (Sylvester and Chen, 1988; Gozde *et al.*, 1989) have used this equation to calculate the heat loss during the soaking period.

$$H_{lost} = 2k_h \pi r_h^2 (T_s - T_R) \sqrt{\frac{t_{soak}}{\pi \alpha}} \quad (4.18)$$

A cylindrically shaped heated zone was assumed in developing the equation. This quantity of heat was deducted from the total heat injected to determine the heat available at the beginning of a production period. Although, the rate of heat loss is very high during the early stages, very few authors tried to find the change of average temperature during the soaking period.

The most popular method for calculating the average reservoir temperature during production is the Boberg and Lantz technique. Performing a heat balance for a cylindrical heated zone, they derived the following equation,

$$T_{avg} = T_R + (T_S - T_R)[\bar{\theta}_r \bar{\theta}_z (1 - \delta) - \delta] \quad (4.19)$$

where, $\bar{\theta}_r$ and $\bar{\theta}_z$ are the unit solutions for conduction in the radial and vertical directions, respectively, and δ gives the fraction of the heat loss due to fluid production. The values of $\bar{\theta}_r$ and $\bar{\theta}_z$ were presented graphically against dimensionless time. The solution given for $\bar{\theta}_r$ was valid for dimensionless time greater than 0.1. Bentsen and Donahue (1969) proposed an alternative solution in terms of a series function which was applicable for a dimensionless time of less than 0.1. They also presented a unit solution for one-dimensional vertical heat loss through conduction. The parameter δ was found by integrating the heat loss due to fluid production at each time step. Gontijo and Aziz (1984) produced the unit solutions with the help of regression analysis. This was done for programming simplicity.

Arthur *et al.* (1991) treated the problem differently. They included a second zone, just outside the hot zone, in their overall heat balance. The outermost boundary temperature was taken to be one degree above the initial reservoir temperature. By so doing, they eliminated the need for calculating the radial heat loss. The average temperature of the warm (outer) zone is important for fluid flow calculation in the later part of a cycle. Although they considered heat exchange between the zones through fluid flow, they ignored conductive heat transfer. The inclusion of conduction is especially important during the soak period when no fluid movement takes place.

A new set of equations was developed (Appendix D) in the present study which included heat conduction between the two zones. All conductive heat transfer terms were calculated using the approximation suggested by Vinsome and Westerveld (1980). A more detailed discussion of their work is presented in Section 4.5. The heat loss rates were evaluated with time-dependent surface temperatures. The need for superposition was avoided by using cumulative project time.

Following are the overall heat balances to calculate the average zone temperatures during the production and soak periods.

Hot zone heat balance:

$$\begin{aligned} \text{Heat content} = & \text{production heat loss} + \text{over- and underburden heat loss} \\ & + \text{warm zone heat loss} - \text{heat gain from warm zone flow.} \end{aligned}$$

Warm zone heat balance:

$$\text{Heat content} = \text{heat loss to hot zone flow} + \text{over- and underburden heat loss} \\ - \text{heat gain from hot zone.}$$

Heat exchanges due to fluid flows during the soak period were considered to be zero.

4.7 Saturation

Earlier CSS analytical models did not involve any fluid saturations, because single phase flow was assumed. Most of these models evaluated only the oil production rate. Water production was calculated from an arbitrary water-oil ratio. No consideration was given to saturation changes or relative permeability.

Jones (1977) introduced an analytical method to evaluate saturation changes based on a water material balance in the hot zone. He correlated these saturation values with relative permeabilities measured in the laboratory. Following Jones, other authors (Gontijo and Aziz, 1984; Sylvester and Chen, 1988; Gozde *et al.*, 1989) used his model or a modified version of it.

Composite elliptical flow models (Stanislav *et al.*, 1987; Obut and Ertekin, 1987), developed mainly for well-testing, used single-phase flow. Hence, the need for saturation calculation did not arise. Arthur *et al.* (1991) employed two different zones to do an overall material balance in both oil and water to calculate the saturation at each time step. Based on their mobile fluid calculation, two different schemes were developed and tested in the present study.

In the first scheme, the traditional approach taken by most authors was followed and an overall material balance of only water in both the hot and warm zones was considered. Although there is evidence of the presence of a gas phase in many reservoirs, the amount of gas in heavy oil reservoirs may be small. It was also assumed that most of the injected steam condensed during the soak period. Both zones were represented by average zone values. Initial mobile fluid saturations were calculated from the following general equation.

$$\text{Initial mobile fluid} = \text{initial volume} + \text{injected volume} + \text{cum. inflow} \\ - \text{cum. production} - \text{cum. outflow.} \quad (4.20)$$

If the fluid saturations in each zone did not add up to unity, the values were normalized. Subsequent saturation values were calculated from a simple material balance on the water,

$$S_{w1} = S_{wc} + (S_{wm1}\phi V_{hot} - q_{w1} + q_{w2})/(\phi V_{hot}), \quad (4.21)$$

$$S_{w2} = S_{wc} + (S_{wm2}\phi V_{warm} - q_{w2})/(\phi V_{warm}), \quad (4.22)$$

$$S_{o1} = 1 - S_{w1}, \quad (4.23)$$

$$S_{o2} = 1 - S_{w2}, \quad (4.24)$$

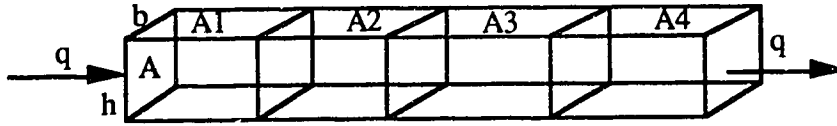
where S_{wm1} and S_{wm2} are the initial mobile water saturations in the hot and warm zones, respectively.

For the second scheme, a material balance on both oil and water was found. It was assumed that the total production time was much larger than the individual production time step. Saturation equations were developed from the continuity equations assuming the change in hot zone volume to be equal to the change in warm zone volume. Arthur *et al.* (1991) normalized the saturation values at each time step, whereas more weight was given to the water balance in the present study. The oil saturation was calculated from the saturation equation at each time step instead of normalizing the values. Arthur *et al.*'s mobile saturation equations and the modified calculation methods for this study are presented in Appendix E. For both schemes, the hot zone water saturation was restricted to $1 - S_{or}$. Mobile water, consequently, was restricted to a maximum value of $1 - S_{or} - S_{wc}$.

4.8 Average Viscosity Calculation

Viscosity is the single most important parameter in the calculation of thermally stimulated oil production calculation. Boberg and Lantz (1966) developed their flow equation solely on the effect of change in oil viscosity in the hot steam zone. They incorporated this effect by increasing the effective wellbore radius. An earlier model by Owens and Suter (1965) used a viscosity-temperature graph to estimate the oil production rate. Closmann *et al.* (1970) evaluated the time average viscosity values to use in a van Everdingen and Hurst (1949) type oil influx calculation, which involved superposition. They did not address the areal distribution of viscosity. Since these early models, all authors have used the average temperature of the hot zone to calculate oil viscosity. The reason for following this procedure is the lack of any simple analytical equation to calculate

a temperature distribution during the production period. Viscosity values found from a viscosity-temperature relationship corresponding to the average zone temperatures cause an overestimation of oil production. These average values do not give the proper weight to the effect of lower temperatures at the outer edge of the averaging area and hence, give lower viscosity values.



$$\mu_{ave} = \frac{A_1\mu_1 + A_2\mu_2 + A_3\mu_3 + A_4\mu_4}{A_t} \quad (4.25)$$

$$(A_t = A_1 + A_2 + A_3 + A_4)$$

An indirect, simple but effective approach was taken in the present study to overcome this limitation. Using Wheeler's (1969) equation, it is possible to calculate all the isotherms at the end of an injection period. As the strips between these isotherms are linear beds in series with the same cross-sectional area, the average viscosity corresponding to the average temperature of each strip was calculated. True area-weighted averages of the oil and water viscosities for each zone were found corresponding to different overall average temperatures. This was accomplished by varying the steam injection time, rate and steam quality. To develop a correlation between the average temperatures and the average viscosities, the total area was kept constant for all calculations. Third degree polynomial equations were derived from the generated data for both the water and the oil. The temperature range covered by these equations was adequate for all the variation in temperature during the production time.

4.9 Flow Reduction Factor

Using the full values of length and height of the fracture in the flow equation produces unrealistic flow rates. In theory, one would get such high rates, but in the actual reservoir there are several factors which would reduce the flow drastically. Three such factors are discussed below.

4.9.1 Vertical Steam Sweep Efficiency

Due to gravity override, the injected steam does not sweep the whole pay thickness. This is true irrespective of the creation of a fracture during injection. Myhill and Stegemeier (1978) examined the oil-steam ratios predicted by different frontal displacement models in steamflood calculations. They compared the results with actual field data and laboratory experiments. The measured values were generally less than the predicted values. They cited steam override in the real situation, which was not addressed by the models they studied, to be one of the factors for such lower values. Van Lookeren (1983) presented several calculations and field data to corroborate this. Even without a thief zone, the sweep efficiency may be as low as 20%. Very seldom does it exceed 70%. Jones (1992) discussed the reasons why analytical cyclic steam stimulation models have not been accepted widely. He showed with the help of a temperature survey in an observation well near an in-progress steam cycle well that only a fraction of the open pay zone took steam. He argued that the common assumption of the entire open wellbore receiving steam injection was one of the major reasons why the predictive flow equations overestimated the flow by factors of two to four. Reis (1990) reported that only 40% of the completed interval accepted steam in a California heavy oil reservoir.

4.9.2 Fracture Parameters

The complexities of steam injection as well as reservoir heterogeneity make the prediction of fracture parameters unique for each oil sand reservoir. Interpretation and analysis of field data play a significant role in characterizing a fracture. Single or multiple well operation, temperature, viscosity, grain size, thief zone, depth of burial, clay content and chemical reaction are among the many other factors contributing to the uniqueness of each oil sand reservoir. The most significant fracture parameters are the height and the half length. Although these parameters may be altered significantly by localized geological effects, general trends in Alberta heavy oil are discussed below.

4.9.2.1 Fracture Height

Arthur *et al.* (1991) presented the only CSS analytical model which included a vertical fracture at the wellbore. They used the total pay thickness (100%) for the fracture height.

Although this ideal situation may exist in some reservoirs, several authors reported partial vertical climb of fracture propagation in Alberta heavy oil.

Leshchyshyn, Farouq Ali, Settari and Chan (1994) reported a fracture height of less than 50% of continuous net pay height. This was attributed to shale heterogeneity. In another work, Leshchyshyn and Kennedy (1994) inferred from a post core clay analysis that the vertical steam fracture climbed at an angle of 45 degrees. This was also supported by an independent analysis of Formation Micro-Scanner (FMS) logs. Lowe and Donovan (1989) observed a vertical fracture profile around the wellbore and steeply rising as it moved out from the wellbore in Athabasca oil sand. Fialka, McClanahan, Robb and Longstaffe (1993) analyzed a post steam core from a Cold Lake area oil sand reservoir. After four cycles, they found the vertical sweep efficiency to be only 60%.

4.9.2.2 Fracture Length

In a fracture growth analysis, Leshchyshyn, Seyer and Langdon (1991) found that only 60% of the calculated fracture length was active with hot fluid (of temperature above 90°C). Many authors assume a complete closure of the fracture during production. Reis (1990) reported formation of vertical fractures in a deeper, less permeable and more consolidated heavy oil reservoir in California, which remained open during production. Chan and Sarioglu (1992), in their discussion on the complexities of the CSS process, noted that numerical simulation studies for different reservoirs suggested the presence of closed but not completely healed fracture. Moreover, fracture length calculated from an analytical relationship is only approximate. In many cases, field observations showed two to five times overestimation of the fracture length calculated by such an analytical formula (Leshchyshyn, 1995).

Flow reduction factor values between 0.20 to 0.50 were used in the present study. This incorporated the effects of all the factors discussed above. These values, along with wellbore fluid heights, were used as fitting parameters to history match the results.

4.10 Relative Permeability

Only two-phase flow was considered in this study: oil and water. This assumption is reasonable when most of the injected steam condenses before the start of the production period and the gas liberated in a heavy oil reservoir is considered negligible.

It is not possible to find a correlation of water and oil relative permeabilities with water saturation which would be applicable to a wide range of reservoirs. Even with the help of experimental data for the same reservoir, it is difficult to match field production data. Gontijo and Aziz (1984) used Farouq Ali's (1982) correlation for a Midway-Sunset field which was originally developed for a Kern River steamflood (Gomma, 1980). Chen and Sylvester (1990) showed that the values found in the Gontijo and Aziz (1984) study were considerably different from the reported field data and these correlations caused significant errors in the oil rate calculation.

In addition, large discrepancies may occur due to hysteresis. Bang (1984) was only able to match field production by adjusting relative permeability in numerical simulation studies. He found that the relative permeability to water at residual oil for imbibition (injection) was about seven times greater than that for drainage (production). Dietrich (1981) also reported that relative permeability curves generated through numerical simulation to reproduce observed water-oil ratios in several CSS operations worldwide, were much lower than those of routine laboratory imbibition water-oil relative permeability tests.

The effect of temperature on the water relative permeability end point is well established. Farouq Ali (1982) concluded from numerical simulation of (Cold Lake, Alberta) viscous oil that the temperature effect on water-oil relative permeability must be taken into account for meaningful history-matching. Dietrich (1981) and Nakornthap and Evans (1986) presented numerical simulation results showing an increase in the irreducible water saturation with temperature. This shift in end point causes a decrease in the water relative permeability values.

For simulation of the Wolf Lake project, Pethrick *et al.* (1988) adjusted relative permeability values, found from experiments, within the bound of the errors. For the present study, the tabulated values of water-oil relative permeability presented in their work were used. These values were adjusted for change in water relative permeability end point due to the effect of temperature.

Chapter V

SOLUTION AND COMPUTER IMPLEMENTATION

A program was written in FORTRAN to implement the ideas described in the previous chapter. The main purpose of this program is to calculate flow rates at each time step during production. Average temperatures of the hot and warm zones at the end of the injection and soak periods are also evaluated. Special attention was paid to avoid iterative procedures. No “trial and error” approach was taken at any level of the calculation. Empirical formulas and correlations were used to minimize data requirements. Whenever needed, cubic spline interpolation and a table look up routine was used to find intermediate values of tabulated data.

5.1 Description of the Model

1. Saturated steam is injected into the wellbore at high pressures, causing formation parting. Fracture half-length is calculated either from a given fluid leak-off coefficient (Carter, 1957) or material balance (Wheeler, 1969).
2. The reservoir is divided into two concentric elliptical cylinders around a vertical fracture at the wellbore. The inner cylinder, which extends from the fracture face to the 100°C isotherm, is called the hot zone. The outer cylinder, which extends from the heated boundary to the drainage boundary, is called the warm zone. The drainage boundary is the isotherm just above the initial reservoir temperature ($16.0 + 0.01^{\circ}\text{C}$).
3. At the end of injection, average temperatures and the distances of the isotherms separating the zones are determined.
4. During soak and production, conduction heat loss to the over- and underburden is calculated. There is no radial heat loss from the outermost boundary. Average zone temperatures are calculated from energy balance equations considering heat loss due to fluid production, heat loss to the confining strata, and convection and conduction heat exchange between the zones (Appendix D).

5. Three different flow equations are used for the three cases to calculate the flow in the hot zone. Interface fluid height and the corresponding pressure are calculated from a material balance equation. It is assumed that steady-state flow takes place in both zones during a time step. Pressure at the wellbore is maintained at a constant level during production for the gravity flow models. Although no flow takes place across the outer boundary, the fluid height is assumed constant (initial reservoir pressure). The elliptical steady-state flow equation is used to determine the rate in the warm zone. Despite steady-state flow during each time step, the overall flow is transient owing to the pressure variation at the hot-warm interface. Flow rates at the beginning of a time step are assumed constant for that step.
6. Heat remaining in the reservoir at the end of each cycle is added to the injected heat in the next cycle, allowing the reservoir temperature to be kept at the initial value at the beginning of each cycle.

5.2 Description of the Subroutines

The subroutines implementing the model are described here in a sequential manner along with the principal features of the main program.

5.2.1 Initialization

Subroutine DATAIN

This is the first subroutine called by the main program. Data are required to be supplied in SI units. There are five sets of input data. The first set needs injection, production, and soak times for each cycle along with steam pressure, saturation temperature and a fluid loss coefficient (optional). The second set is comprised of porosity, formation thickness, injection rate, steam quality, absolute reservoir permeability and initial reservoir temperature. Compressibilities, saturations and initial reservoir pressure are specified in the third set. The fourth set provides thermal conductivities and heat capacities of the reservoir and the confining strata. The final set includes all the relative permeability data. Data are provided in free format.

Subroutine SPLINE

This subroutine calculates all the spline coefficients for the tabulated relative permeability data.

Subroutine OVISC

Oil and water viscosities and densities are calculated with the help of this program. Viscosity values at initial reservoir temperature are calculated here before the start of the injection period.

5.2.2 Injection Period

The main program initializes all the project and cumulative values at this stage. Maximum and minimum production limits of 100 m³/day and 1m³/day, respectively, are also set at this time. The maximum number of cycles is supplied and all the cycle calculation values are initialized.

Subroutine PVTIN

This routine calculates the viscosity, density and heat capacity of the steam, water and oil. The latent heat of vaporization is also evaluated. At this point, all the values are calculated at steam temperature.

Subroutine TEMPGAUSS

Hot and warm zone boundaries are calculated by this program, along with the fracture length. The fluid leak-off velocity can be found in three different ways: supplying of leak-off coefficients as direct input, calculating the leak-off velocity through the subroutine LEAKOFF or using Wheeler's (1969) material balance equation with a known fracture length. Wheeler's equations are integrated using 16-point Gaussian quadrature. Average temperatures at the end of injection for each zone are also calculated here. In the case of an unknown fracture length, it can be found either from Carter's or Wheeler's equation. For repeat cycle calculations, the heat remaining from the previous cycle is added in the form of a dimensionless quantity to the heat input in the present cycle.

Subroutine PRESSURE

Pressures at the interface and the outer boundary are calculated for the approximate solution to the flow into a wellbore at the centre of an elliptical drainage system. Pressure at the wellbore is controlled by an exponential function of production time.

5.2.3 Soak Period

Subroutine SOAKTEMP

This program evaluates the average zone temperatures at the end of the soak period. Parameters for the fitting function are first evaluated. It also calculates the heat loss to the over- and underburden during this period. A time step size of 1 day was used for the short soak period. Moreover, at high temperatures the heat loss rate varies considerably for a small change in temperature. A 1 day time step is used for retention of better accuracy.

At this point, the main program calculates all the initial mobile saturations and PVT data at average temperatures. Saturations for the first production time step are evaluated and limits are checked. The oil in place in the hot zone is also calculated. Then the production stage calculation values are initialized.

5.2.4 Production Period

Relative permeabilities and mobilities for the first production time step are evaluated here. In addition to the table look-up (subroutine SEARCH), relative permeability calculations from correlations are provided for. Wellbore fluid height and all flow rates are calculated next. Maximum and minimum flow rates are checked. Cycle cumulative values are updated.

Subroutine SATN

This program calculates the saturation values based on the flow rates evaluated at the present time. Options for an oil- and water-based material balance calculation as well as only water based calculation are provided. The new saturation values are used for the next time step.

Production results for the time step are written here. Then fluid heights at the hot and warm zones as well as at the interface are updated.

Subroutine AVPRODTEMP

This routine evaluates the average zone temperatures at each production time step. The conduction, heat flow from the hot zone to the warm zone is multiplied by a scale-down factor. This is done in accordance with the assumptions made for the flow reduction factor. Fifty percent of the formation thickness was considered active in the heat exchange. Heat lost to the over- and underburden and through fluid production is also calculated by this program.

The main program is looped with a time increment of two days until the end of production. Cycle results are then written and project cumulative values are updated. The heat remaining in the reservoir is calculated at this time before the start of the next cycle calculation. The procedure is repeated until the end of the cycles is reached. A flow diagram of the computer program is shown in Figure 5.1.

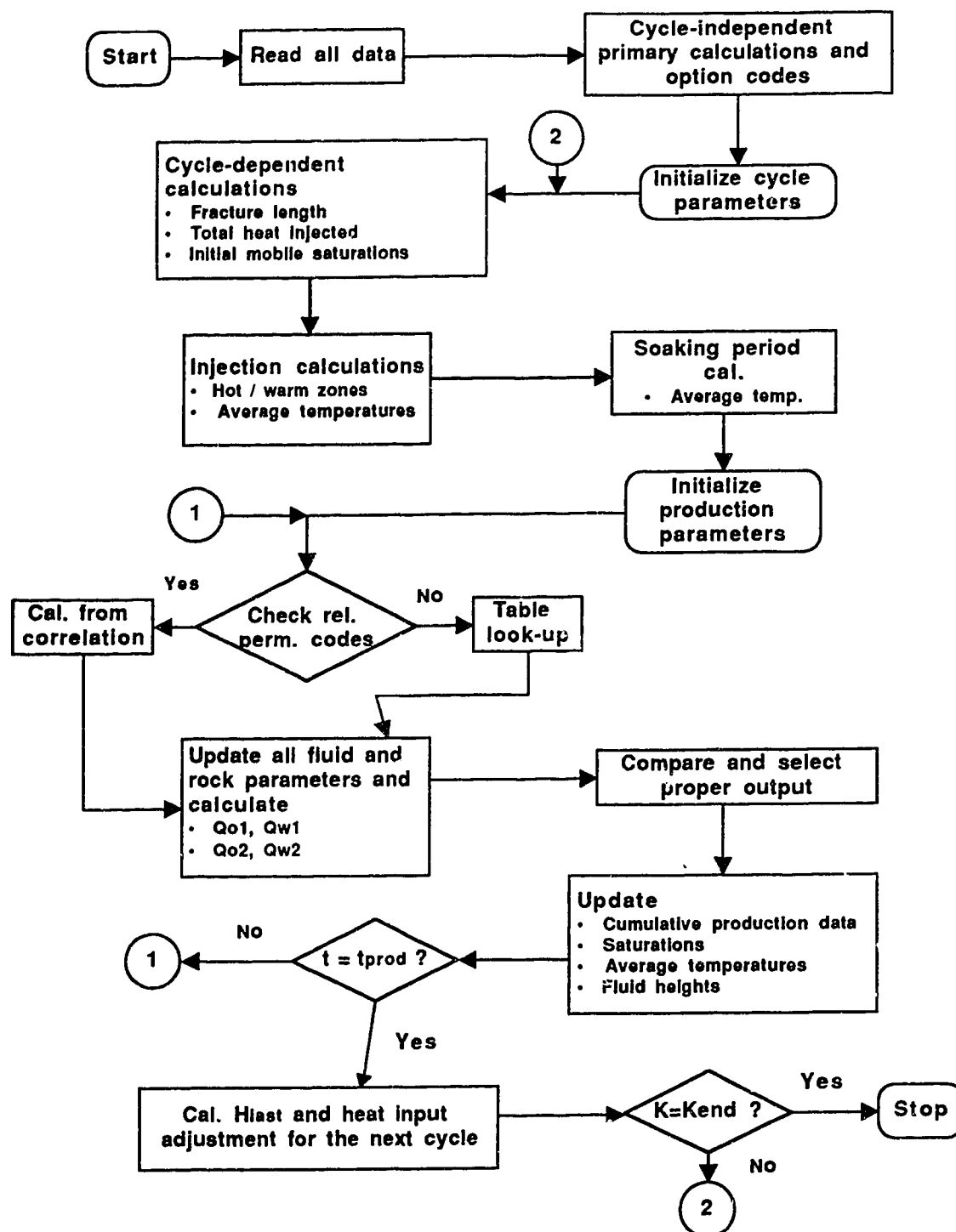


Figure 5.1—Computational flow diagram of the model.

Chapter VI

RESULTS AND DISCUSSION

This study examines Cyclic Steam Stimulation (CSS) performances under fractured as well as unfractured wellbore conditions. Flow into a completely closed fracture which involves Elliptic Flow into a circular Well (EFW) is investigated. A closed-form as well as an approximate solution to this problem is examined. Based on the results of these studies, a partially open fracture situation is investigated with the help of the new model discussed in Chapter IV. To verify the effectiveness, as well as the limitations of the new model, an extensive sensitivity study is conducted. The effects of changes in downhole steam quality, formation thickness, steam injection rate, time step size, steam soak period, steam temperature, hot zone boundary temperature and initial reservoir temperature are discussed. Two different methods of calculating the saturations are examined. The effect of temperature change on the water relative permeability end point is also studied.

The new model investigates the effects of conventional method of evaluating the oil and water viscosities at each time step during production. Results from a new and much improved method, as discussed in Chapter IV, are presented. The effect on the average temperature due to conduction heat loss from the hot inner zone to the warm outer zone is investigated.

Sample results are discussed and interpreted for each of the above mentioned aspects of the CSS process in this chapter. Figure 6.1 shows the investigation structure of this study. The objectives are to explore the existing concepts and to provide a better understanding of the CSS process. The relative importance of different phenomena on the overall CSS process is investigated.

6.1 Simulation Data

The most frustrating part of this study was the lack of available field data. All the past and present operators in Cold Lake, Wolf Lake and Marguerite Lake heavy oil pilot and commercial projects were contacted. Data were also requested from AOSTRA and ERCB. All these efforts came to naught. Either the data were confidential or they were on sale for a

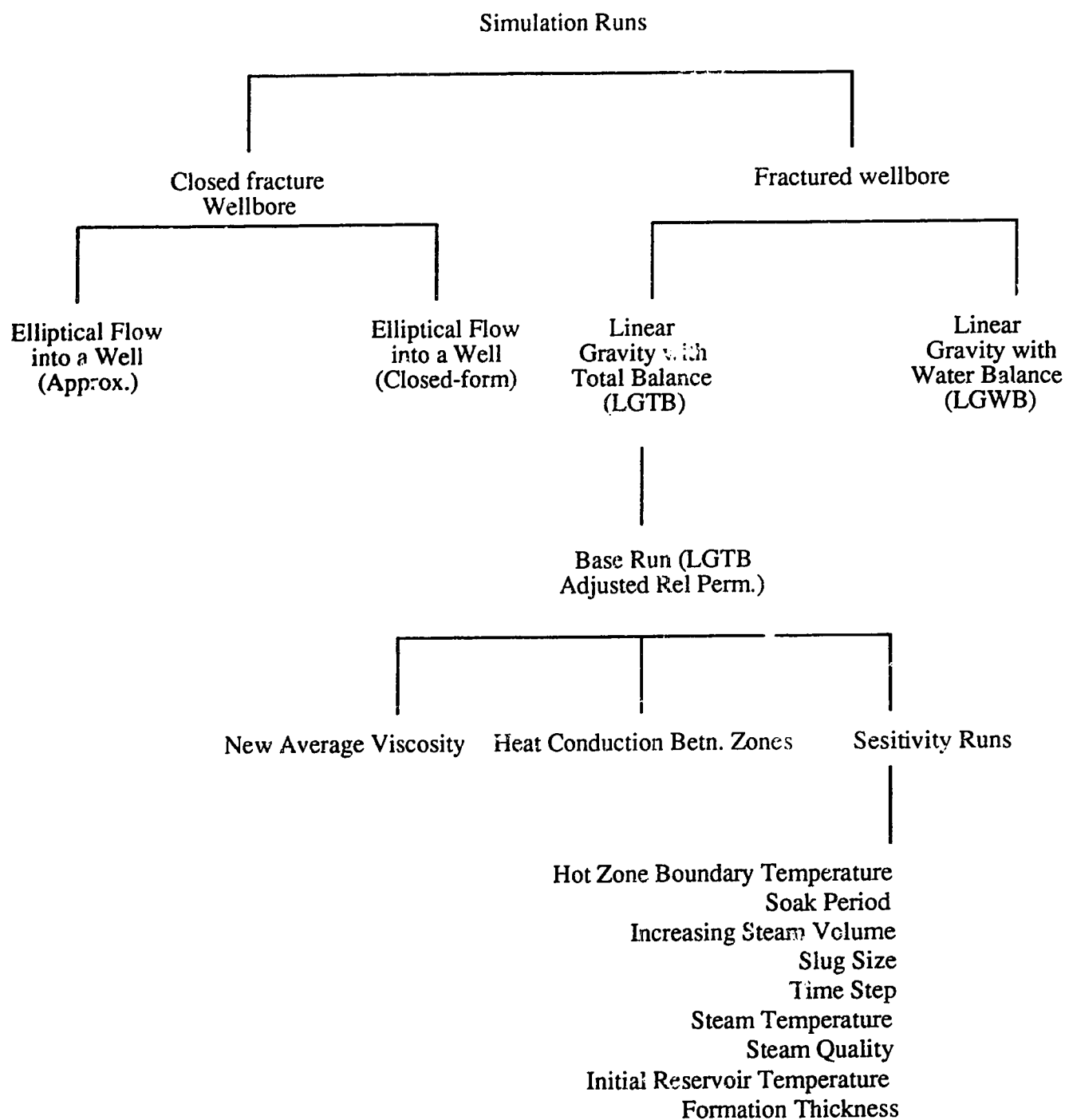


Figure 6.1—Overall scheme of the simulation runs conducted.

price beyond the means of the present undertaking. This study was conducted using the only published data (Pethrick *et al.*, 1988) on the Wolf Lake project, jointly owned by Petro-Canada and BP Resources Canada Limited. The simulation input data are shown in Table 6.1 and the oil-water relative permeabilities are shown in Table 6.2. The correlations used to calculate the fluid properties are presented in Appendix F.

The fracture equations do not account for geological stresses or change in stress. The criterion for the fracture model is same as specified by Pethrick *et al.* (1988) that the pressure at the leading edge of the fracture is 8500 ± 500 kPa at the end of the injection period. No injection restriction was imposed. This is the approximate fracture propagation pressure.

At BP's former Marguerite Lake lease, bitumen is produced at an approximate depth of 450m (Buckles, 1979) primarily from the lower Cretaceous Clearwater formation. Wells are predominantly in 220 m \times 100 m five-spot configuration. Based on the net present value of the project, Pethrick *et al.* optimized the injection and production strategies of individual wells in Wolf Lake projects. Prior to this optimization, several years of CSS production data from BP's Phase A Pilot in the Wolf Lake project were matched to validate the thermal simulator. The agreement between the simulation results and field behaviour allowed a high degree of confidence in the optimization strategy. The final strategy in a 220 m spacing is shown in Table 6.3. This data has been used as the base run for all the experiments in the present work.

For the initial investigation and the sensitivity study, the first five cycle results are used. Several production performance parameters are used to analyze the results. Project efficiency is compared on the basis of the oil-steam ratio (OSR). The operational criteria are based on a calendar day oil rate (CDOR). The remaining efficiency parameter used is the water-oil ratio (WOR).

6.2 Elliptical Flow Into a Well (EFW)

Two different approaches were taken to study this problem. The approximate method was tried to verify the merit of further analysis by the closed-form solution. The closed-form solution required some more rigorous calculation.

Table 6.1—Simulation input data.

Porosity, fraction	0.305
Permeability, μm^2	1.0
Initial reservoir pressure, kPa	2750.0
Initial oil saturation, fraction	0.66
Initial reservoir temperature, $^{\circ}\text{C}$	16.0
Irreducible water saturation, fraction	0.34
Residual oil saturation, fraction	0.35
Rock compressibility, kPa^{-1}	0.45E-6
Water compressibility, kPa^{-1}	0.45E-6
Oil compressibility, kPa^{-1}	0.34E-6
Oil thermal expansion coefficient, $^{\circ}\text{C}^{-1}$	0.848E-3
Reservoir specific heat, $\text{kJ m}^{-3}\text{K}^{-1}$	2350.0
Reservoir thermal conductivity, $\text{kJ m}^{-1}\text{d}^{-1}\text{K}^{-1}$	149.6
Cap/base rock specific heat, $\text{kJ m}^{-3}\text{K}^{-1}$	2350.0
Cap/base rock thermal conductivity, $\text{kJ m}^{-1}\text{d}^{-1}\text{K}^{-1}$	149.6
Oil viscosity at 16°C , mPa.s	81000.0
Oil viscosity at 100°C , mPa.s	115.0
Oil viscosity at 200°C , mPa.s	6.8
Net pay, m	23.8
Fracture half length, m	240.0

Table 6.2—Water-oil relative permeability (Pethrick *et al.*, 1988).

S_w	k_{rw}	k_{ro}
0.3200	0.0000	1.0000
0.4300	0.0025	0.6440
0.5450	0.0100	0.3910
0.5929	0.0200	0.2420
0.6359	0.0330	0.1380
0.6760	0.0530	0.0610
0.7145	0.0730	0.0300
0.7530	0.1130	0.0120
0.7700	0.1200	0.0000

Table 6.3—Operational data.

Cycle	Steam Slug Size (m ³)	Injection Time (days)	Soak/down Time (days)	Production Time (days)	Cycle Time (days)
1	6250	25	15	89	129
2	7000	28	15	123	166
3	7500	30	15	135	180
4	8000	32	15	150	197
5	8250	33	15	161	209
6	8500	34	15	174	223
7	8750	35	15	188	238
8	9000	36	15	202	253

6.2.1 EFW Approximate Solution

Initial investigation of this problem was done with the help of an approximate solution. An exponential decline curve, $P_{wf} = P_I \exp(-t/d)$, was used to calculate the bottomhole flowing pressure. The value of P_I was fixed at 1500 kPa below the steam injection pressure for each cycle and d was varied from 260 in the 1st cycle to 90 in the 5th cycle for best matching. The interface pressure of this model was approximated using an infinite integral solution and a material balance equation. This was based on Arthur *et al.*'s (1991) solution procedure.

Results of the approximate as well as the closed-form solution are presented in Figure 6.2 through Figure 6.8. The analysis for the closed-form solution will be presented in the next section. Figure 6.2 shows the cycle oil production along with BP's simulation results. A fairly good match was obtained by adjusting the wellbore fluid pressure. Predicted production in the 3rd cycle is about 100 m³ less than the simulation value. An over-production of about the same amount in the 4th cycle kept the cumulative oil production very close to the simulation result. This can be seen in Figure 6.4, where both the BP simulation and the approximate solution predict the same total amount of oil at the end of five cycles. In the history-matching effort, more emphasis was given to match the oil production and let the water production be according to the relative permeability distribution. Figure 6.3 shows the cycle water production of the EFW schemes and the BP simulation run. It can be seen that the predicted water production by the approximate solution is consistently below the simulation values for all the cycles. Although the general trend of increasing water production is seen, no attempt was made to adjust the relative permeability curves. Any adjustment for hysteresis or temperature effect would have produced even less water. Cumulative water production at the end of five cycles is only 9,042 m³ compared to 23,724 m³ projected by the BP simulation (Fig. 6.5). A new set of relative permeability values could be generated to force a match. The objective of the study was to remain as close to the original simulation input data as possible and explore the actual results of various schemes. No forcing of the solution was done for this reason.

Because of the incorrect estimation of water production, one cannot put much confidence in the performance parameters predicted by this model. Cycle OSRs (Fig. 6.6) and CDORs (Fig. 6.7) matched the values predicted by the BP the simulation fairly closely. The effect of low water production can be seen in Figure 6.8, where the WOR varied from

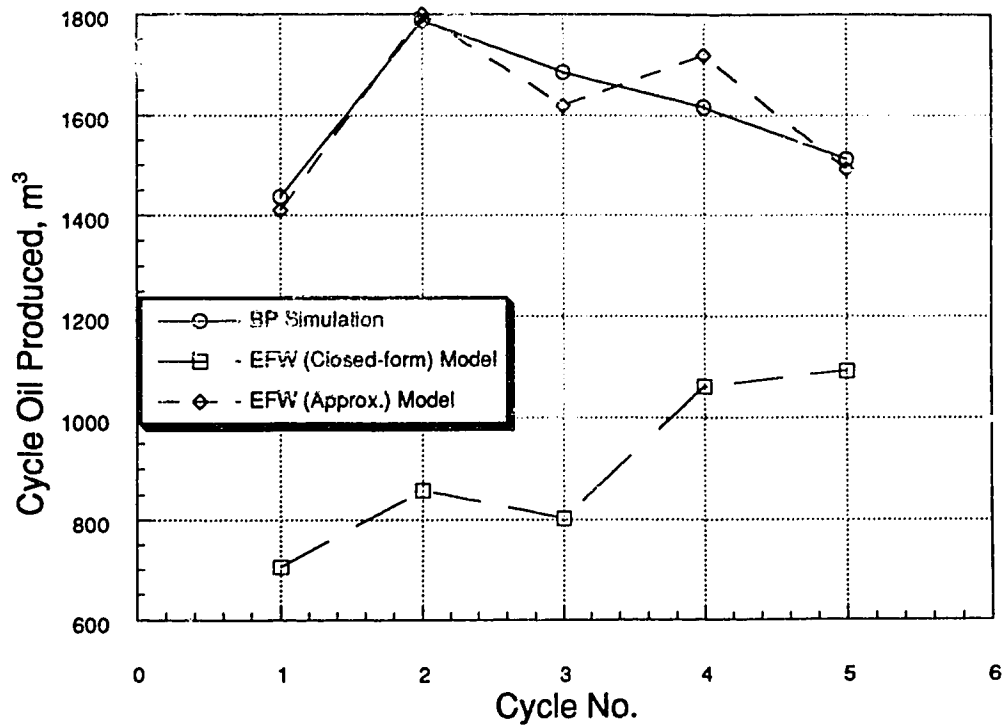


Figure 6.2—Comparison of cycle oil production for closed fracture models.

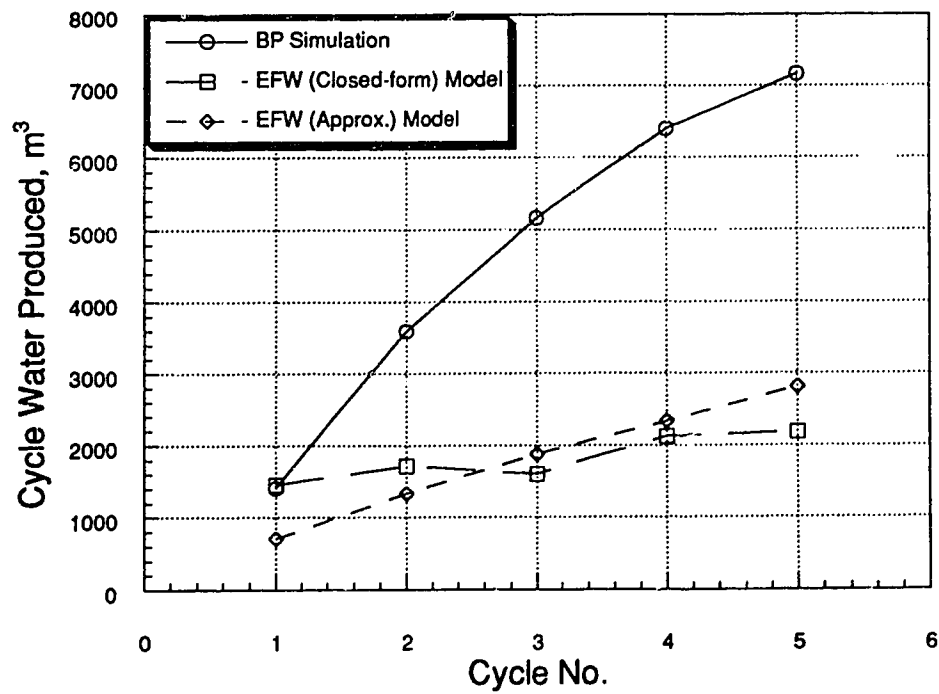


Figure 6.3—Comparison of cycle water production for closed fracture models.

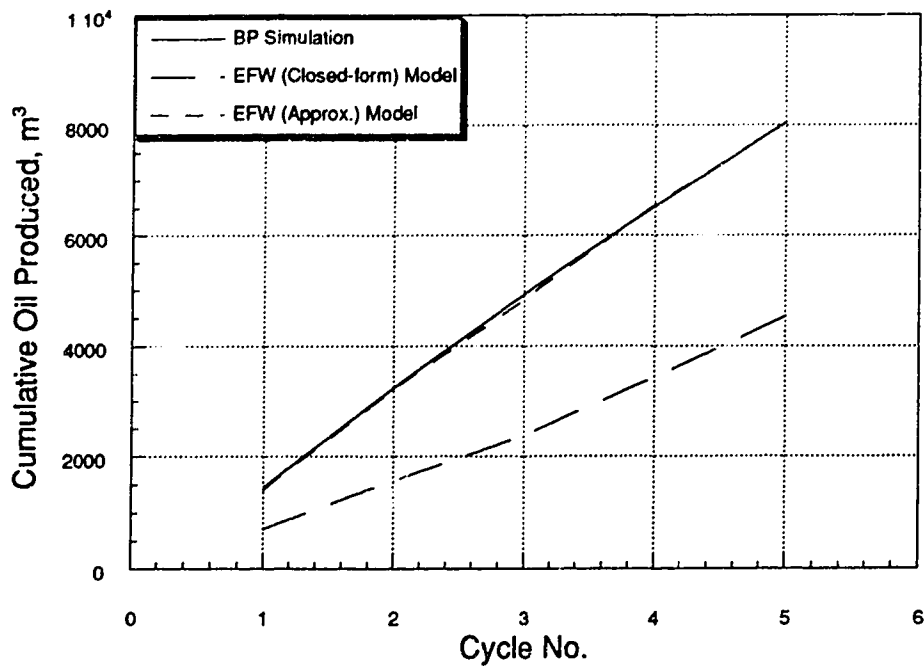


Figure 6.4—Comparison of cumulative oil production for closed fracture models.

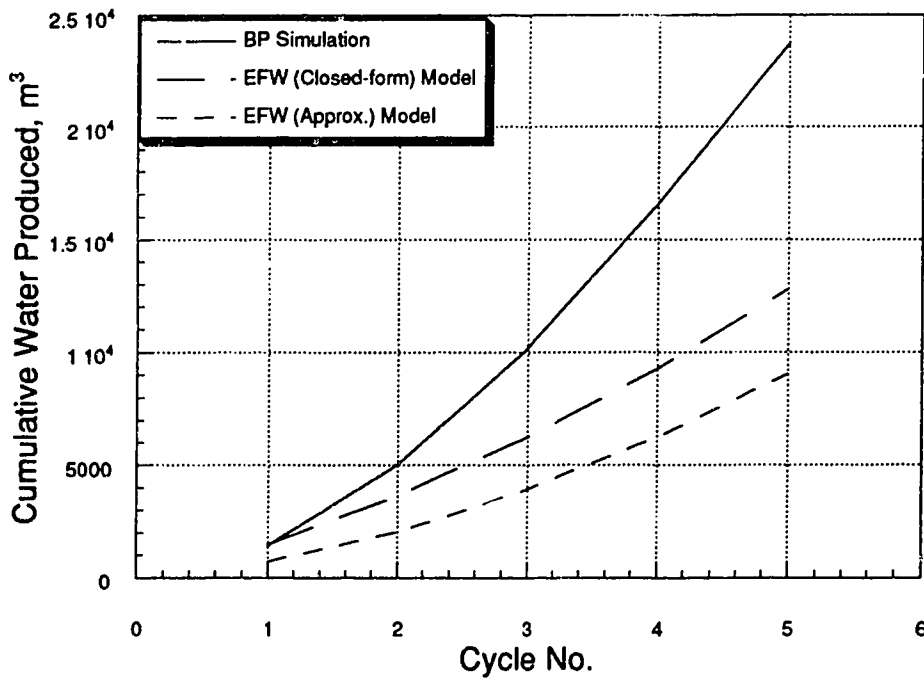


Figure 6.5—Comparison of cumulative water production for closed fracture models.

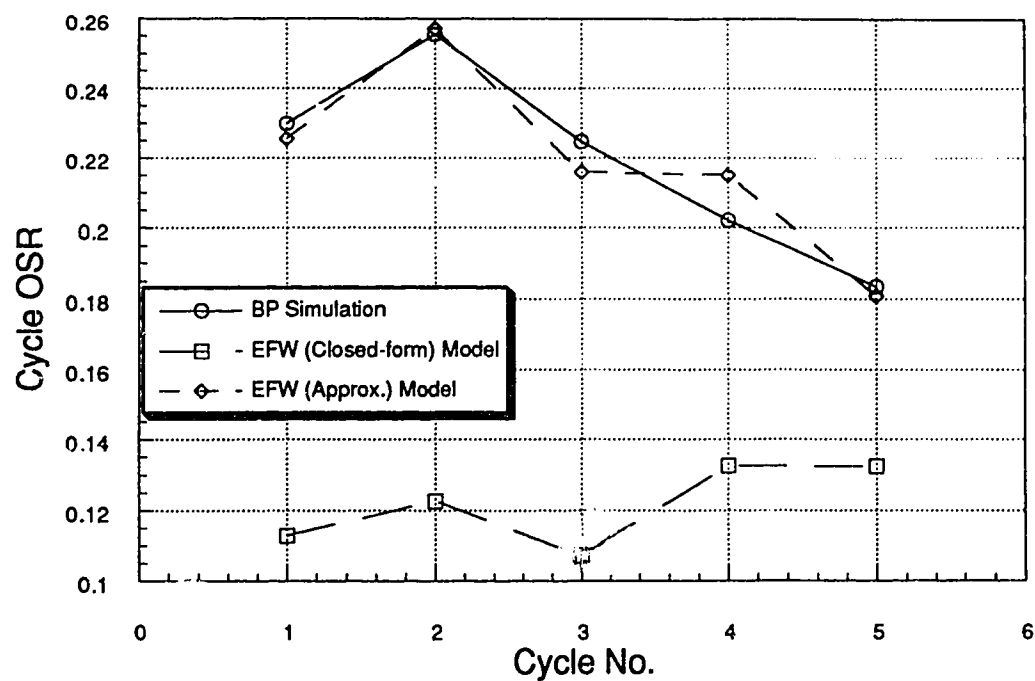


Figure 6.6—Comparison of cycle oil-steam ratio for closed fracture models.

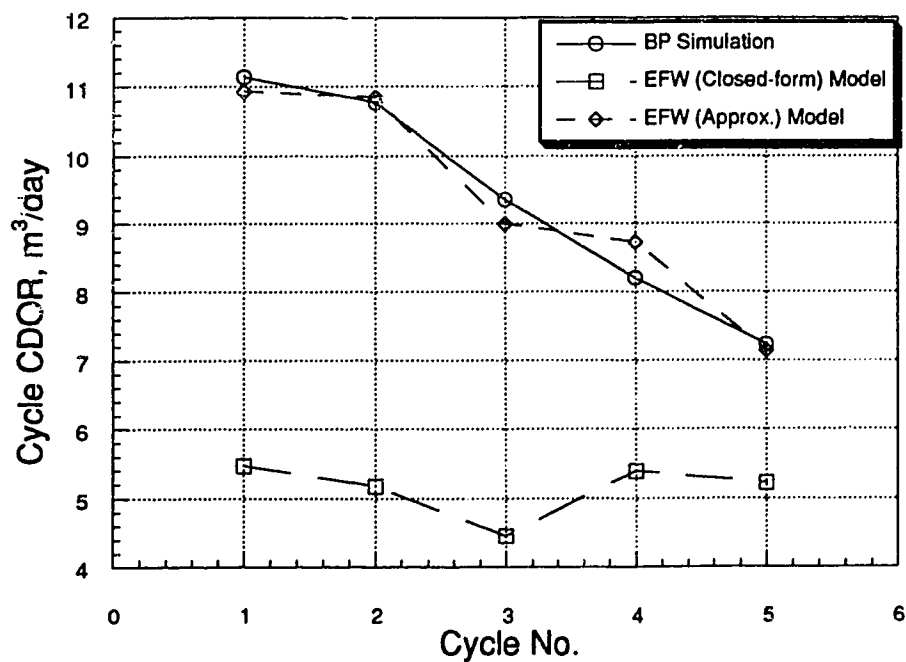


Figure 6.7—Comparison of calendar day oil production rate for closed fracture models.

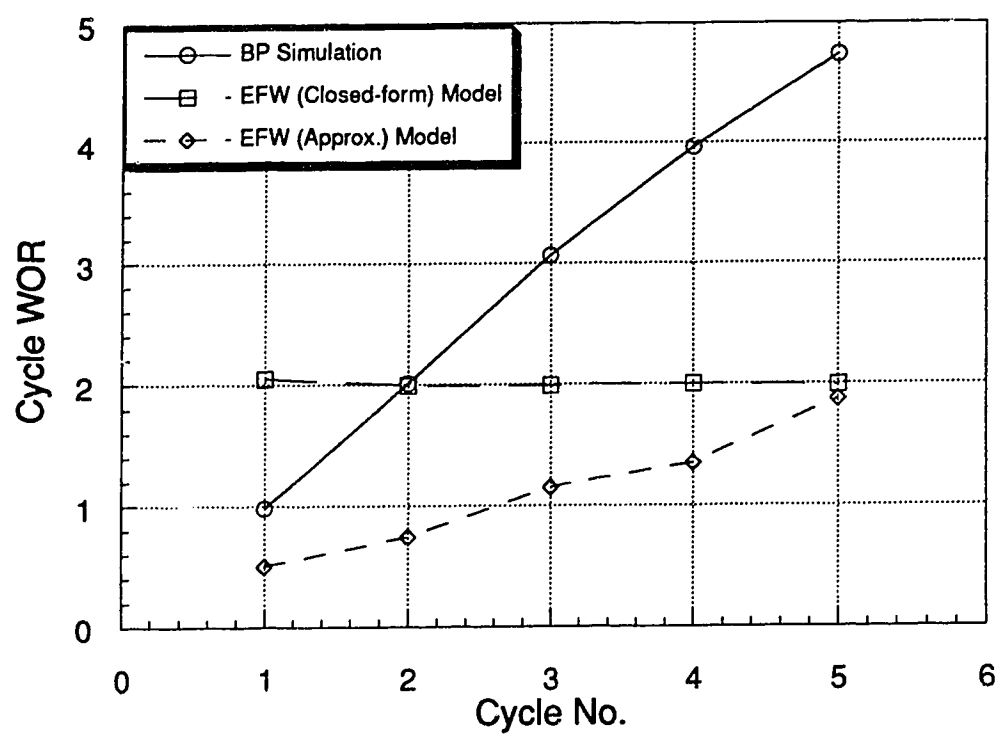


Figure 6.8—Comparison of cycle water-oil ratio for closed fracture models.

a low of 0.5 in the 1st cycle to about 2.0 in the 5th cycle. These values are somewhat lower than the reported average field results (Farouq Ali, 1994) from the Cold Lake area.

6.2.2 EFW Closed-form Solution

The approximate method gives an inconclusive answer regarding flow geometry. Although the oil production was matched satisfactorily, water production was far below the simulation results. This discrepancy did not support a correct interpretation of the flow geometry assumption, as all input data were unmodified. Before getting into any mechanistic analysis, it was decided to conduct further investigation with the help of a closed-form solution of the problem (van der Ploeg *et al.*, 1971).

The closed-form solution requires the computation of the coefficient A_{N0} . This involved integration of several functions which are described in Appendix B. A Gaussian quadrature method was employed to do these integrations. The calculated geometric parameters of the inner hot ellipse were used as the input data ($a=240$ m, $b=2-3.5$ m, $r_w=0.2$ m). The average value of A_{N0} was evaluated to be 2.05. After observing low flow rates in all the cycles, the wellbore fluid height was fixed at 0.0 m to achieve the maximum flow potential.

Figure 6.2 compares the cycle oil production of both the EFW models with the BP simulation. Although the shape of the closed-form solution curve is similar to the approximate solution, the flow volumes are the lowest for the closed-form solution. While the water production for the 1st cycle is as high as the simulation result, it drops drastically in the 2nd cycle (Fig. 6.3) and falls below the approximate solution after that. The cumulative oil production is only half of that predicted by the BP simulation (Fig. 6.4). It should be noted that the approximate solution uses pressure drawdown as the driving force. To achieve a higher production rate to match the BP simulation results, three different options were available to calculate the average pressure of the hot zone: average pressure calculated from an infinite integral solution (Arthur *et al.*, 1991), saturated pressure corresponding to the average temperature and average pressure corresponding to the average fluid height of the hot zone. The maximum of these values was used. Moreover, higher flow reduction factors were used to match the results. Tarnim and Farouq Ali (1995) reported less oil production also for the approximate model using the same flow reduction factors for both models. This produced even lower rates for the closed-form solution. The total water production at the end of the 5th cycle is substantially higher than

the approximate solution but about half of the simulation results (Fig. 6.5). Higher prediction by the closed-form solution was due to the large amount of water production in the 1st cycle.

Due to the low oil production, both cycle OSRs (Fig. 6.6) and cycle CDORs (Fig. 6.7) were much lower than the simulation values. The 3rd cycle produced the lowest CDOR of $4.4 \text{ m}^3/\text{day}$ as well as the lowest OSR of 0.107. Interestingly, the WOR remained constant at 2.0 for all cycles (Fig. 6.8). The reason for such behaviour is not understood. This is close to the average WOR for the first 5 cycles in other Cold Lake area operations (Farouq Ali, 1994).

Lower production rates for the EFW models indicate that a circular well at the centre of an elliptical drainage boundary does not represent the true flow geometry in the field. Any fracture at the wellbore which is created during injection does not completely close during production. Even if it is closed, it does not heal and considerable high residual permeability remains in the fracture plane. Although discrepancies in oil and water production volumes are evident, curves for all the parameters followed the same general trend for both cases. The cycle water production and consequently the WOR curve followed different directions. This could be attributed to the large difference in 1st cycle water production between the closed-form and the approximate solutions. Average temperature and saturation calculations for a subsequent cycle depend on heat remaining in the reservoir and the last saturation values from the previous cycle. The relative permeability curves and the nature of the flow equation determine the 1st cycle response.

6.3 New Model

From the investigation of flow in an elliptical drainage system with a circular well at the centre, it is found that the flow rates are much lower than the BP simulation results. Although the approximate solution predicted satisfactory oil production, this was achieved using much higher flow reduction factors than the probable field values. Both the approximate and the closed-form solution predicted much lower water production than the BP simulation results.

A new flow geometry is proposed for the new model. It is assumed that the vertical fracture created during the injection period does not close completely during the production period or it leaves behind a vertical plane with a high residual permeability. Linear gravity

flow will take place from a long narrow rectangular block of hot mobile oil into this highly permeable vertical plane. For the nature of the flow equation, this model will also be called the Linear Gravity flow model. The flow reduction factor was increased from 0.25 in the 1st cycle to 0.50 in the 8th cycle. The wellbore fluid height was fixed at 19.5 m for all cycles.

6.3.1 Saturation Schemes

Two different saturation calculation schemes have been tested. In the first scheme, in accordance with the technique used in all radial flow analytical models, oil and water saturations during production are calculated based on an overall material balance of water in both the hot and the warm zones. This model is called the Linear Gravity flow based on Water Balance (LGWB). For the second scheme, the material balance was done on both the oil and the water. This will be called the Linear Gravity flow based on Total Balance (LGTB).

Cycle oil productions for the two saturation models are shown in Figure 6.9. Model LGWB consistently produced slightly more oil at each cycle. Model LGTB produced the same amount of oil for each of the first three cycles, after which the oil production fell off. Overall, both models were able to predict the oil production fairly closely to the results given by the BP simulation. The maximum difference in production was only 7%. This can be seen more readily in Figure 6.10 showing the cumulative oil production. The production forecasted by the LGWB model was only 200 m³ more than the BP simulation after 5 cycles. The accuracy for water production was not as good. After the 2nd cycle, the water production kept declining for the LGWB model. On the other hand, the LGTB model produced a considerably more water than the BP simulation (Fig. 6.11). It overestimated water production by 125% in the first cycle and about 60% in the 5th cycle. It should be mentioned that no modification of the relative permeability curves was made for either model. Emphasis was placed on matching the oil production and history-matching parameters were adjusted independently for each model. Because of the higher production in the 1st cycle, the cumulative water production for model LGWB was within a reasonable range of the BP simulation value whereas, model LGTB predicted 60% more total water production. Figure 6.12 displays the cumulative water production for all the models.

The production performance parameters found from these models cannot be accepted for making operational decisions. Close matching of oil production generated good

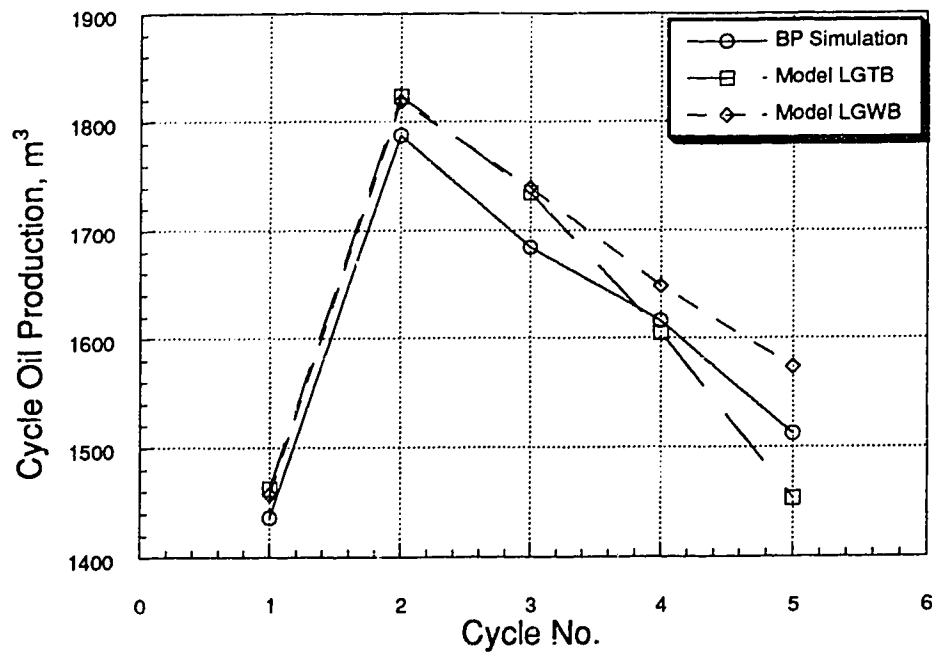


Figure 6.9—Comparison of cycle oil production for fractured wellbore models.

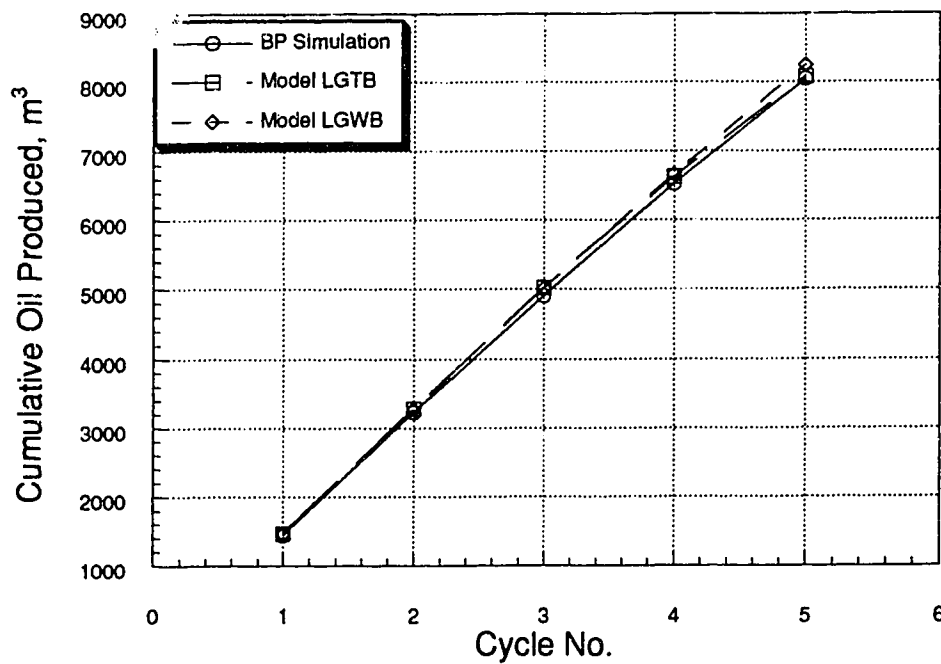


Figure 6.10—Comparison of cumulative oil production for fractured wellbore models.

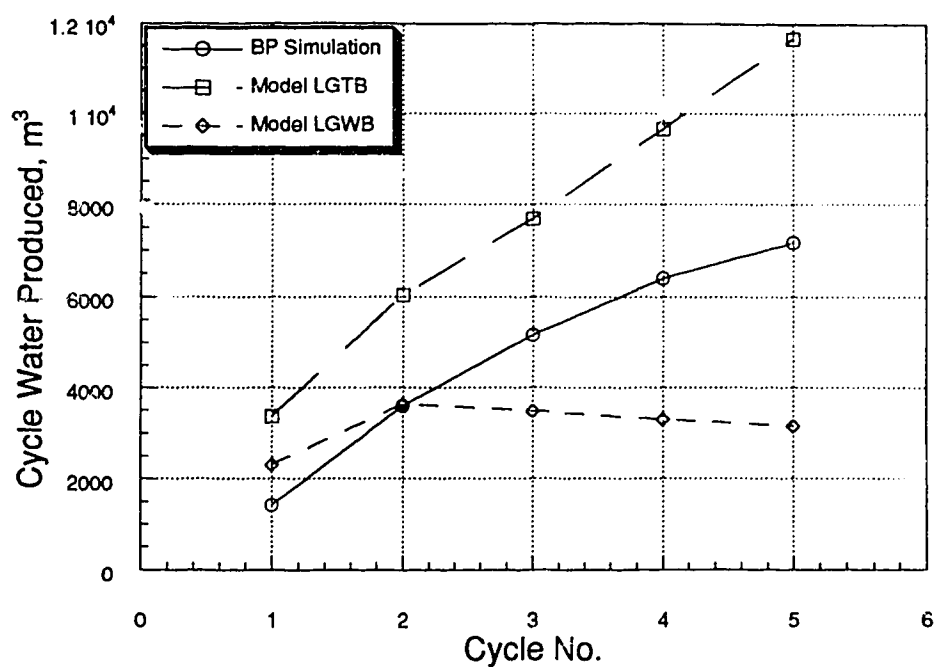


Figure 6.11—Comparison of cycle water production for fractured wellbore models.

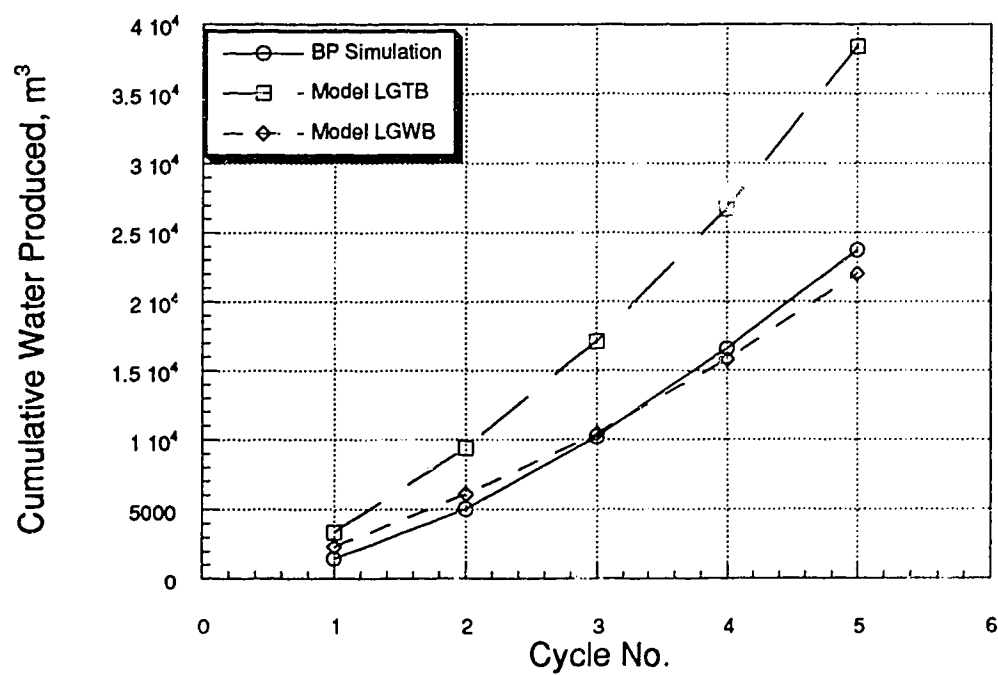


Figure 6.12—Comparison of cumulative water production for fractured wellbore models.

agreement of the related parameters – OSRs (Fig. 6.13) and CDORs (Fig. 6.14) but, the WOR for LGTB was two times higher than the BP simulation due to much higher water production. Interestingly Figure 6.15 shows that LGWB has a constant WOR of 2.0 for all the cycles. The EFW closed-form solution also produced the same WORs. No explanation could be found for such a behaviour.

It is evident from the results that just considering the water balance of the system in calculating saturation does not produce the expected amount of water. The constant value of 2.0 is contrary to the increasing WOR with increasing cycle numbers as reported in almost all field observations as well as in the BP simulation. On the other hand, model LGTB produced from one and a half times to two times more water for each cycle. Both the cumulative water production and the WOR curves look like they have been shifted upward from the BP simulation values. Neither of these saturation calculation schemes meets all the boundary conditions as rigorously as in a numerical simulation. Each model gives approximate values. Moreover, they are also somewhat sensitive to the time step size. More accurate values are found from smaller steps, although larger steps do give acceptable results (detailed analysis is presented in the sensitivity study).

6.3.2 Effect of Temperature on Relative Permeability

Frizzell (1990) did an extensive analysis of 15 years of thermal laboratory data to determine the effect of temperature on relative permeability and the saturation end-points in heavy oil reservoirs. He cited several studies and concluded that the irreducible water saturation increased with increasing temperature. Observing the sub-parallel nature of the WOR curve of model LGTB and the BP simulation in Figure 6.15, intuitively one would conclude that incorporating the effect of temperature on the water end-point saturation would improve the results. Several adjustments were made to include this effect in the relative permeability curve and Figure 6.16 shows the final form of the adjusted relative permeability values. These were not changed or readjusted for the entire project time. A cubic spline interpolation scheme was used to determine the intermediate values.

Results from this experiment are presented in Figure 6.17 through Figure 6.23. Oil production from each cycle is shown in Figure 6.17. It can be observed that a very good match was achieved with the BP simulation. Excellent agreement can also be seen in the cumulative oil production plot (Fig. 6.18). Figure 6.19 shows the cycle water production

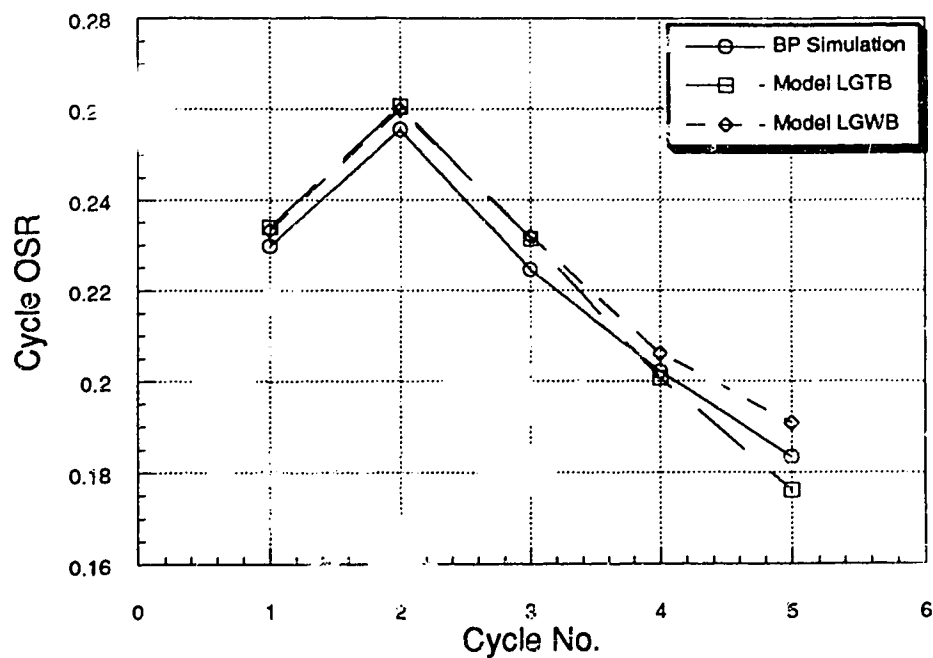


Figure 6.13—Comparison of cycle oil-steam ratio for fractured wellbore models.

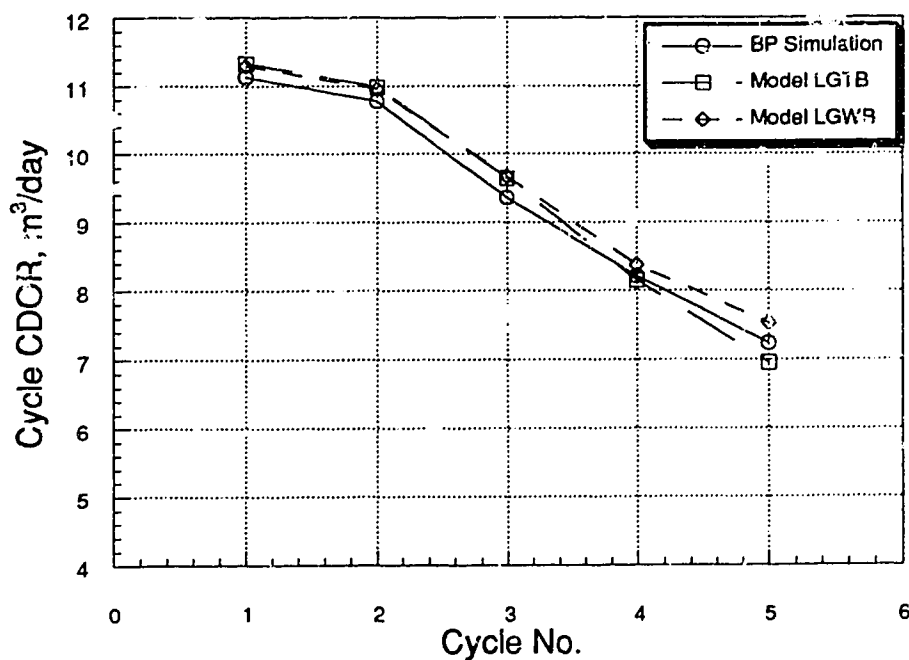


Figure 6.14—Comparison of calendar day oil production rate for fractured wellbore models.

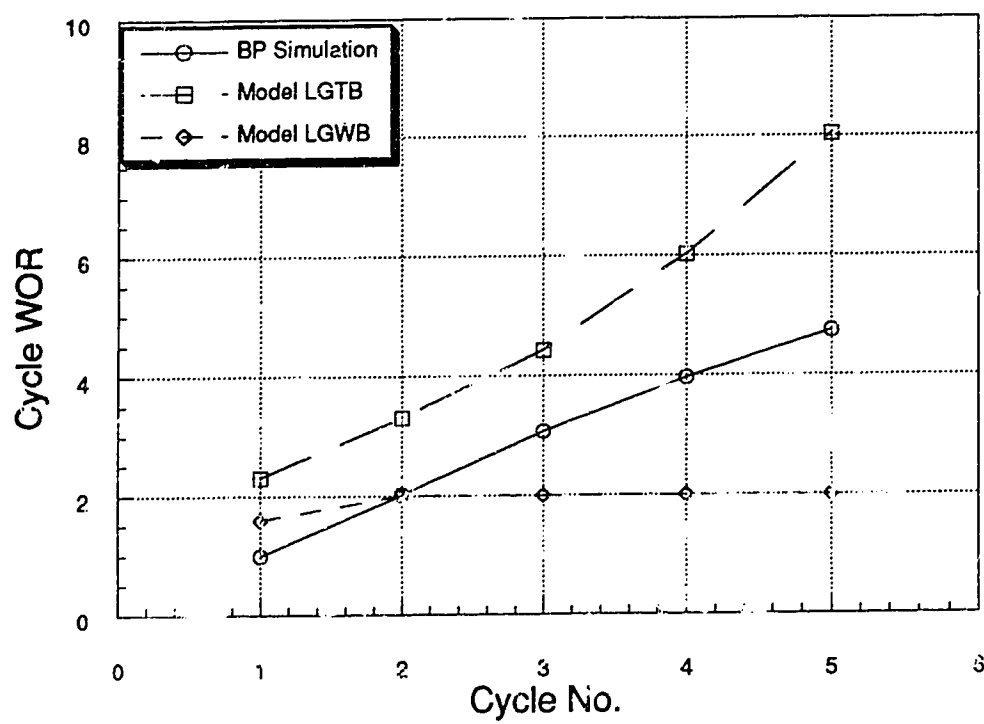


Figure 6.15--Comparison of cycle water-oil ratio for fractured wellbore models.

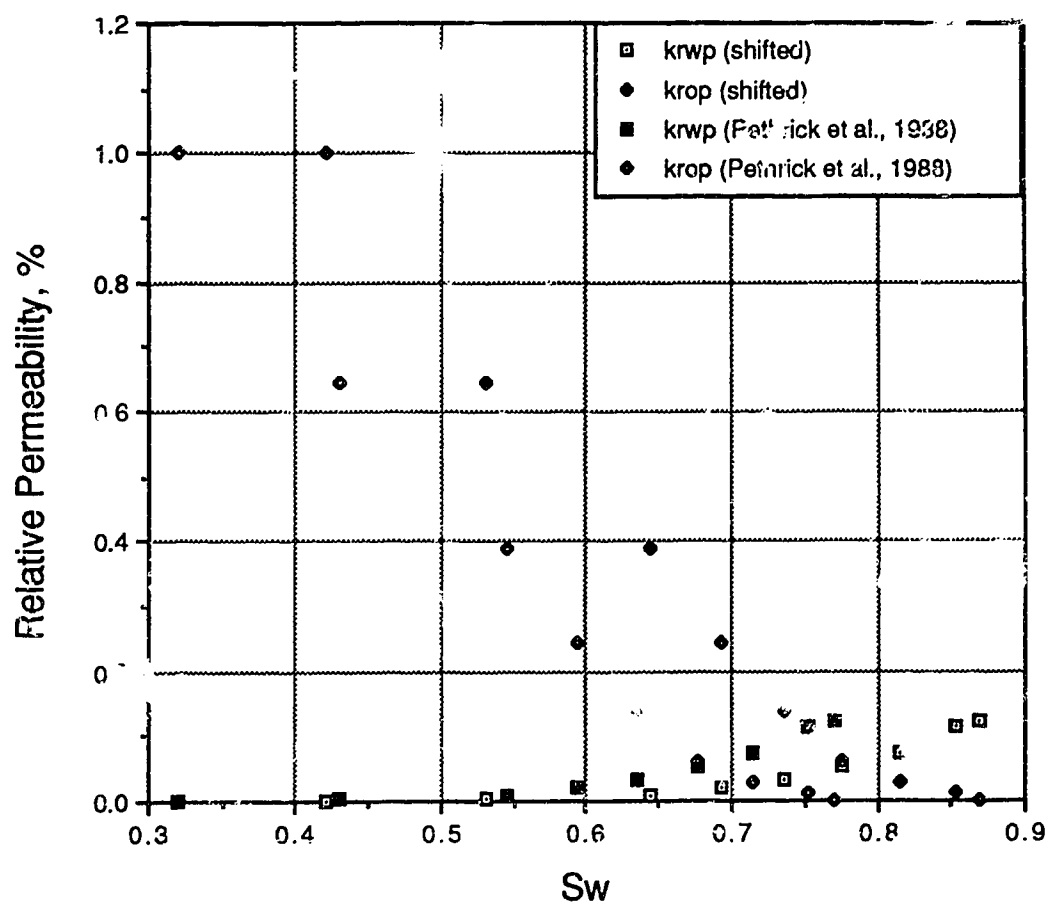


Figure 6.16— Adjusted relative permeability.

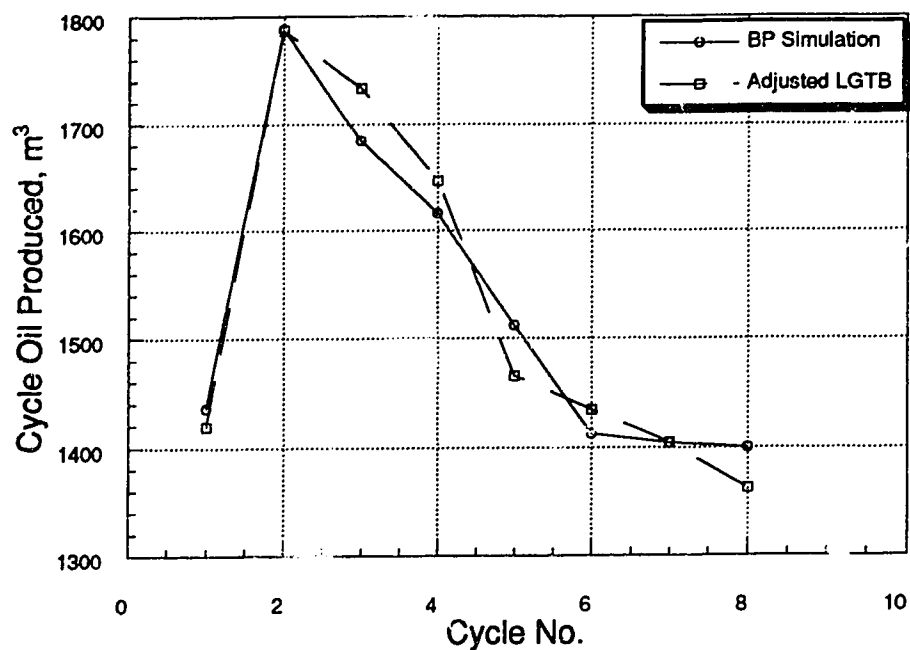


Figure 6.17—Oil production at each cycle for model LGTB, with adjusted relative permeability due to temperature effect.

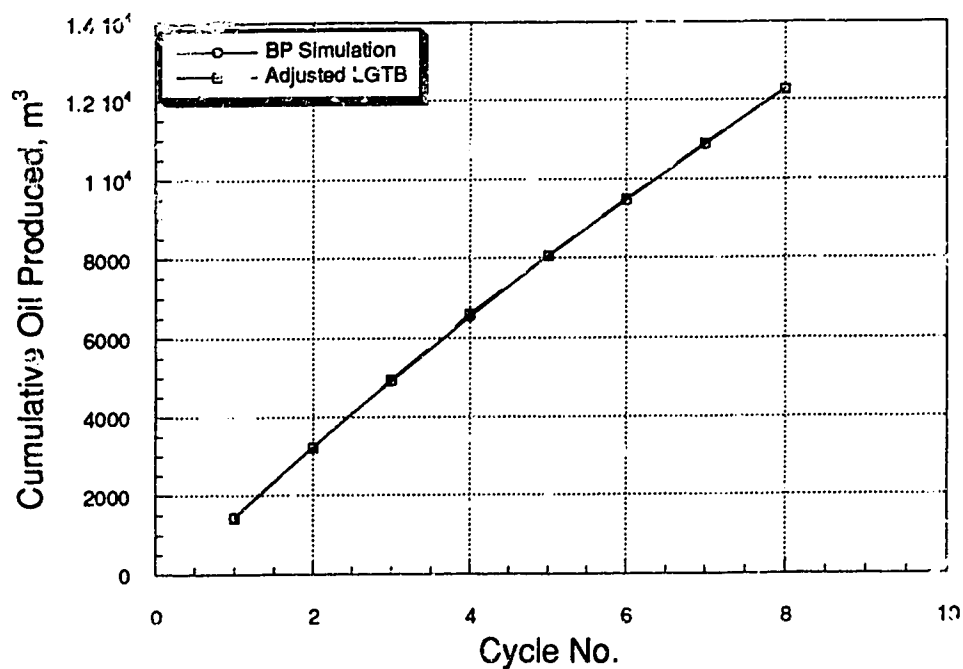


Figure 6.18—Cumulative oil production for model LGTB, with adjusted relative permeability due to temperature effect.

from model LGTB with and without the effect of temperature on the water end point saturation. Improvement of the water production forecast can be seen readily. A fairly good match is achieved up to the 5th cycle. The adjusted LGTB still produced a much larger volume of water for the last three cycles. Such high water production could be due to relative permeability hysteresis. However, it is believed that the hysteresis effect is more pronounced in the early cycles, whereas the water production is higher in the last three cycles. Two possible explanations for later cycle high water production are found in the literature. Vittoratos (1990, 1991) attributed this to the formation of a well defined single phase emulsion flow in which the water content rises with cycle number. Other authors also reported a similar observation (Gallant, Stark and Taylor, 1993). Karyampudi (1995) reported the change of reservoir rock wettability near the wellbore from water-wet to oil-wet, because of exposure to high temperature steam. This causes reduced oil mobility and a higher water cut. Adjustment to the relative permeability curve reduced the cumulative water production by 30% up to the 5th cycle (Fig. 6.20) .

Excellent agreement was achieved for both the OSR (Fig. 6.21) and the CDOR (Fig. 6.22). For the first four cycles, WORs are approximately equal to the actual cycle numbers. Figure 6.23 shows the WOR. Excessively high WORs are seen for cycles 7 and 8. They can be disregarded for any operational or economic analysis. Figure 6.24 shows the oil recovered as a percentage of the original oil in place. At the end of 8 cycles, which is towards the end of the operational life of a well in Cold Lake, 15% of the oil has been recovered. This is close to the average ultimate recovery of 20% in Cold Lake projects (Boone, Gallant and Kry, 1993). Very little oil was produced from the warm zone in all runs.

The overall performance of the adjusted LGTB model was very good. It successfully matched most of the BP simulation results. The first five cycles of this model have been used as a base run for all the sensitivity runs.

6.4 Effect of Viscosity

The most significant parameter for flow calculation in thermal oil recovery processes is the oil viscosity. So far, no one has attempted to calculate an average viscosity based on the actual areal distribution of temperature during production. Results from the two methods of calculating viscosities are presented in this section. In the direct method, the average zone temperature is found from a heat balance equation at each time step and the corresponding

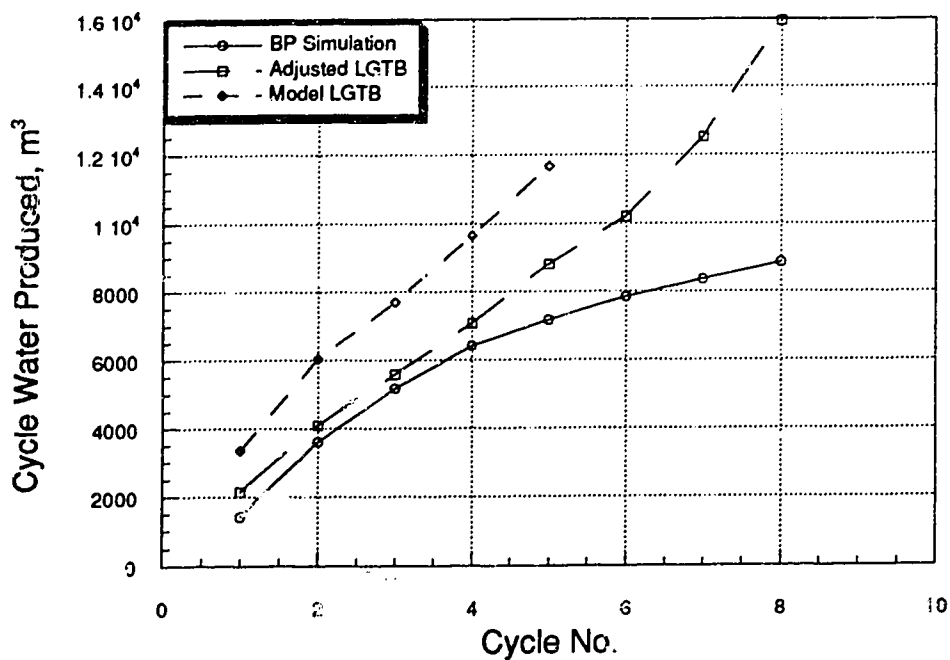


Figure 6.19--Water production at each cycle for model LGTB, with adjusted relative permeability due to temperature effect.

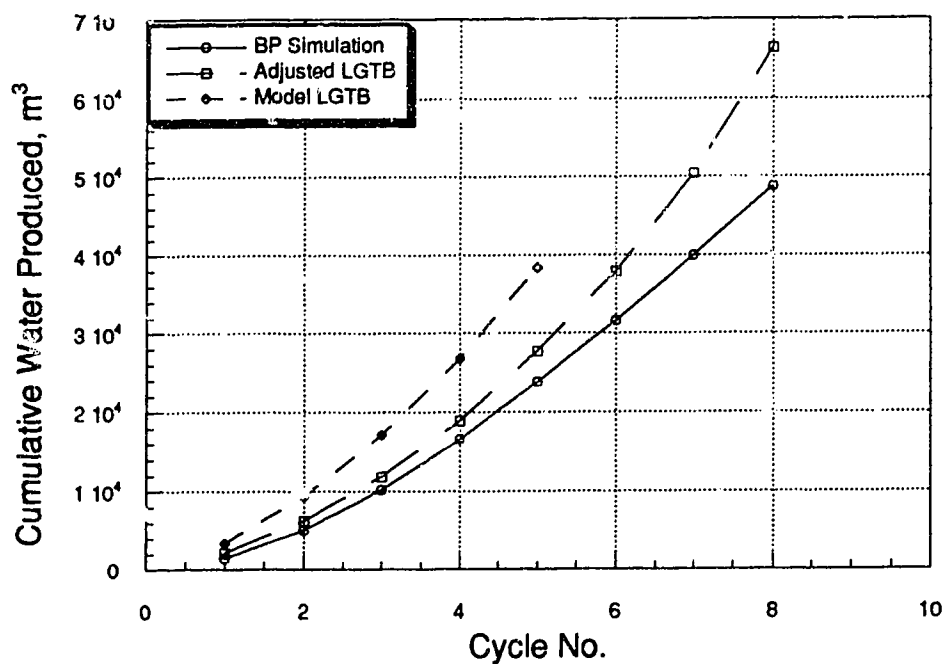


Figure 6.20--Cumulative water production for model LGTB, with adjusted relative permeability due to temperature effect.

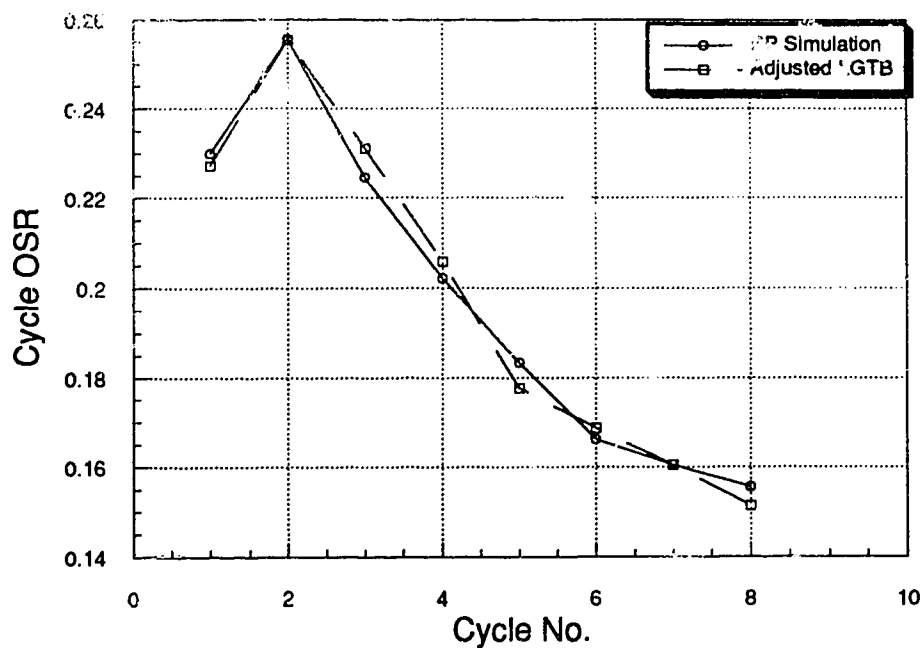


Figure 6.21—Oil-steam ratio for model LGTB, with adjusted relative permeability due to temperature effect.

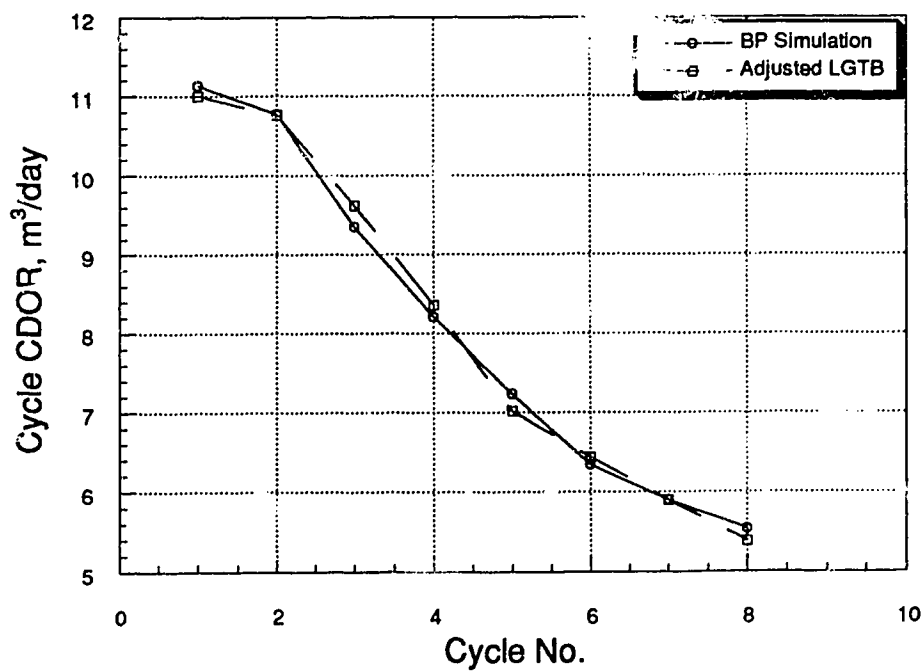


Figure 6.22—Calendar day oil production rate for model LGTB, with adjusted relative permeability due to temperature effect.

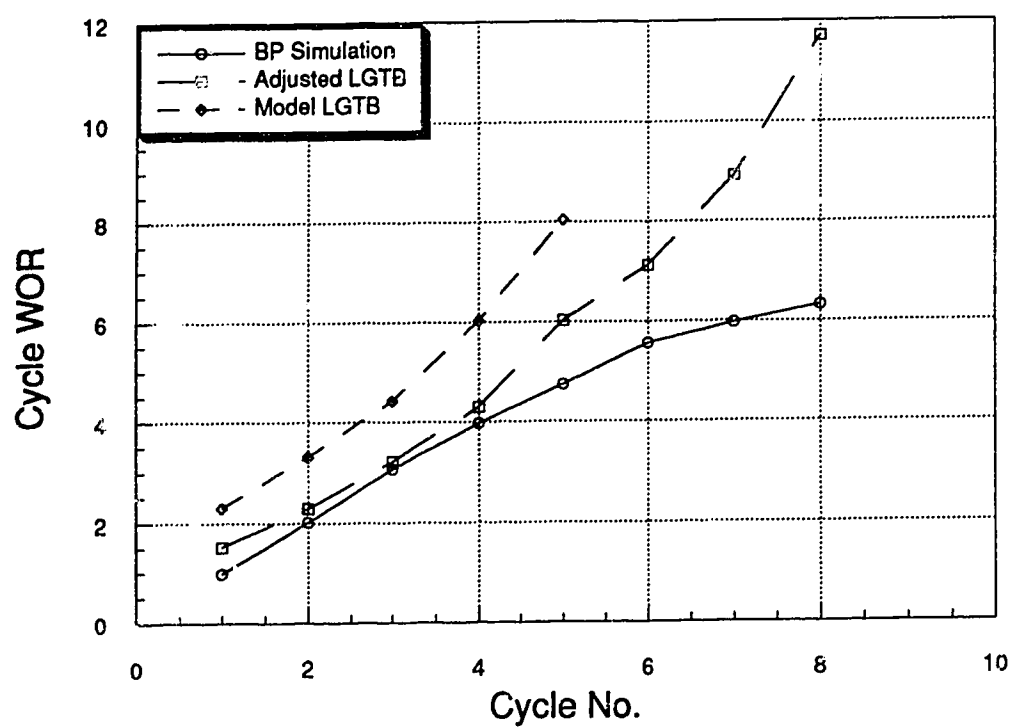


Figure 6.23—Water-oil ratio for model LGTB, with adjusted relative permeability due to temperature effect.

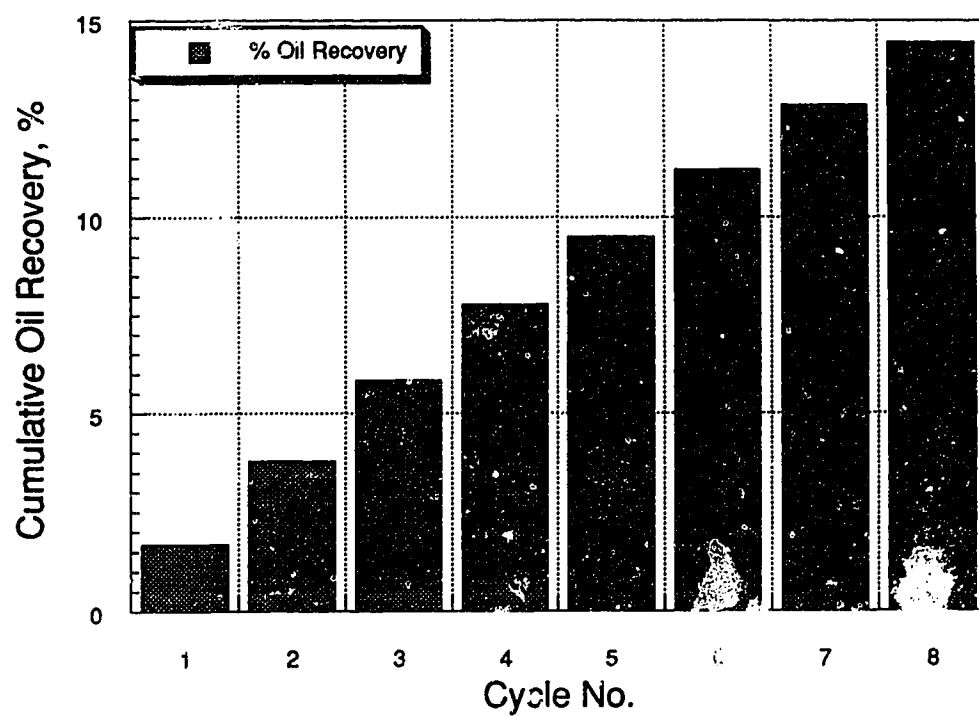


Figure 6.24—Predicted oil recovery as a percentage of original oil in place.

viscosity is calculated from a viscosity-temperature relationship (i.e. $\mu = ae^{b/T}$). The average method uses a viscosity-temperature relationship based on an area weighted temperature distribution for the same average zone temperature. A detailed description of the method is presented in Section 4.8 of Chapter IV.

Average temperatures of both the hot and the cold zones are calculated using Eqn. 4.12. Isotherms are found by increasing the value of the y coordinate (ξ in dimensionless form), which is the perpendicular distance from the fracture face. Increase of ξ is continued until the 100°C isotherm is reached, and then the average hot zone temperature is calculated using the trapezoidal rule. The step size of this incremental distance was varied to check the sensitivity of the average temperature (average viscosity). For the 1st cycle, dimensionless step sizes of 0.02 (0.476 m), 0.01 (0.238 m), 0.008 (0.1904 m) and 0.005 (0.119m) yielded average hot zone temperatures of 190.62°C, 197.49°C, 198.41°C and 199.0°C respectively. When the dimensionless step size of 0.005 needed 17 steps to reach the 100°C isotherm, step size 0.02 needed only 5 steps to reach the same isotherm. Decreasing the step size beyond 0.005 (0.119 m) did not change the average temperature much. The 100°C isotherm varies from 2 m in the 1st cycle to about 5 m in the 8th cycle. Step sizes may gradually be increased with the cycle number without losing accuracy. Slightly higher step size (0.015) may change the cyclic production responses but it would not cause any considerable error in ultimate recovery (less than 5%). Step size of 0.005 has been used for the 1st cycle in the present study.

The oil viscosity calculated by the direct method is much lower than that from the average method. At 134°C the direct method estimates an oil viscosity 6 times lower than the average method. At higher temperatures, this difference is reduced considerably. Figure 6.25 shows the variation of oil viscosities with temperature calculated by both methods. It can be seen that even at 178°C the direct method underestimates the oil viscosity value by 3 times. The reason for this discrepancy is the lack of any provision in the direct method to accommodate the influence of a rapidly decreasing viscosity values towards the hot zone boundary. At higher temperatures, this difference is smaller than at lower temperatures. This is due to the highly non-linear nature of the viscosity-temperature relationship. The average method gives a proper weight to the higher viscosity values near the hot zone boundary in calculating the overall zone viscosity. Clearly, this method produces more accurate and representative results. Because of the almost linear nature of the water viscosity-temperature relationship, differences in the water viscosity remain essentially constant across the temperature range. Figure 6.26 shows only 30% underestimation in the

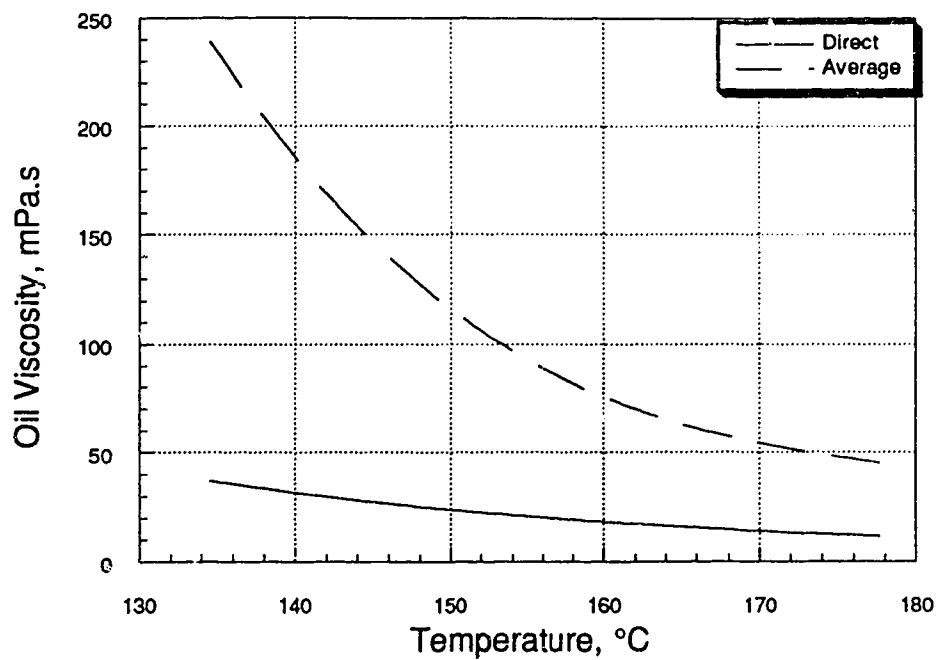


Figure 6.25—Comparison of area weighted average oil viscosity and direct values from the average temperature.

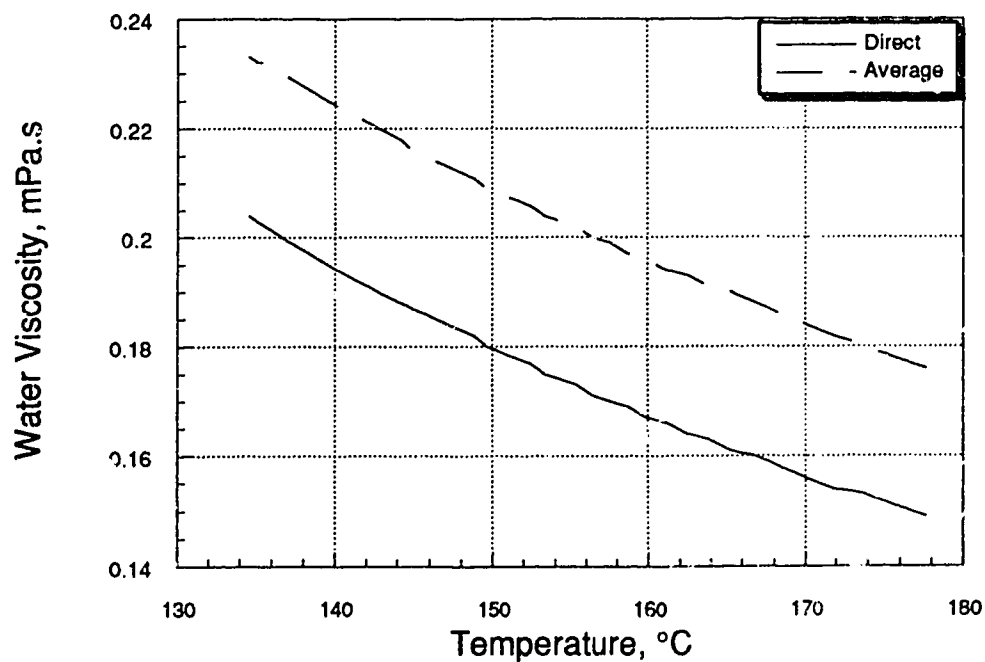


Figure 6.26—Comparison of area weighted average water viscosity and direct values from the average temperatures.

water viscosity calculation by the direct method. This is due to the small variation in water viscosity with change in temperature. The consequence of lower oil viscosity on computation by the direct method can be seen in Figure 6.27 where the cumulative oil production has been plotted against time. After 673 days the direct method produces 3,689 m³ of extra oil which is 45% more than the average method. Most of this oil is produced in the early cycles when the maximum oil is available in the hot zone (Fig. 6.28).

A higher production in early cycles portrays a deceptively high efficiency. Figure 6.29 shows the cycle OSRs for both the methods. For the first two cycles, the direct method shows around two times more oil production for the same amount of steam injected in the average method. The CDORs are also much higher for the first two cycles. Figure 6.30 shows a rate of 30 m³/day for the 1st cycle and 18.5 m³/day for the 2nd cycle. These are considerably higher than the average Cold Lake operation (10.0–12.0 m³/day) reported elsewhere (Farouq Ali, 1994). For high early cycle production, the CDOR fell below the average method value in the 3rd cycle. The effect of the oil viscosity difference is greatest in the first two cycles. Consequently, much less water was produced by the direct method during these two cycles. The WOR jumped from 2.5 in the 2nd cycle to 5.5 in the 3rd cycle. A lower water viscosity computed by the direct method aggravated the situation further which is seen in Figure 6.31.

The results and analysis presented above clearly show that the conventional direct method of oil/water viscosity calculation produces inaccurate and misleading results. Because of the extremely important role played by the oil viscosity in flow calculation, utmost care should be taken to estimate its value correctly.

6.5 Conduction Between the Two Zones

In the analytical models, most authors (Boberg and Lantz, 1966; Jones, 1977; Gontijo and Mac, 1984; Sylvester and Chen, 1988) used a single heated zone around the wellbore. The temperature in the heated zone at the end of the injection period was assumed to be the saturated steam temperature. The temperature beyond the heated zone was assumed to be the initial reservoir temperature. This problem was then solved in both the vertical and the radial directions as a hot body initially at a constant temperature cooling in an infinite medium through conductive heat transfer only. In warmer reservoirs, the step function temperature profile may not contribute any error beyond the uncertainty of the reservoir input data. For Canadian heavy oil reservoirs, where the initial formation

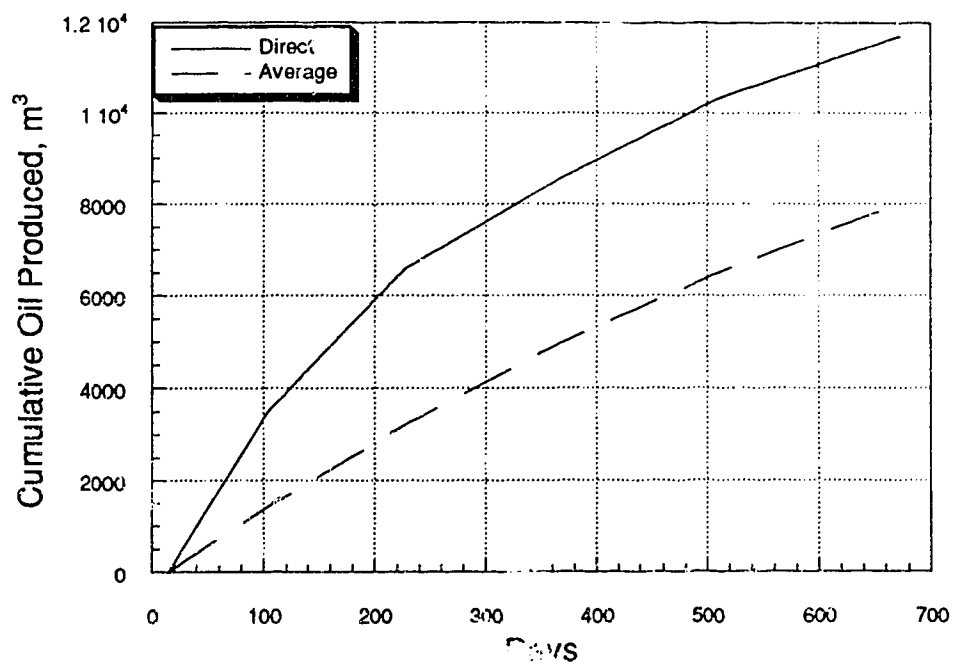


Figure 6.2.—Effect of different methods of oil viscosity calculation on cumulative oil production.

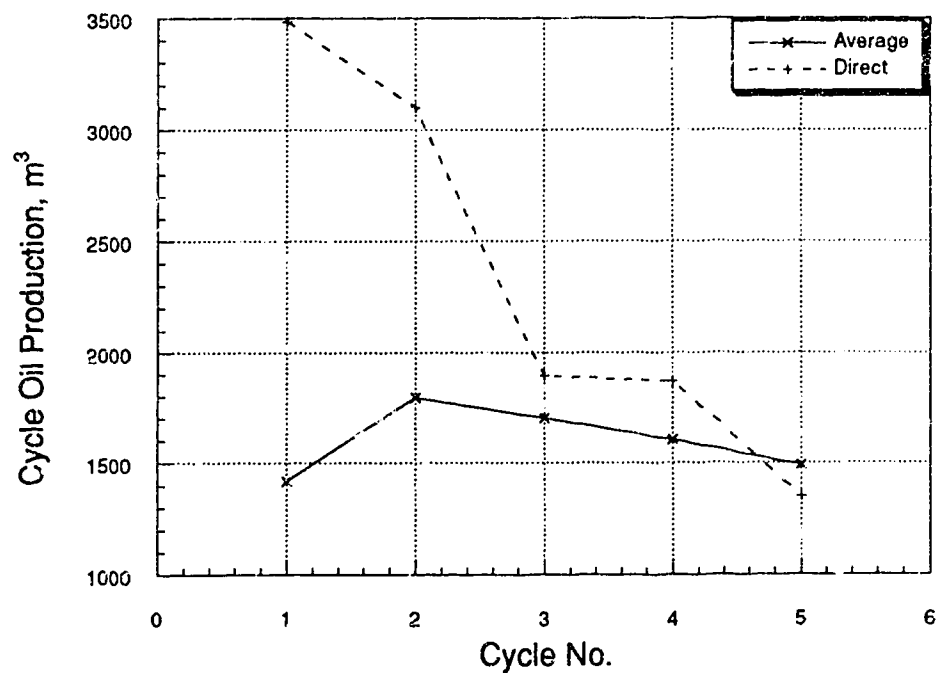


Figure 6.28—Effect of calculating oil viscosity without areal average temperature on oil produced at each cycle.

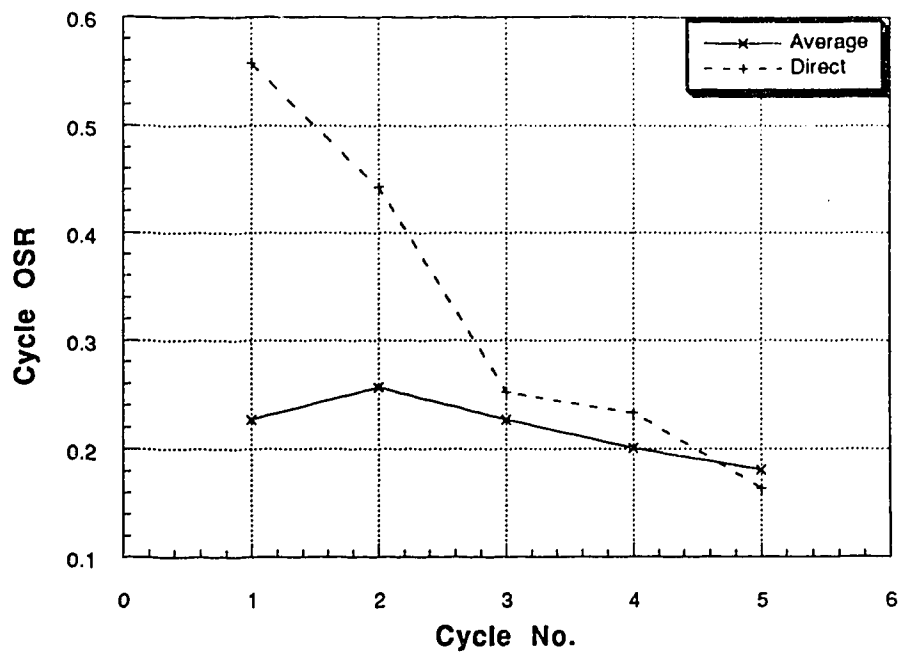


Figure 6.29—Effect of calculating oil viscosity without areal average on cycle oil-steam ratios.

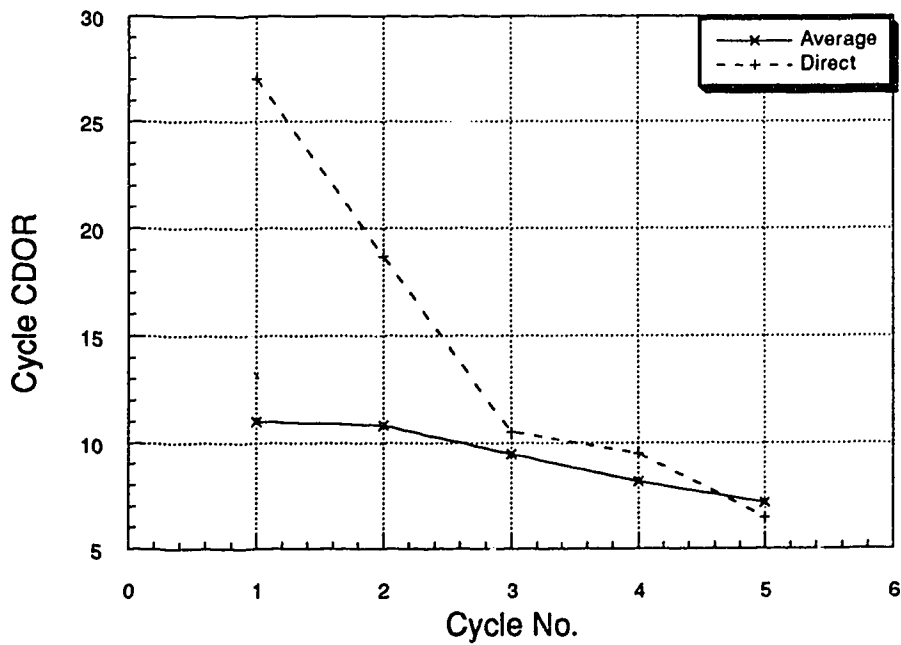


Figure 6.30—Effect of calculating oil viscosity without areal average on cycle calendar day oil rates.

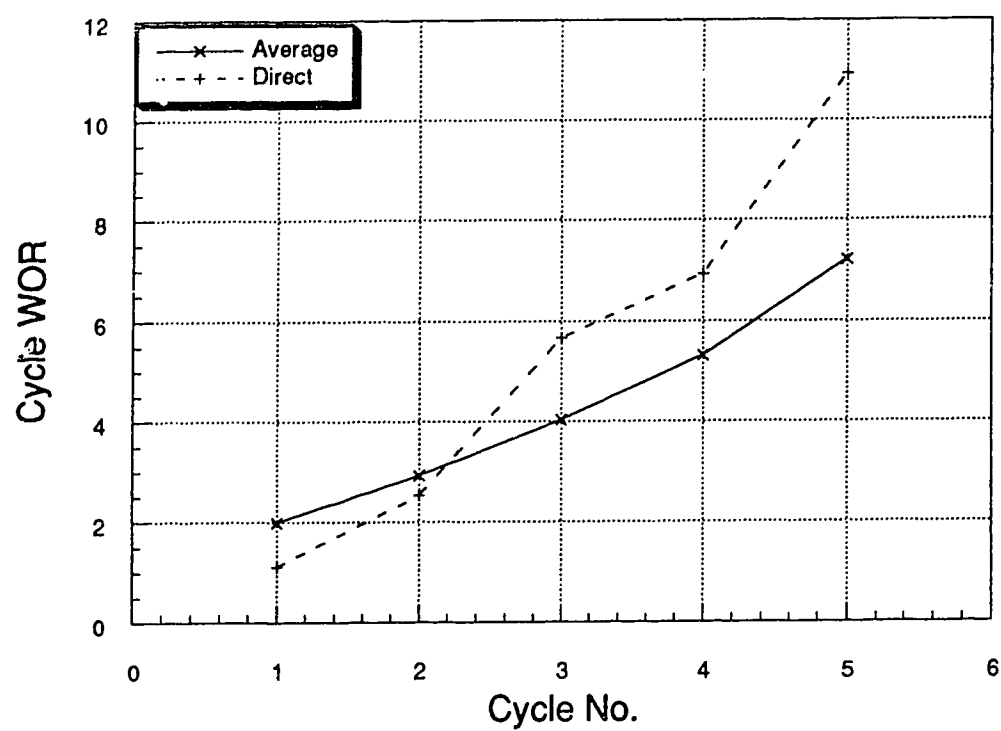


Figure 6.31—Effect of calculating oil viscosity without areal average on cycle water-oil ratios.

temperature varies between 13°C and 18°C and the typical steam injection temperature is about 300°C, a step function temperature profile at the hot zone boundary would create considerable error in the heat loss calculation. One way to overcome this problem is to create a warm buffer zone between the hot zone and the cold outside zone. Seba and Perry (1969) took a similar approach for a radial model and considered average temperature changes in a smaller cold zone as opposed to an infinite radius. They maintained the hot zone temperature at the saturated steam temperature for the entire project time. Obviously, this would predict a highly optimistic oil production for most cases. Arthur *et al.* (1991) took the right approach in considering a hot and a warm zone in their heat calculation of an elliptical drainage system. The rate of heat loss from the inner hot zone during soak is very high. As there is no fluid flow during soak, the only mode of heat transfer is conduction. The contribution of conduction during the early stage of production between the two zones is also quite significant. Arthur *et al.* (1991) ignored this important aspect of the heat balance and considered only convective heat transfer between the hot zone and the warm zone. Heat loss to the over- and underburden was through conduction only. A new set of equations including conduction between the two zones was developed (Appendix D) in the current study. The importance of the conduction term is presented in this section.

Figure 6.32 shows a comparison of the average hot zone temperature profiles of three cycles during production. It can be seen that the temperature at the beginning of production is higher for no conduction heat loss to the warm zone at each cycle. The curves are flatter too. On average, the difference in temperatures for the two cases through the entire production period is more than 20°C. Due to the higher temperatures calculated, the model with no heat conduction between the two zones produced 27% more oil (Fig. 6.33). Most of this oil was produced in the first two cycles when the effective conductive heat transfer between the two zones was at a maximum. Figure 6.34 shows a sharp drop in cycle oil production after the 2nd cycle. The cumulative water production was also 27% higher in the no conduction model after 673 days of production (Fig. 6.35).

Favourable OSRs (Fig. 6.36) and CDORs (Fig. 6.37) are predicted as a consequence of the higher average temperature in the hot zone. The effect of excluding the conduction term on WORs is not as acute. The effect of high oil production in the first two cycles kept the water production somewhat lower and a moderate jump in WOR can be observed after the 2nd cycle. Figure 6.38 shows the changes in WORs for both cases.

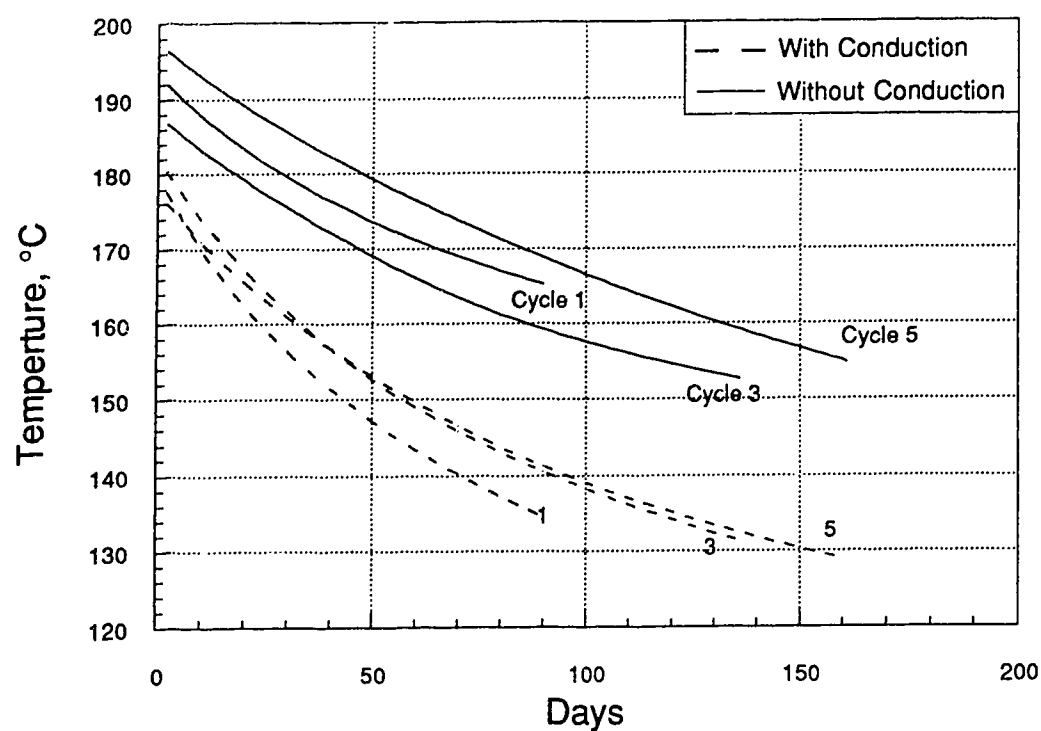


Figure 6.32—Effect of conduction heat loss on average hot zone temperature.

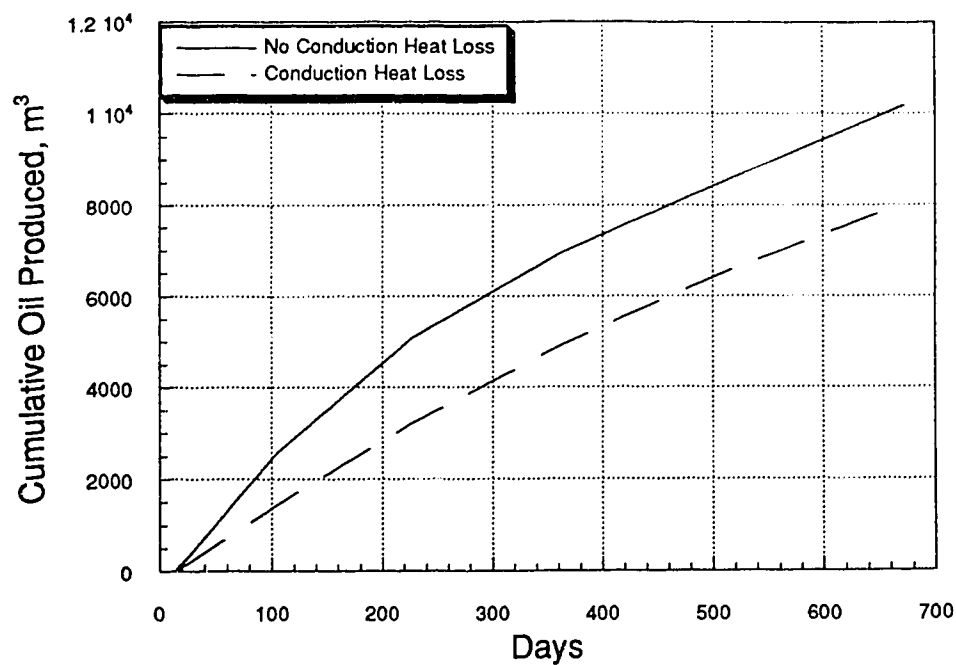


Figure 6.33—Effect of conduction heat loss from the hot zone to the warm zone on cumulative oil production.

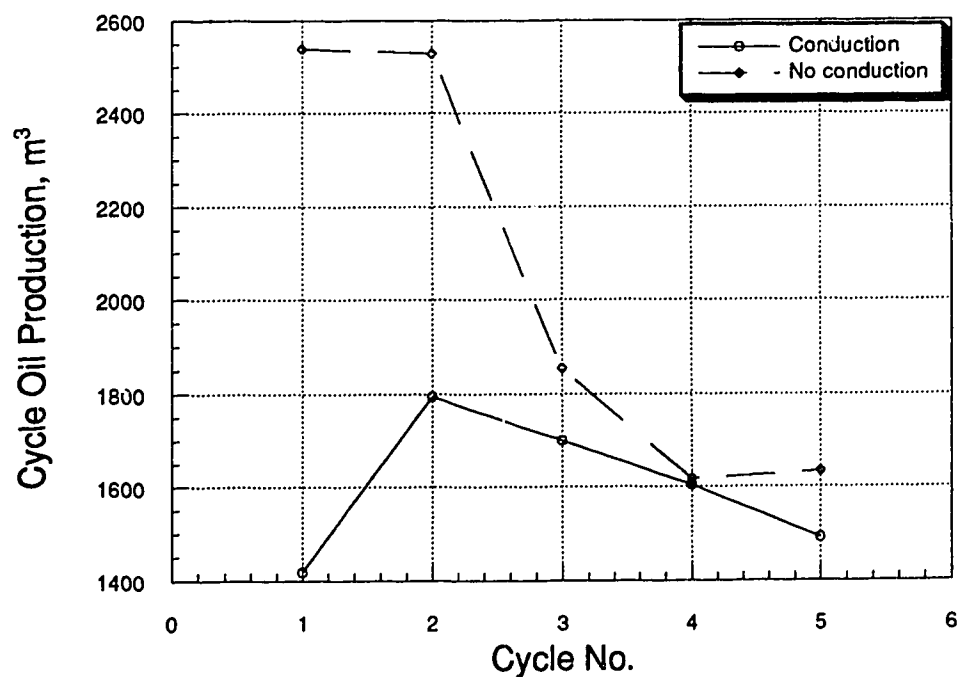


Figure 6.34—Effect of conduction heat loss from the hot zone to the warm zone on cycle oil production.

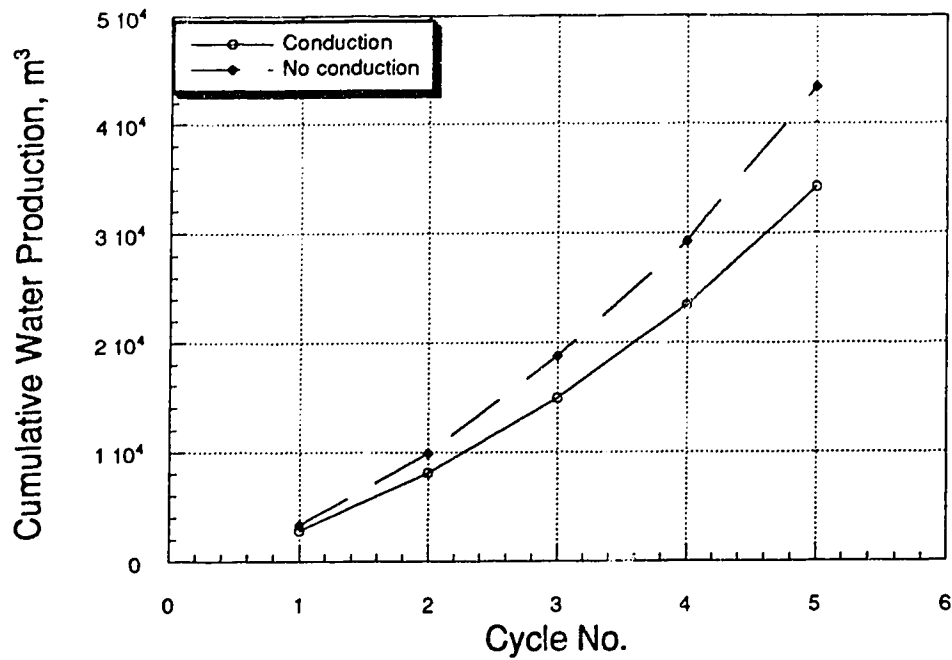


Figure 6.35—Effect of conduction heat loss from the hot zone to the warm zone on cumulative water production.

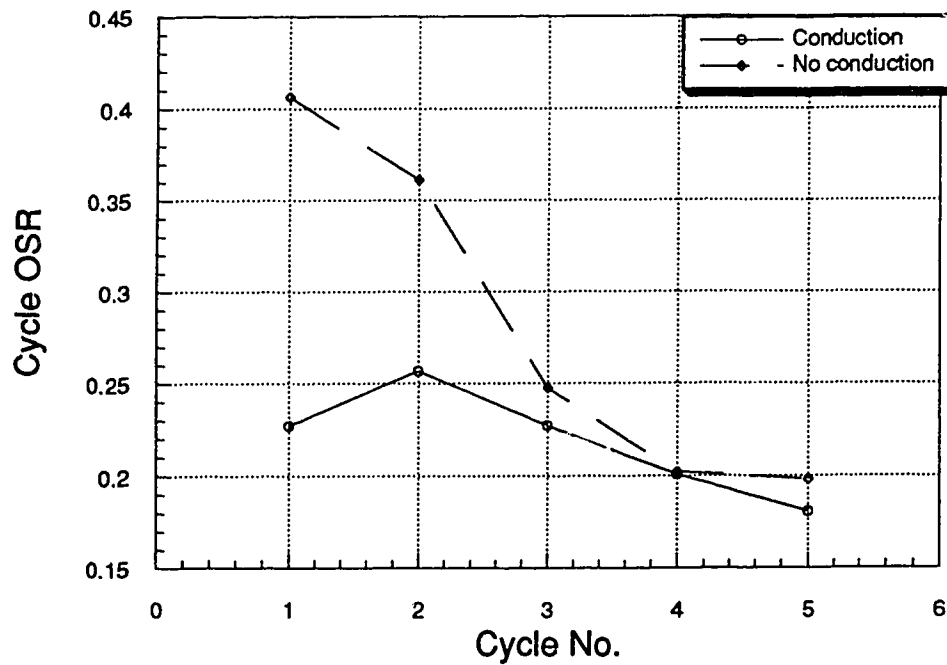


Figure 6.36—Effect of conduction heat loss from the hot zone to the warm zone on cycle oil-steam ratios.

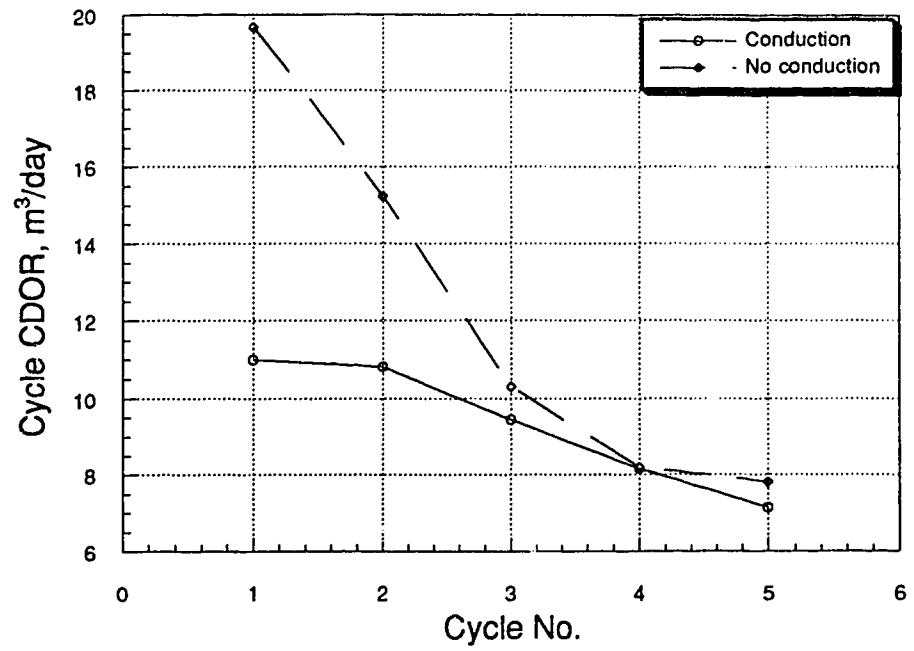


Figure 6.37—Effect of conduction heat loss from the hot zone to the warm zone on cycle calendar day oil rates.

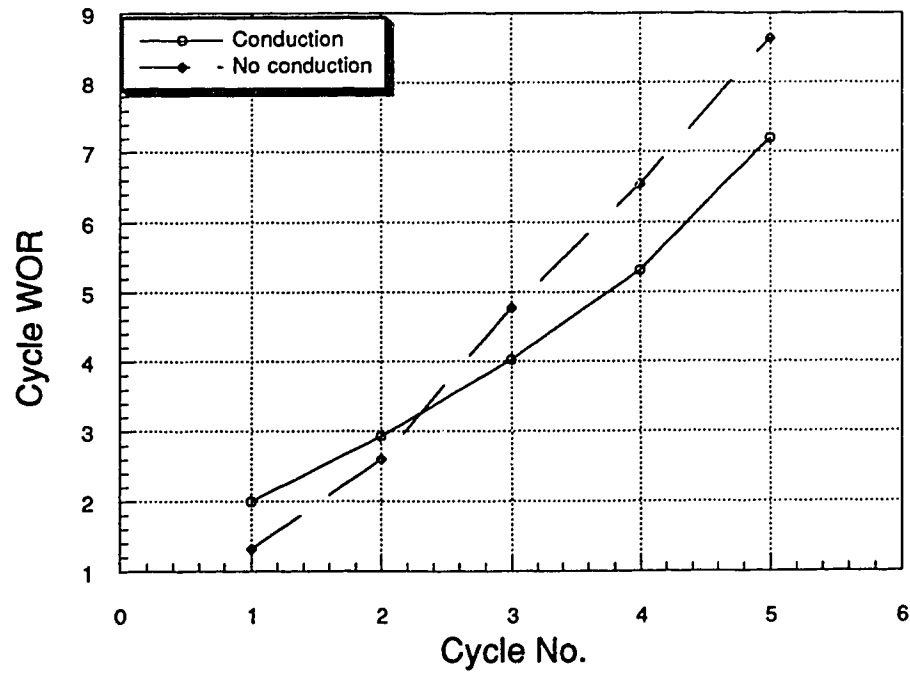


Figure 6.38—Effect of conduction heat loss from the hot zone to the warm zone on cycle water-oil ratios.

Tables 6.4 and 6.5 show the changes in the hot zone average temperature during the soak period with and without conduction heat loss, respectively. In Table 6.5 we can see that the hot zone average temperature dropped about 5 to 7°C during the 15 day soak period in all cycles. The heat loss was only to the over- and underburden through conduction. The warm zone, which is a large area, did not gain any heat from the hot zone during this period and the average temperature dropped from 1 to 4°C due to heat loss to the over- and underburden. When the conduction term is included in the heat balance, there is a significant temperature drop in the hot zone during soak. Table 6.4 shows a 21°C average temperature drop in the 1st cycle and a drop of 12°C in the 5th cycle. Although the initial temperature before soak is around 190°C, the heat transfer rate decreases with increasing cycle number due to the inclusion of the total project time in the heat loss equation. This has been discussed in Chapter IV. The warm zone average temperature increased by 6°C in the 1st cycle and 2.5°C in the 5th cycle. Considering the large volume of the warm zone, this indicates significant heat gain during the soak period. This temperature increase did not enhance the flow rate from the warm zone, because the highest temperature is only 33.8°C, but heat losses from the hot zone reduced the flow rate considerably from that zone.

6.5.1 Relative Error Compared to Erroneous Viscosity Calculation

The exclusion of conductive heat transfer between the hot and the cold zone produced 27% more cumulative oil after 673 days of production. The effect of the “Direct” method of calculating average viscosity on oil production is more severe. The lower values of oil viscosity, calculated by this method, produced about 46% more total oil than predicted by the BP simulation during the same production time. This shows relatively the more importance of proper evaluation technique of viscosity; which is, in fact, the most important parameter in thermal recovery flow calculations.

6.6 Sensitivity Study

Although the new model successfully matched the BP numerical simulation results, a sensitivity analysis has been made to determine the limitations of the model. Both physical

Table 6.4 —Average temperature change (°C) during soak with conduction.

	Cycle No.	1	2	3	4	5
Hot Zone	Soak (Beg.)	198.31	191.89	196.02	190.45	188.59
	Soak (End)	177.67	175.2	180.31	177.23	176.12
Warm Zone	Soak (Beg.)	27.93	26.92	27.73	26.50	25.91
	Soak (End)	33.88	31.05	31.05	29.37	28.46

Table 6.5—Average temperature change (°C) during soak without conduction.

	Cycle No.	1	2	3	4	5
Hot Zone	Soak (Beg.)	198.31	189.95	192.6	185.66	202.26
	Soak (End)	191.98	184.1	186.85	180.25	196.45
Warm Zone	Soak (Beg.)	27.93	26.21	26.96	25.5	28.17
	Soak (End)	27.01	25.40	26.12	24.11	24.71

and operational parameters are selected for examination. The first five cycles of the adjusted LGTB model are used as a base case to measure sensitivity against.

6.6.1 Hot Zone Boundary Temperature

The hot zone boundary temperature was selected to be 100°C. Pethrick *et al.* (1988) argued that at that temperature, heavy oil in the Marguerite Lake had a satisfactorily high mobility. The choice of this temperature is quite arbitrary. One has to look at the relative permeability, absolute permeability of the reservoir and oil viscosity-temperature relationship to decide upon a boundary temperature for a given reservoir. Even then one can argue about the validity of such a decision.

Accordingly, the base run hot zone boundary temperature was fixed at 100°C. Four different temperatures – 80°C, 90°C, 110°C and 120°C – were studied to see the effect of the variation of temperature. Figure 6.39 depicts the cycle oil production for each case. Lower temperature settings (80°C, 90°C) produced much less oil in the early cycles than the base case, but picked up production in the later cycles. This is expected as the hot zone gradually gets heated with increasing cycle number. On the other hand, higher temperature settings (110°C, 120°C) consistently produced more oil in each cycle, with decreasing production at later cycles. In the case of 110°C there was an unexpected jump in production in the 4th cycle. This could be the result of a combination of saturation and average temperature calculation at the end of the 3rd cycle. The overall project performance can be seen from the cumulative oil production diagram (Figure 6.40). Total oil production from the 80°C setting was considerably lower than the base run. A setting of 90°C produced 8% less oil than the base case; the 110°C setting produced 9% more oil (748 m³) than the base run. A further increase of the hot zone boundary temperature (120°C) produced only a nominal increase in cumulative oil (1%) at the end of 5 cycles. From the general trends of the curves it can be said that any temperature setting between 90°C and 120°C of the hot zone boundary would give very similar ultimate recoveries. The difference in the performances would be in the early cycle production. A temperature of 100°C seems to be a balanced choice for this particular case. Figure 6.41 shows the water produced at each cycle. A steady increase of water production can be seen with increase of the boundary temperature. Incremental total production of 3,000 m³ can be seen with each increase of temperature up to 110°C. Additional production is about 1,800 m³ for the 120°C setting. These results are shown in Figure 6.42.

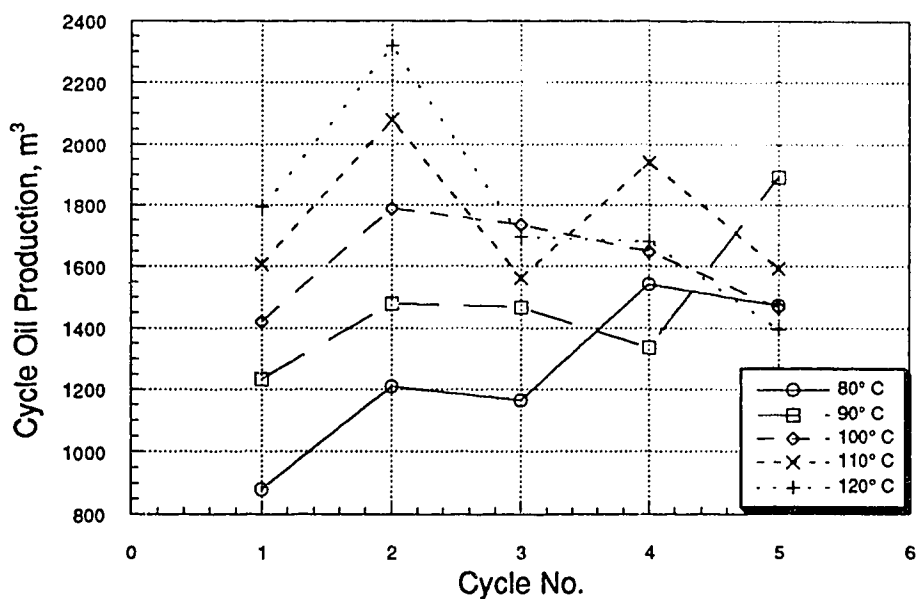


Figure 6.39—Oil produced at each cycle for various hot zone boundary temperature values.

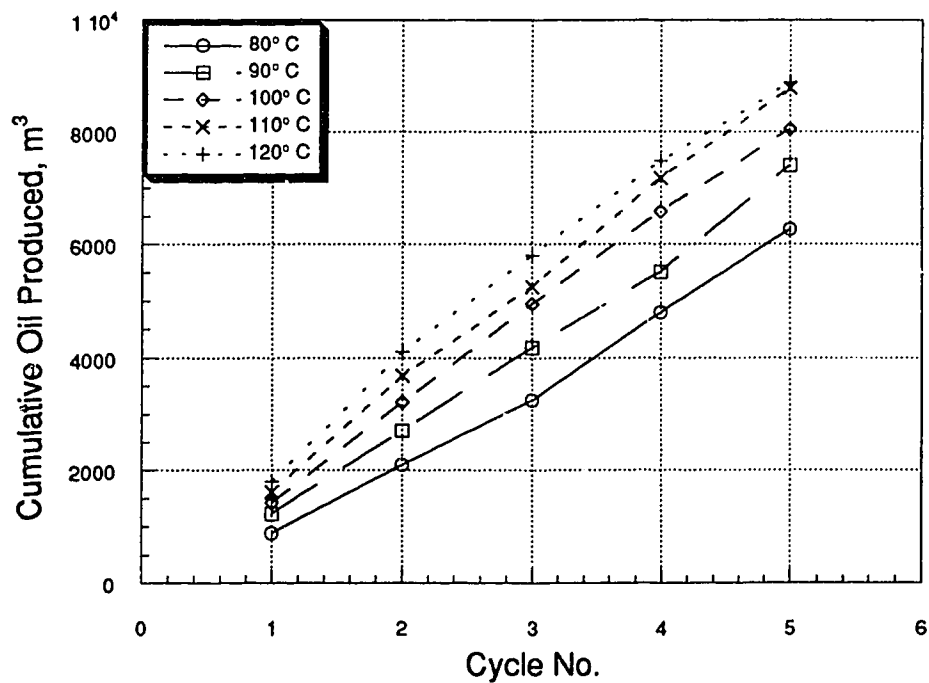


Figure 6.40—Cumulative oil production for various hot zone boundary values.

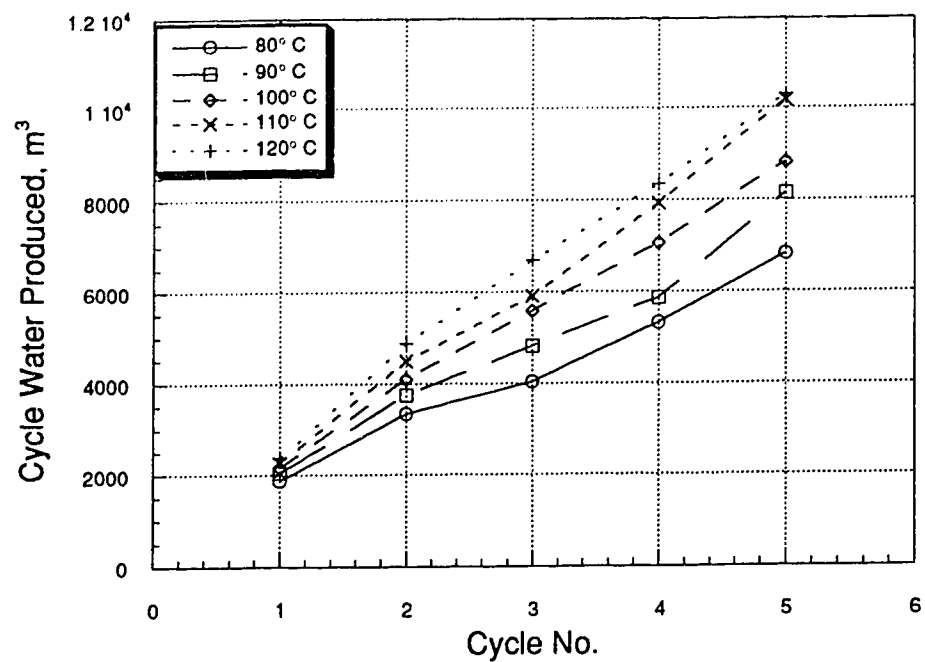


Figure 6.41—Water production at each cycle for different hot zone boundary values.

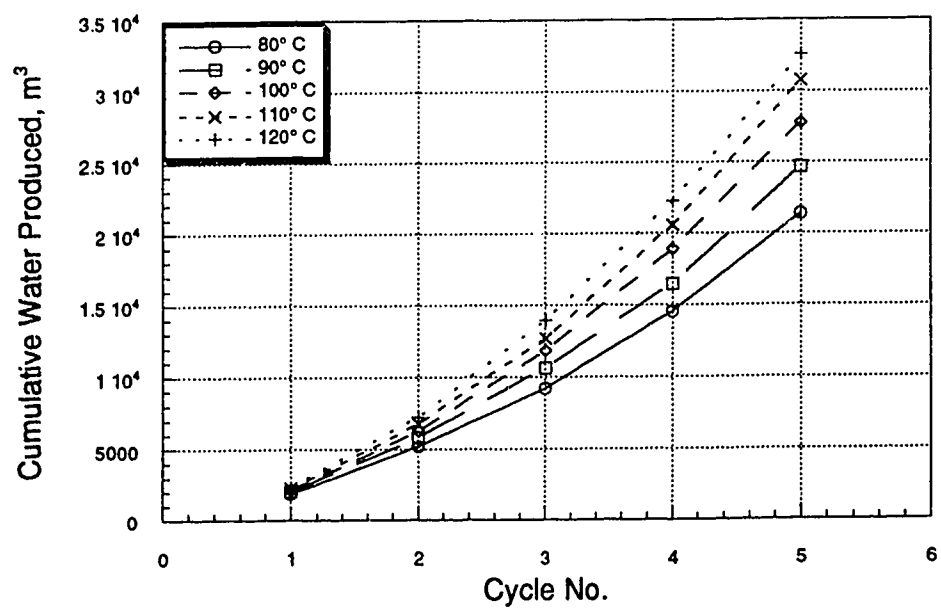


Figure 6.42—Cumulative water production for various hot zone boundary temperature values.

Without going into individual analysis of the performance parameters for each case, the general trends are discussed here. The lower temperature cases have better OSRs in the later cycles. The OSRs in the first two cycles increase steadily with increasing boundary temperature (Fig. 6.43). A similar trend can also be seen in the CDORs (Fig. 6.44). Water cuts are much higher in the first two cycles for the lower temperature settings. Figure 6.45 shows the WORs. It can be concluded that the benefits in the early cycles for a higher temperature setting are traded off with lower efficiency in the later cycles. With an 8 to 9 percent difference in total oil production at the end of 5 cycles, the sensitivity of the model to the setting of hot zone boundary temperature is very little, provided the temperature is not set lower than 100°C.

6.6.2 Soak Time

A soak period is unavoidable in the field because of the time needed to change the well from the injection phase to the production phase. Different authors have expressed contradictory opinions about the benefit of a soak period. Chen (1987) suggested a minimum possible soak period for the best oil production. Niko and Troost (1971) experimentally found that the oil production was insensitive to soak time. Treballe, De Paz and Martinez (1993) also found that soak time had very little influence on recovery. With the help of a three-dimensional numerical simulation they varied the soak time from 15 to 360 days and concluded that an inactive well did not compensate for the deferred production. Ferrer and Farouq Ali (1977) observed that soaking produced more oil for a high viscosity oil compared to the no-soak condition, whereas the situation was reversed for a lower viscosity oil. Resistance to the flow of oil because of water and steam saturation around the wellbore outweighed the benefit of viscosity reduction in the latter case. On the other hand, field data and numerical simulations have shown the benefit of an optimum soak period. Optimum soak period theory is based on the assumption that all of the steam does not condense right after the injection period. A few days are needed for the steam to condense and transfer its latent heat to the reservoir. On the other hand, this period cannot be too long. Otherwise too much heat would be lost to the over- and underburden. Adams and Khan (1969) reported an optimum period of 9 days in a California reservoir.

The present model assumes immediate condensation of the steam after the injection period and does not account for any steam distillation. In a cold heavy oil reservoir, this

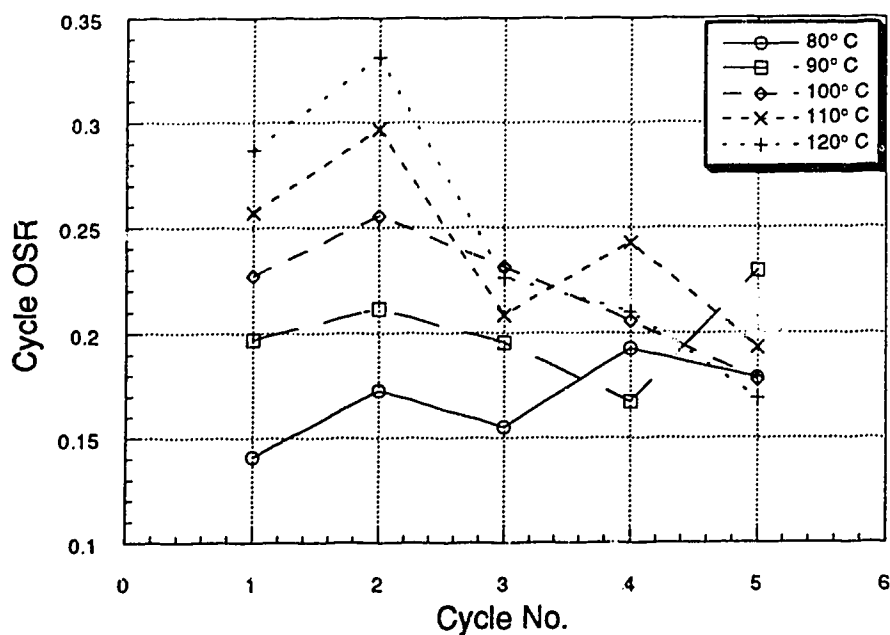


Figure 6.43—Oil-steam ratio at each cycle for various hot zone boundary values.

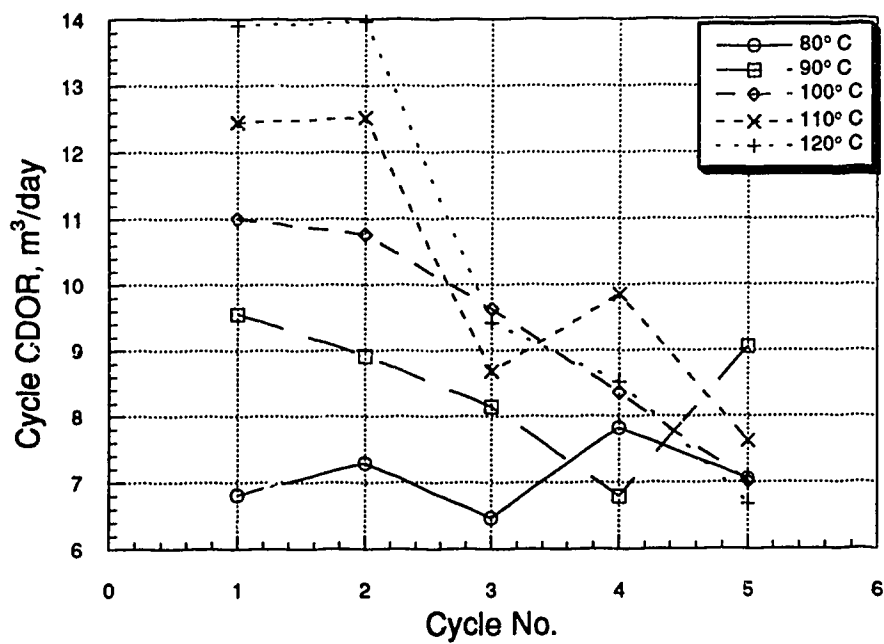


Figure 6.44—Calendar day oil production rate at each cycle for various hot zone boundary values.

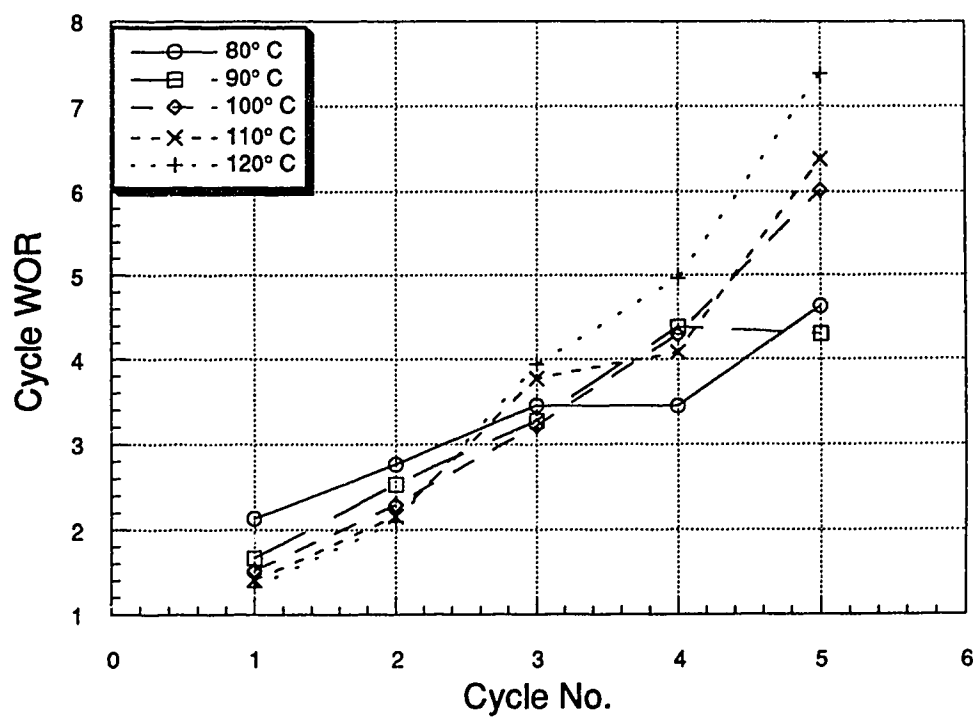


Figure 6.45—Water-oil ratio at each cycle for various hot zone boundary values.

would not be too unrealistic. Different soak periods between 0 to 18 days were considered. As shown in Figure 6.46, cycle oil production steadily decreased with an increase of soak time up to the 2nd cycle. After the 3rd cycle, higher soak periods (15, 18 days) produced a little more oil than the lower soak times (5, 9 days). This is due to more available oil and late heating of the formation. A better picture of the performances can be seen in Figure 6.47 where cumulative oil productions are displayed. A no-soak time produced the highest amount of oil at the end of 5 cycles. This is expected with the assumptions made for the model. Total oil production always declined with the increase of soak time but for a wide variation of soak period between 5 to 18 days the decrease was only about 5%. Except for the no-soak line, all the other curves in both cycle (Fig. 6.48) and cumulative (Fig. 6.49) water production diagrams clustered together to see any significant difference between them. Although these results suggest better performance with a shorter soak time, loss of recovery does not increase significantly with a longer soak period beyond 5 days. To prevent loss of production due to shut-in, a soak period between 0 to 5 days seems to be the best strategy. Remembering the limitation of this model mentioned earlier, caution should be taken in using this model to establish soak periods in any CSS operation.

6.6.3 Increasing Steam Volume

Several experiments were done with the steam injection strategy. The first of these tests was increasing the steam injection volume. Injection periods for each cycle were kept constant for all the tests. The injection rate was varied from 150 m³/day (cold water equivalent, CWE) of steam to 400 m³/day. Figure 6.50 shows a steady and uniform increase in oil production at each cycle. This was due to increased heat input into the reservoir. For each m³/day (CWE) increase in steam injection, about 5 m³ of incremental oil was produced in the 1st cycle. Incremental oil production per cubic meter of CWE decreased with an increasing amount of steam injection. An increase of injection rate from 150 m³/day to 200 m³/day for a total of 148 days of injection time over the 5 cycle period, produced 32.3 m³ of incremental oil per m³/day rate increase. For the same operation period, the incremental oil was 27.5 m³ per m³/day for a rate increase from 300 m³/day to 400 m³/day. Cumulative oil production for each case is shown in Fig. 6.51. The diminishing return with increasing steam injection rate was also observed by Martin (1967) and Davidson *et al.* (1967). In a steamflood study, Hong (1994) observed a similar trend. Boone *et al.* (1993) suggested a strategy of massive steam injection (over 2,000 m³) for short periods (hours) as opposed to a constant lower injection rate for longer period to

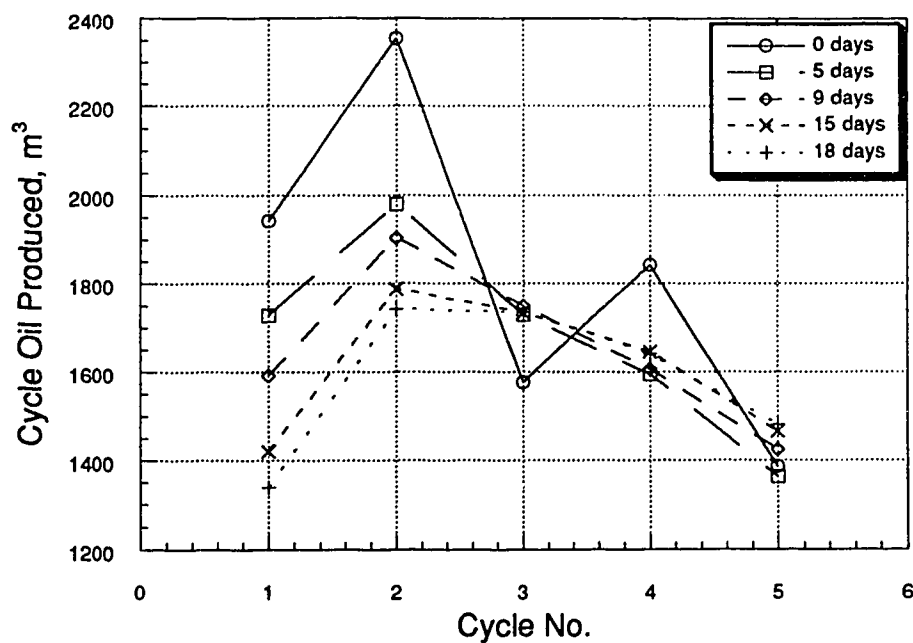


Figure 6.46—Oil production at each cycle for different soak periods.

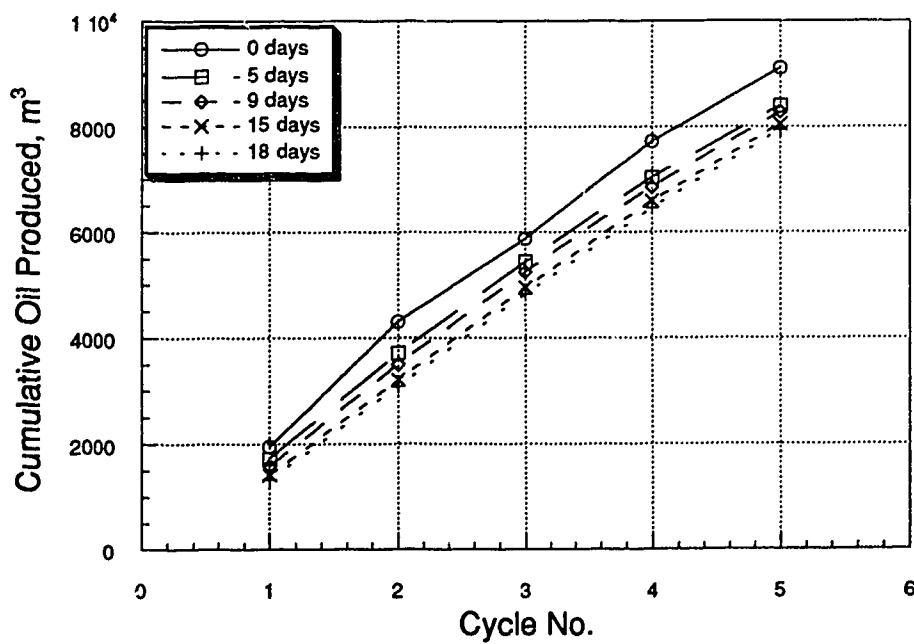


Figure 6.47—Cumulative oil production for different soak periods.

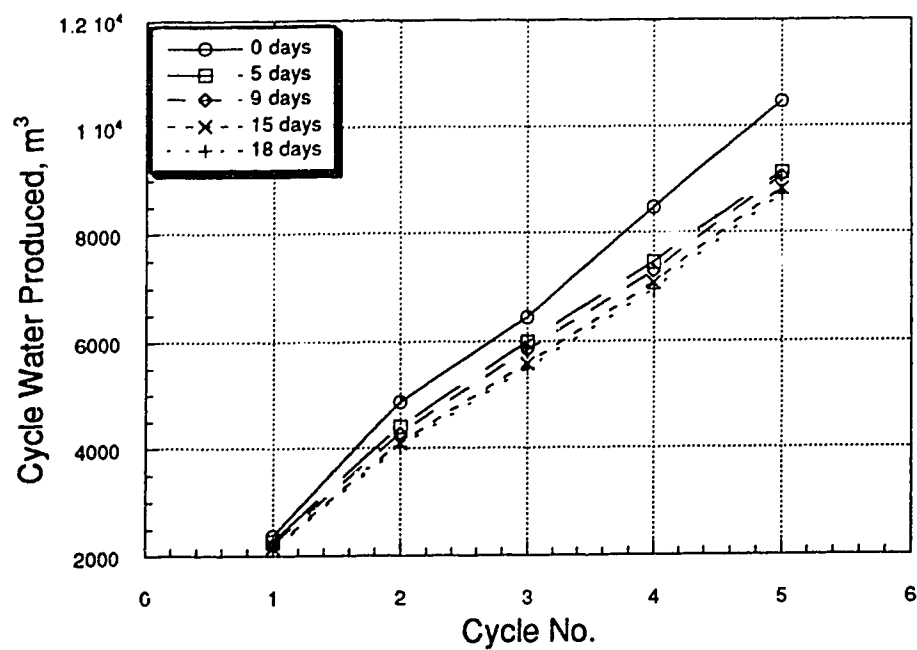


Figure 6.48—Water production at each cycle for different soak periods.

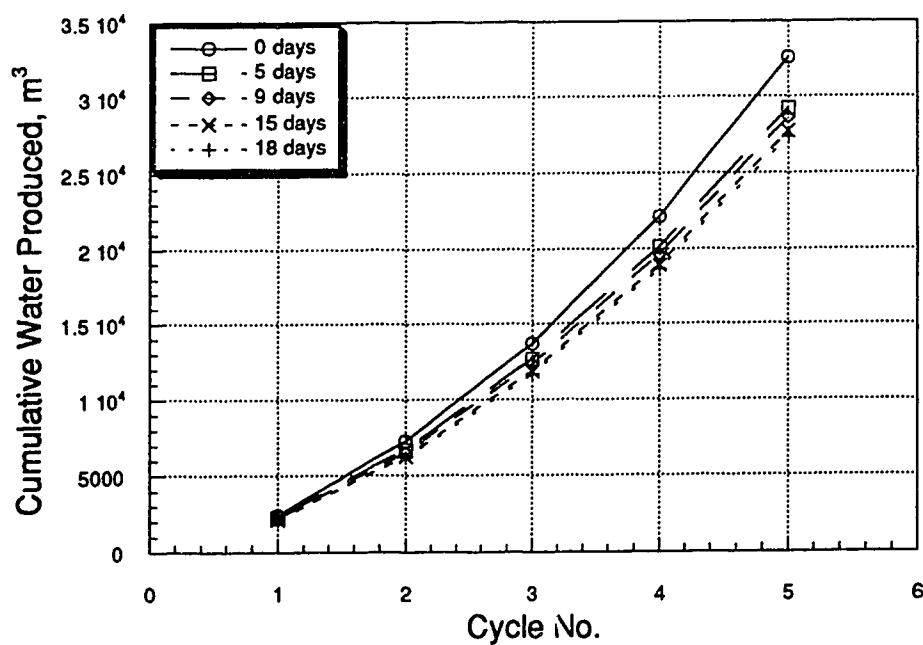


Figure 6.49—Cumulative water production for different soak periods.

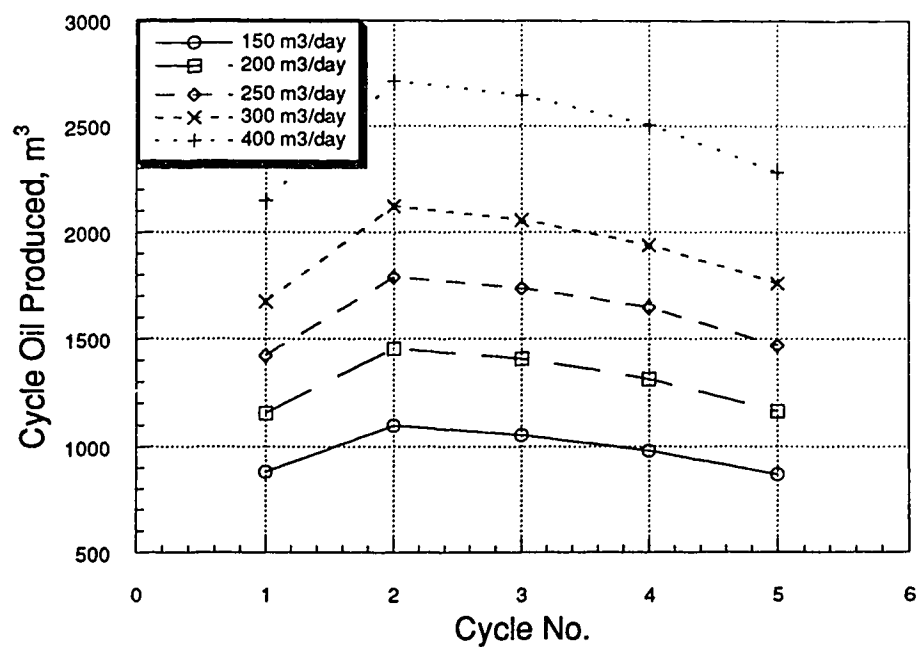


Figure 6.50—Oil production at each cycle for various steam injection rates.

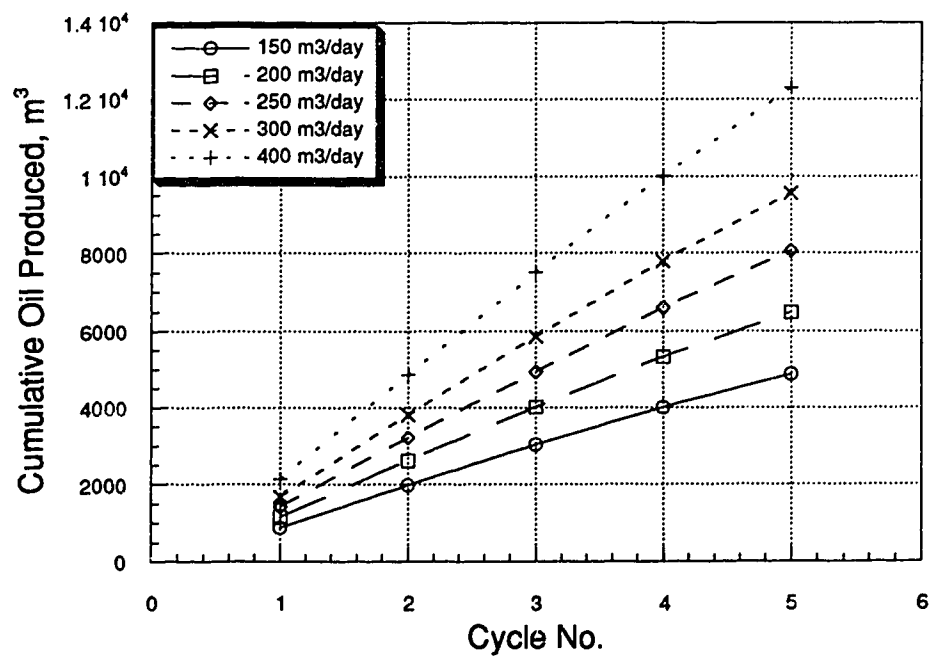


Figure 6.51—Cumulative oil production for different steam injection rates.

increase the areal thermal conformance. This strategy was based on changing fracture orientation and geometry. Increased steam production involves higher boiler capacity and higher operational costs. A detailed calculation of heat loss through the tubing has to be included in the analysis. Economic factors play an important role in steam injection strategy. Decisions regarding injection rates have to be based on cost per cubic meter of oil produced. Cycle water (Fig. 6.52) and cumulative water production (Fig. 6.53) increased proportionately in a similar manner.

The production performance parameters give an excellent perspective on the steam injection strategy. Whereas higher injection rates produced lower OSRs (Fig. 6.54), CDORs (Fig. 6.55) varied inversely with injection rate. Better OSRs were achieved through lower injection rates. Both 150 m³/day and 200 m³/day attained identical values, whereas 400 m³/day was the worst performer. Obviously any increase of injection rate would produce even lower OSRs. Depending on the operational break-even point, field capacity and initial investment, each reservoir would have a different optimum strategy. Shepherd (1979) also found that increasing steam volume increased the CDOR, although recovery from a well was not significantly affected. Figure 6.56 shows lower WORs for higher injection rates. This could be explained as a result of larger contact area for increasing injection rates. Steam travels farther from the wellbore allowing a higher oil cut.

6.6.4 Slug Size

About fifty percent of the cost in thermal projects involve generating steam. It is very important to explore the injection strategy with a given steam generating capacity. In the BP simulation a total of 37,000 m³ CWE of steam was injected with increasing slug sizes. Three more simulation runs were conducted with different slug sizes. Large-small-large (LSL), constant and decreasing slug sizes were used, keeping the total steam volume same. Table 6.6 shows the four steaming schemes.

Figure 6.57 shows the cycle oil production. Both the LSL and the decreasing slug strategy produced the same maximum oil in the 1st cycle with slug sizes of 8,250 m³ and 10,000 m³ respectively. With the lowest slug sizes, the decreasing slug scheme produced less than 300 m³ of oil for each of the last two cycles. With the decrease of slug size, the LSL oil production dropped abruptly in the 2nd cycle and then gradually picked up after that. A constant slug size produced little more oil than the increasing slug size for the first two cycles and then the production decreased steadily for the next three cycles. Figure 6.58

Table 6.6—Slug sizes (m³) for steaming schemes.

<i>Slug Schemes</i>	<i>Cycle Number</i>				
	1	2	3	4	5
Increasing	6250	7000	7500	8000	8250
LSL	8250	6020	7020	7520	8190
Constant	7400	7400	7400	7400	7400
Decreasing	10000	9016	8010	5024	4950

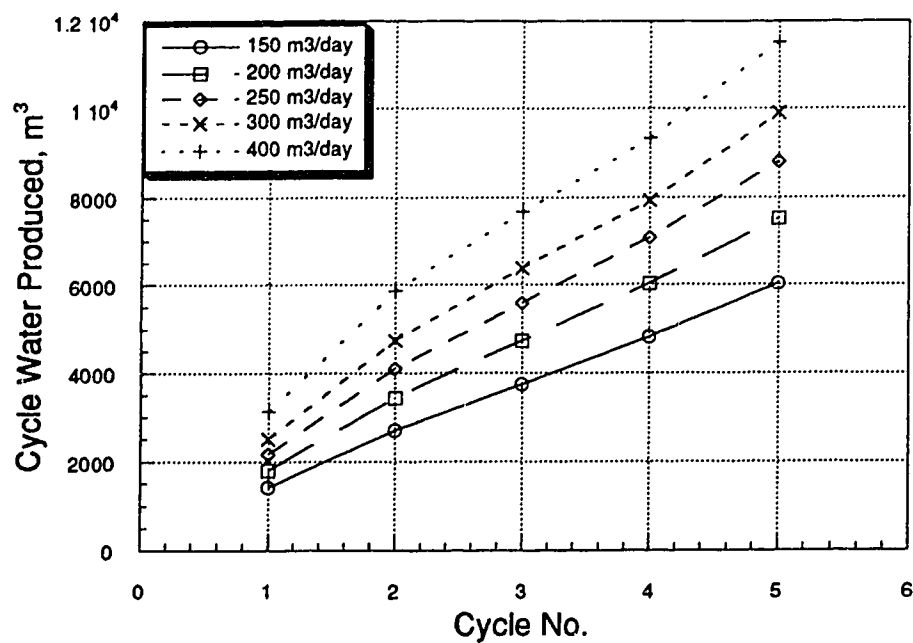


Figure 6.52—Water production at each cycle for different steam injection rates.

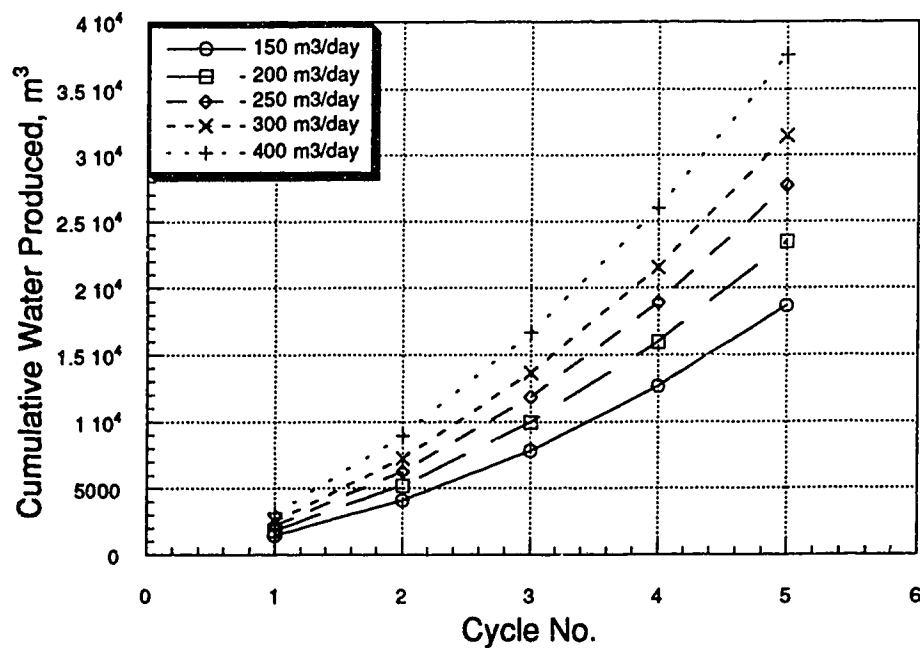


Figure 6.53—Cumulative water production for various steam injection rates.

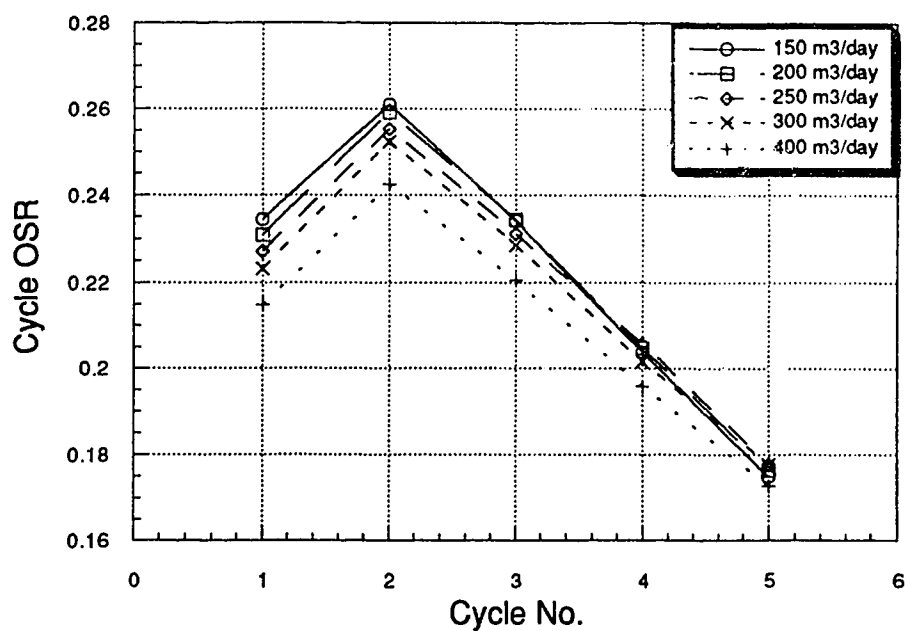


Figure 6.54—Oil-steam ratio at each cycle for various steam injection rates.

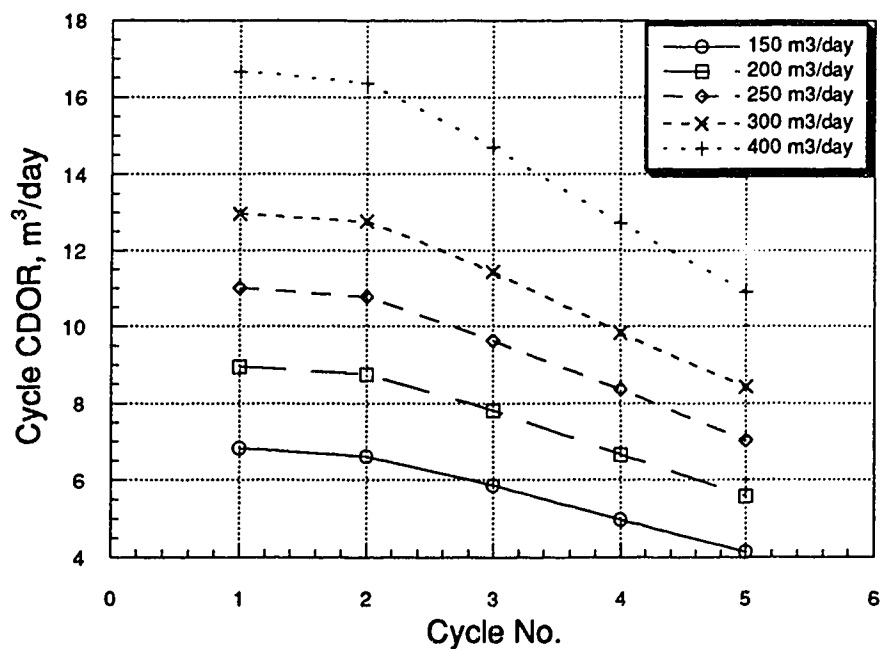


Figure 6.55—Calendar day oil production rates for different steam injection rates.

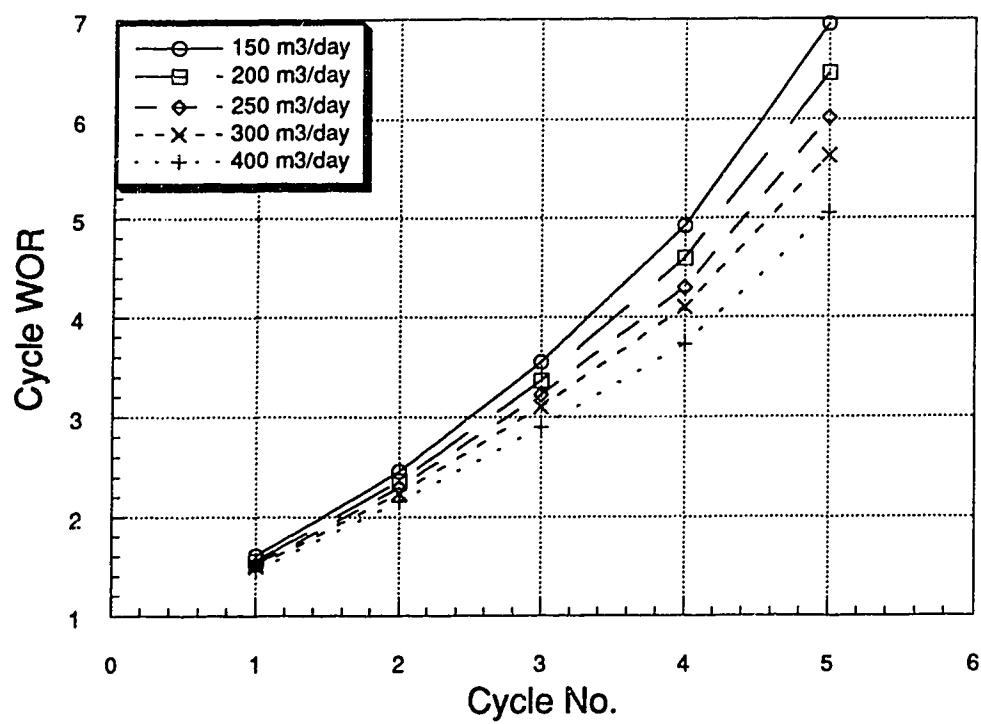


Figure 6.56—Water-oil ratio at each cycle for different steam injection rates.

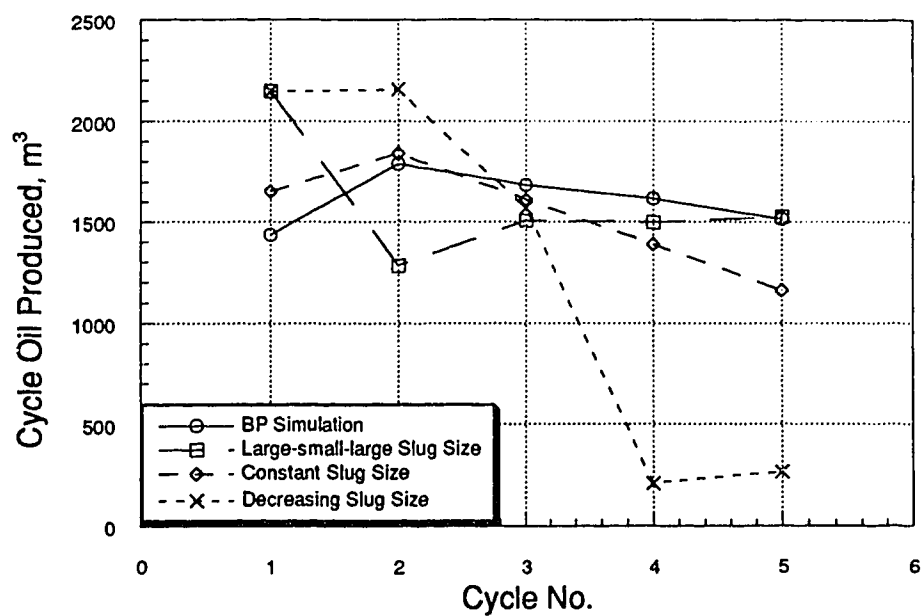


Figure 6.57—Oil production at each cycle for different slug sizes with constant total steam.

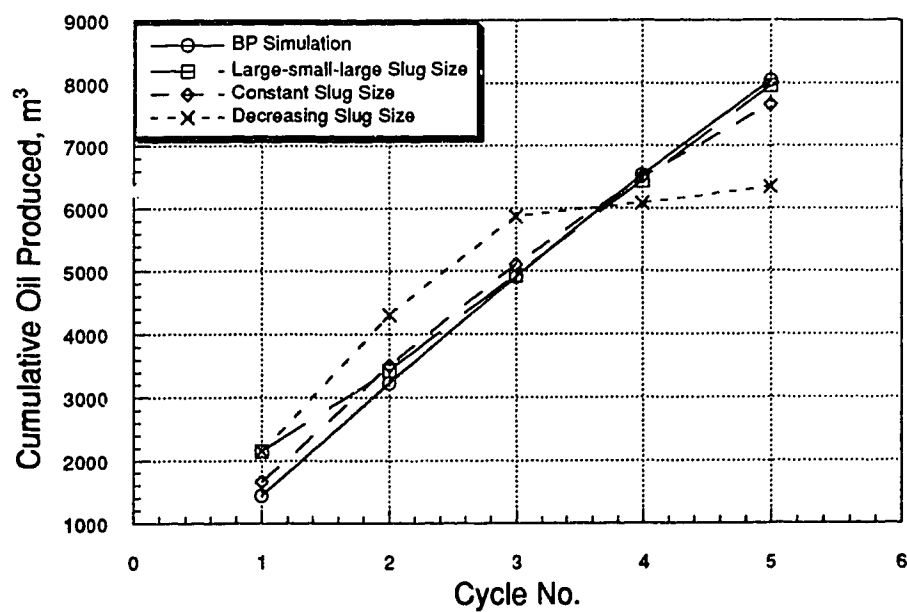


Figure 6.58—Cumulative oil produced for different slug sizes with same total injected steam.

gives a better idea of the overall performance in terms of the total oil recovery. The increasing slug size (BP simulation) produced the maximum amount of oil after 5 cycles, doing marginally better than the LSL scheme. The constant slug strategy produced 5% less oil than the increasing slug strategy. The decreasing slug size strategy was the worst performer of all the schemes with 21% less oil production. From these results, it is seen that with a large slug size much oil can be produced in the 1st cycle but, reduction of slug size reduces the subsequent cycle production drastically. It is very important to fill up the voidage in the reservoir with increasing slug sizes. Decreasing the slug size after an initial large steam volume does not expand the hot zone any more. It would fill up the already heated zone and just bring up the temperature without reaching new oil. Cycle water production (Fig. 6.59) for each of the schemes was much higher than for the increasing slug size scheme. Consequently all the three cases produced more water after 5 cycles (Fig. 6.60), with the decreasing slug size strategy producing the maximum water.

Figure 6.61 shows the OSRs for each cycle. Again, increasing the slug size shows the best overall performance. The same conclusion can be made from the CDORs (Fig. 6.62). The WORs for all four cases were fairly close except for a dismal performance again by the decreasing rate scheme. The WOR value rose over 30 for the last two cycles. Figure 6.63 shows the results. With much less heat supplied, the reservoir average temperature would drop favouring large water production from the same heated zone created in the 1st cycle. Unless one is aiming for high oil production in the first couple of cycles, increasing the slug size is the best injection strategy in CSS operation. A close second would be the LSL injection with a quick pay-off in the 1st cycle without losing much overall efficiency.

6.6.5 Time Step

Analytical models, from the nature of their solution procedure, should not be sensitive to time step sizes. In this particular model, the most important factor for flow calculation is oil viscosity. Viscosity for the next time step is calculated from the current average temperature. As the average temperature is a function of time, so is the viscosity. The highly non-linear relationship between temperature and viscosity may make this model sensitive to time step size. Gontijo (1983) reported a considerable production drop with an increase of the time step size using a similar viscosity calculation method. Figure 6.64 shows the effect of different time step sizes on cycle oil production: 0.5, 1.0 and 2.0 days show virtually no difference. The first significant change in production pattern is seen

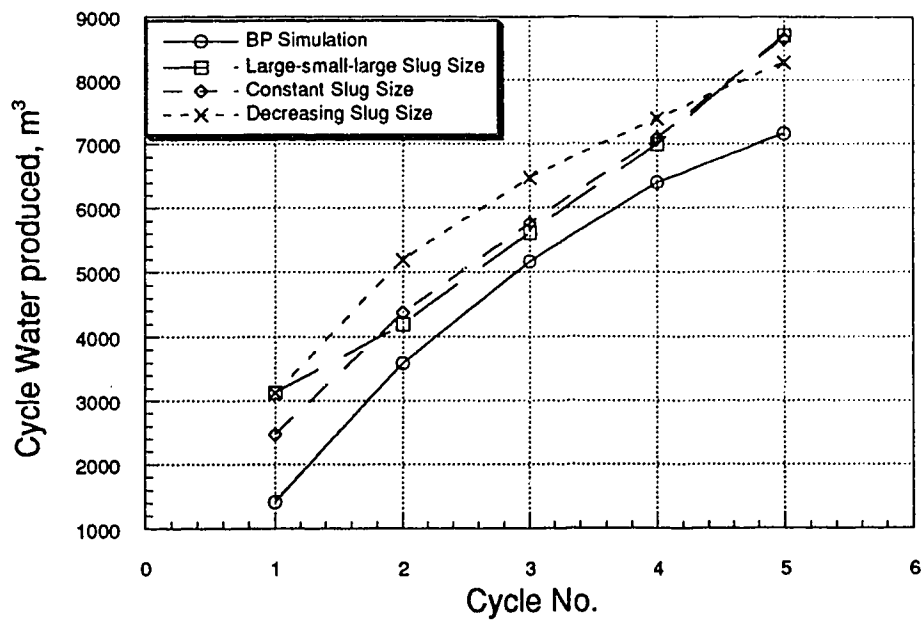


Figure 6.59—Water production at each cycle for various slug sizes with constant total injected steam.

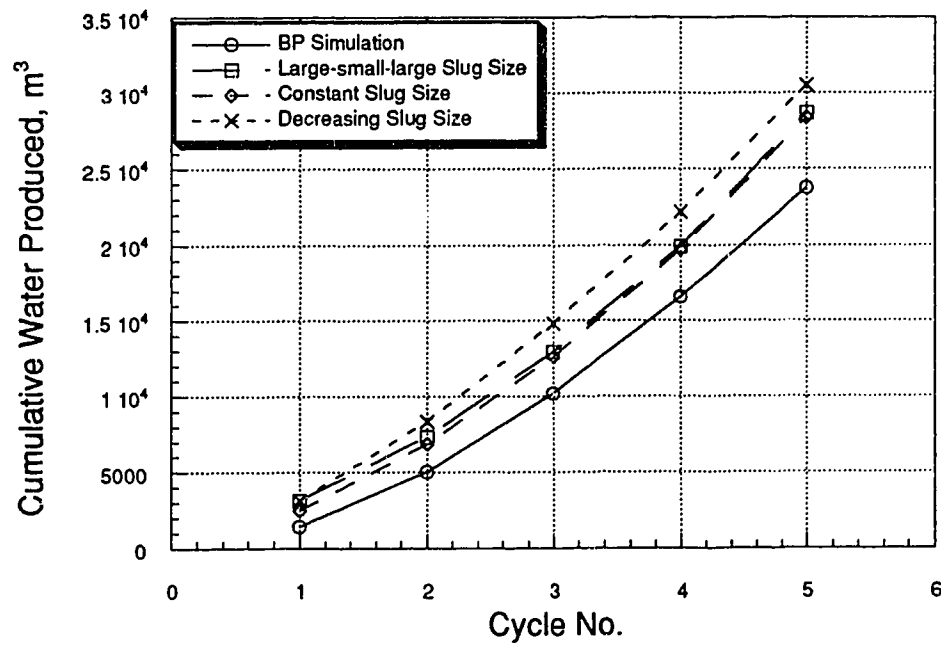


Figure 6.60—Cumulative water production for various slug sizes with constant total injected steam.

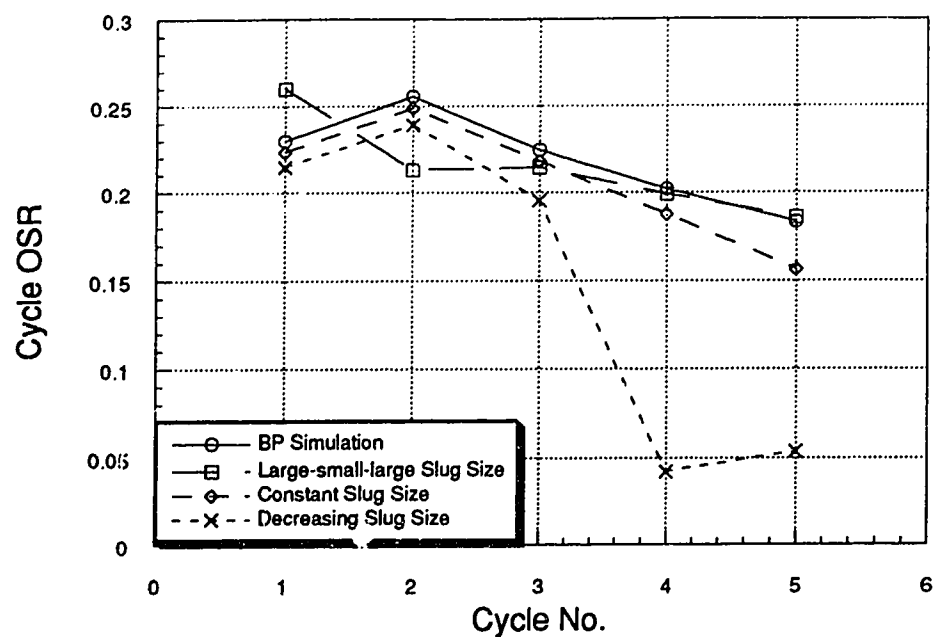


Figure 6.61—Oil-steam ratio at each cycle for various slug sizes with constant total injected steam.

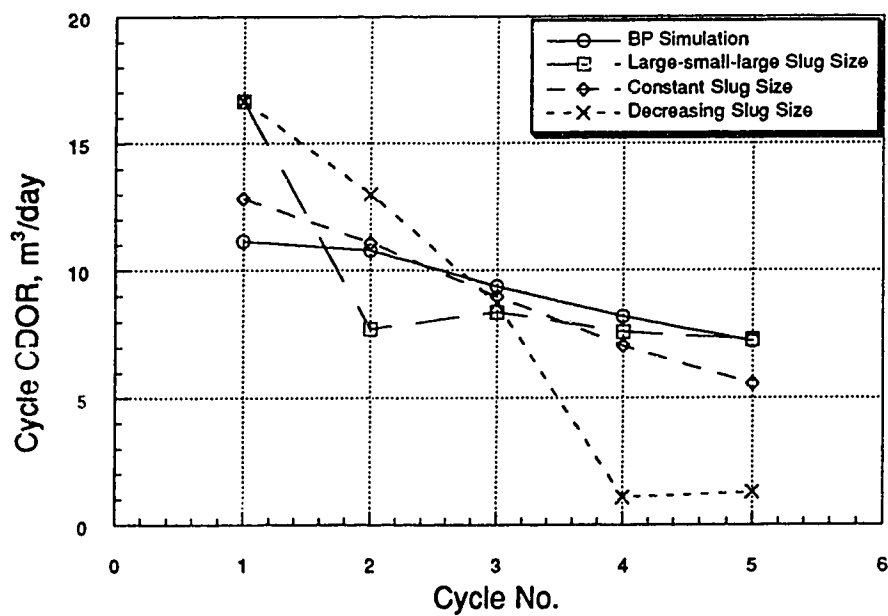


Figure 6.62—Calendar day oil production rate at each cycle for various slug sizes with constant total injected steam.

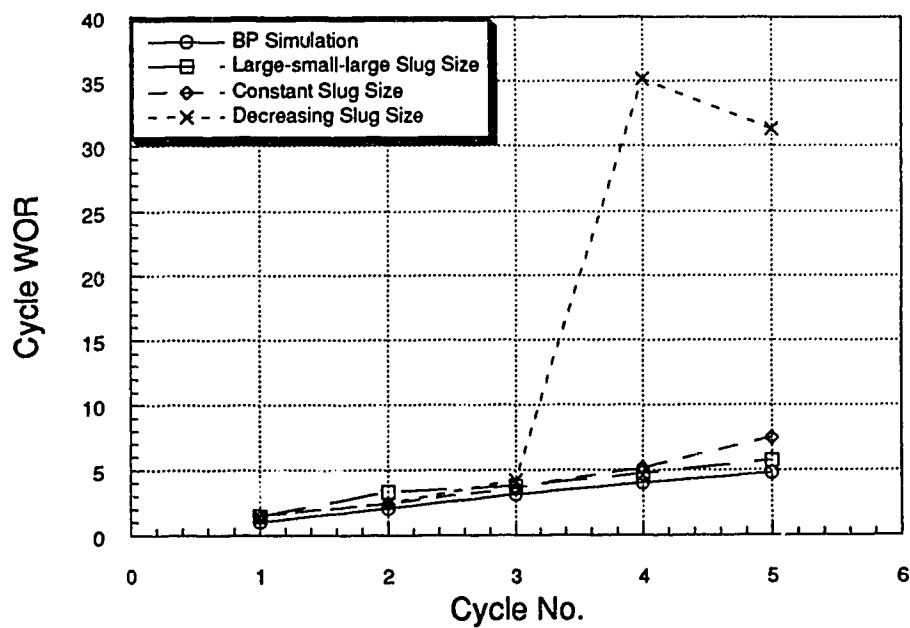


Figure 6.63—Water-oil ratio at each cycle for various slug sizes with constant total injected steam.

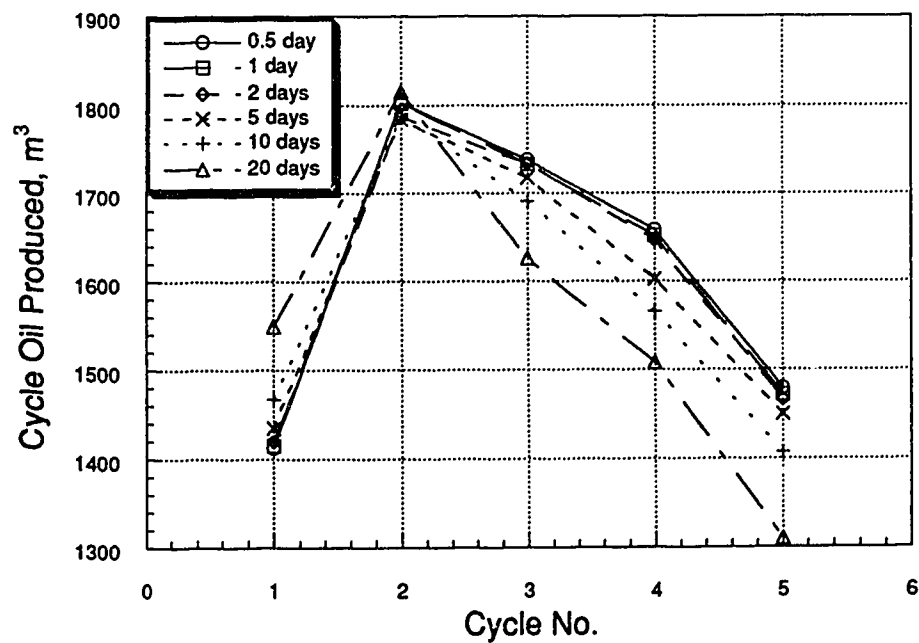


Figure 6.64—Oil produced at each cycle for various production time-steps.

when the step size is increased to 5 days. The 1st cycle production increases and starts dropping from the 3rd cycle. An increment to 10 days still follows the 0.5 day trend reasonably closely. Doubling the time to 20 days changes the production pattern considerably. In terms of cumulative oil production, the differences for all cases are very small. A 20 day step produced 283 m³ less oil than the 0.5 day case after 600 days of production, which is less than 3.5% production loss. Figure 6.65 shows the results. Cycle water (Fig. 6.66) and cumulative water (Fig. 6.67) curves for all the cases are so close that it is difficult to distinguish one from the other. The improved response toward time step size is due to the adaptation of the “Average” method of oil viscosity calculation. In this method, the oil viscosity is not as sensitive to temperature changes as the “Direct” method. All the runs in the present study used a 2 day time step size. This enabled faster computation without losing accuracy.

6.6.6 Steam Temperature

Another feasible option to increase the heat input into the reservoir is to increase the steam temperature. The cost of producing steam at higher pressure or to superheat the injected steam is high. Two runs were conducted to see the benefit of high temperatures. Steam saturation temperature (pressure) was increased by 50°C and 70°C above the base run. Steam quality for each case was kept at 0.75 to see the effect of temperature. This would actually be disadvantageous for higher temperature, as the latent heat content decreases with increasing pressure. Steam enthalpy remains almost constant with less latent heat at a higher temperature. Figures 6.68 and 6.69 show the effect of higher temperature on oil production rates and average hot zone temperatures respectively for the first cycle. Higher temperature enabled higher rates for the high temperature cases. Figure 6.70 shows the cycle oil production. For the higher temperatures, the 1st cycle production was higher and after that the responses were somewhat erratic. Cumulative oil productions are shown in Figure 6.71. It can be seen that higher temperatures produced a larger amount of oil. Interestingly, increasing the temperature from 50°C to 70°C produced marginal incremental oil after 5 cycles. Even the 50°C case produced only 7% incremental oil. Although increasing temperature makes the oil more mobile, more heat is also lost in these cases. Moreover, the total heat input remains almost constant. In Figure 6.72, it can be observed that at a higher temperature the fluid heat loss is higher. Both cycle water (Fig. 6.73) and cumulative water (Fig. 6.74) follow similar trends as oil production. From these results, it can be concluded that increasing the steam temperature follows the law of diminishing

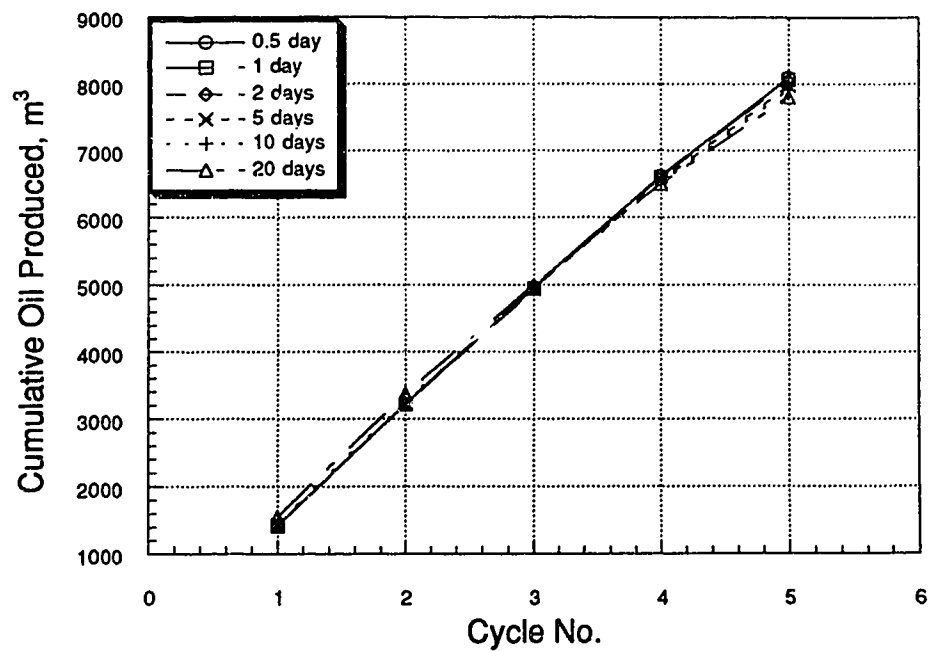


Figure 6.65—Cumulative oil production for various production time-step sizes.

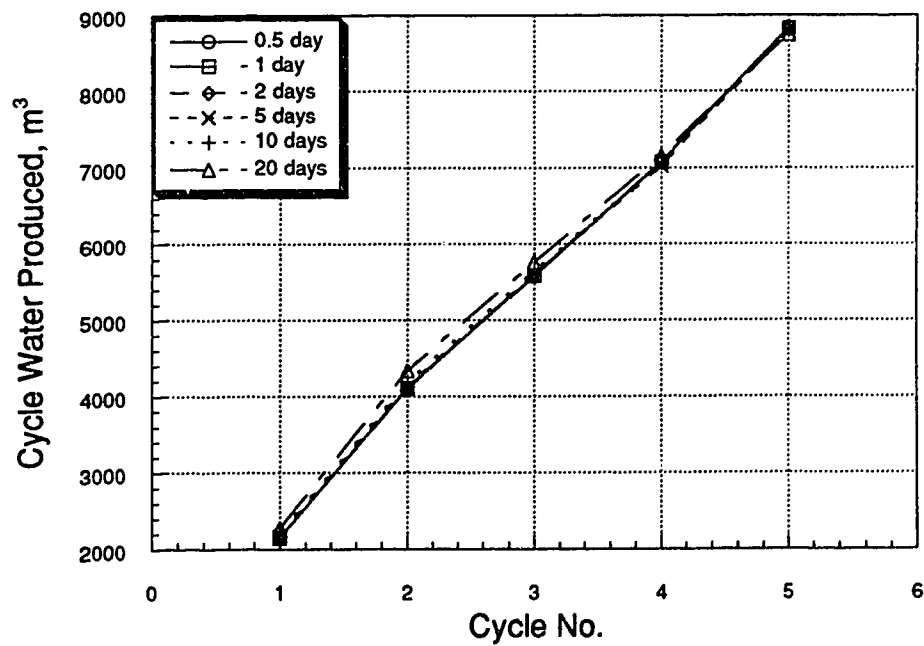


Figure 6.66—Water production at each cycle for various production time-step sizes.

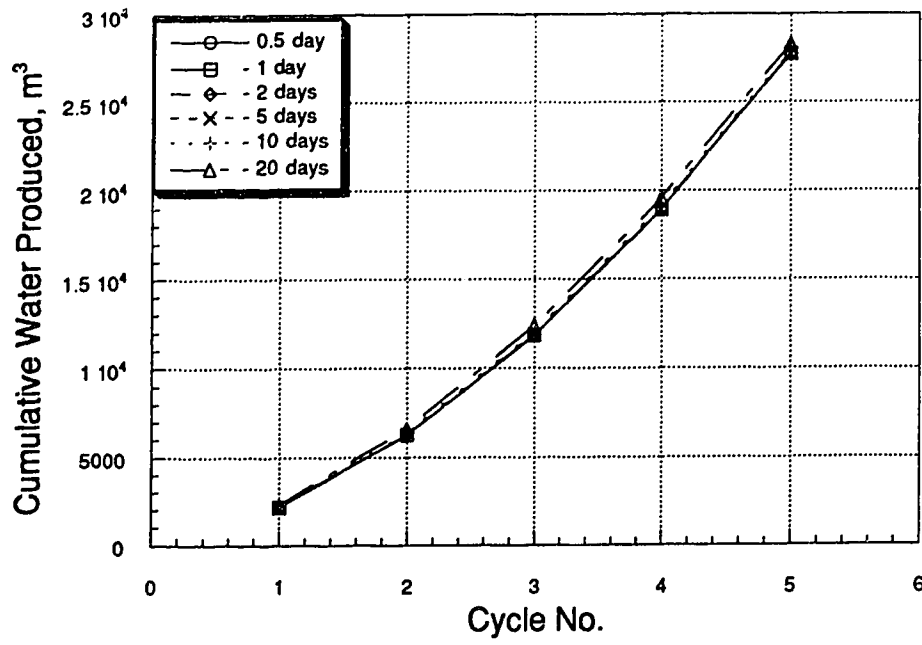


Figure 6.67—Cumulative water production for various production time-step sizes.

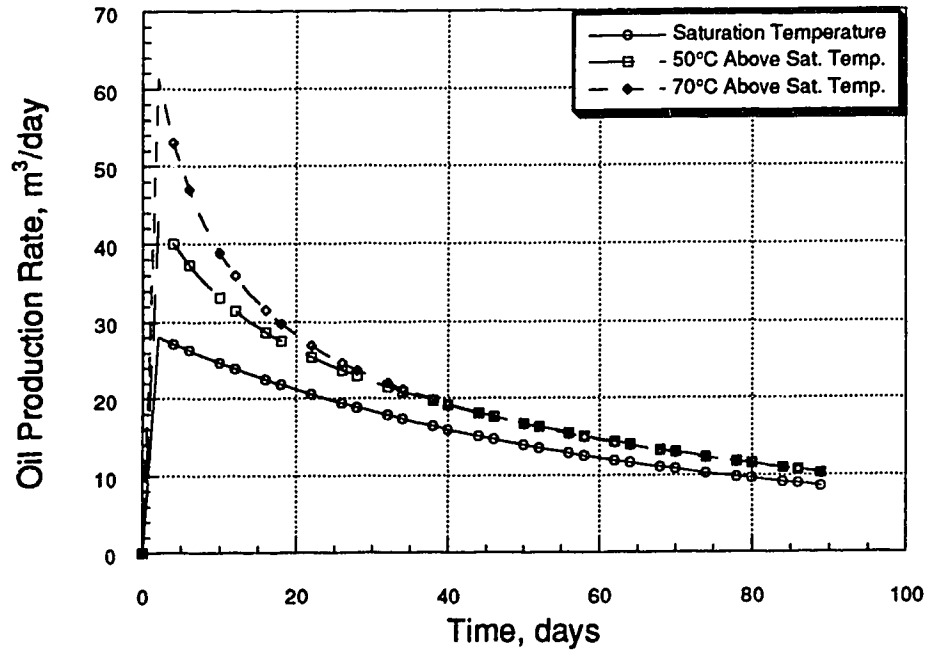


Figure 6.68—Effect of steam temperature on 1st cycle oil production rate.

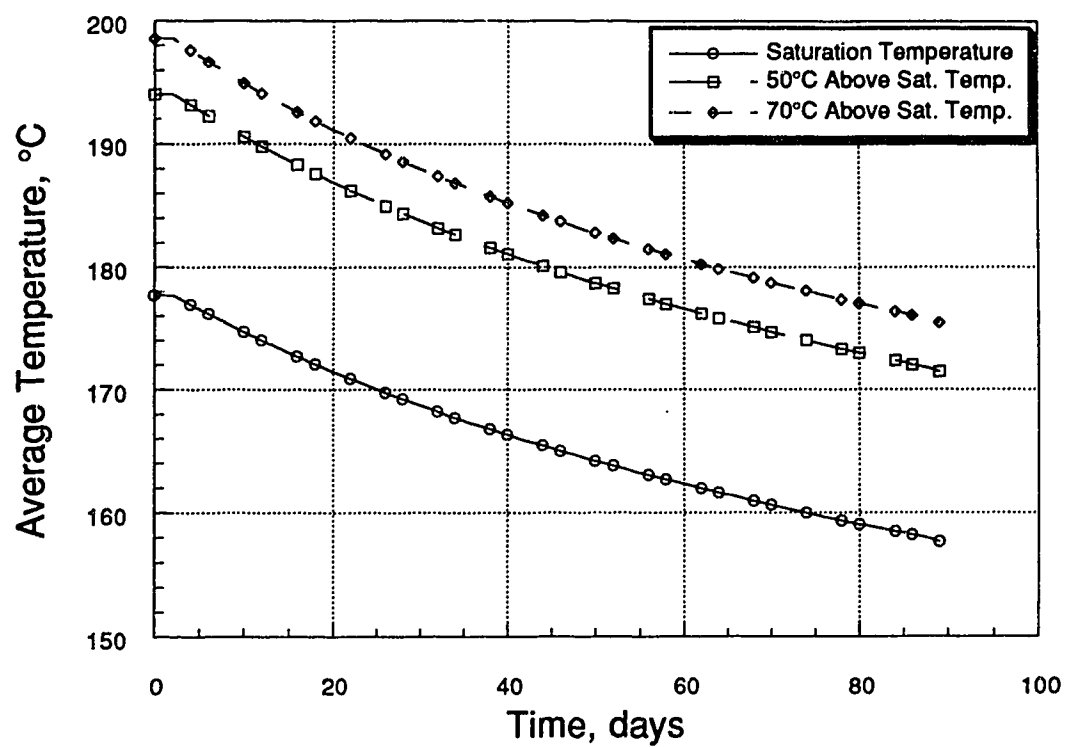


Figure 6.69—Effect of steam temperature on 1st cycle average hot zone temperature.

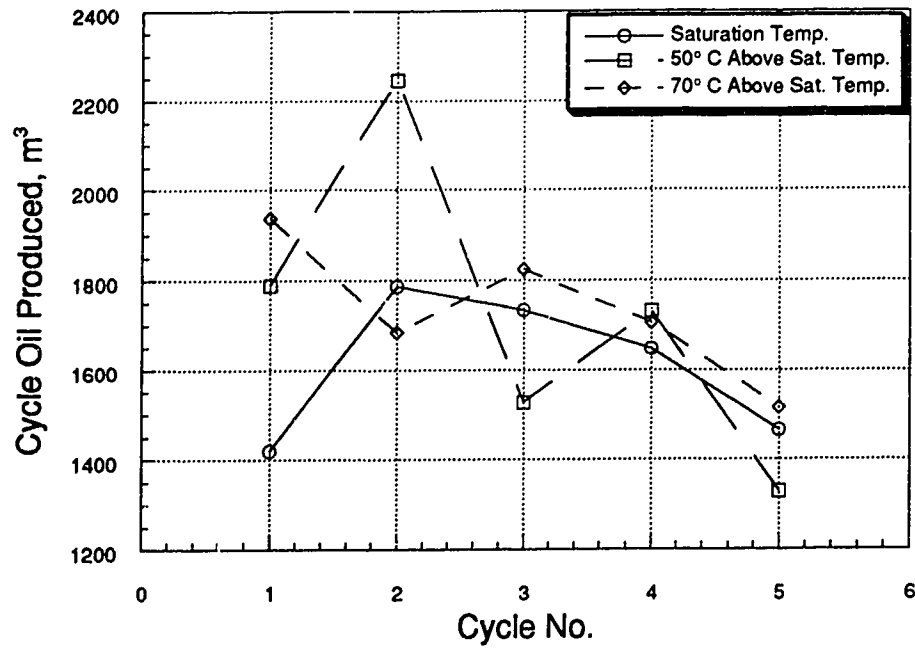


Figure 6.70—Oil production at each cycle for different steam temperatures.

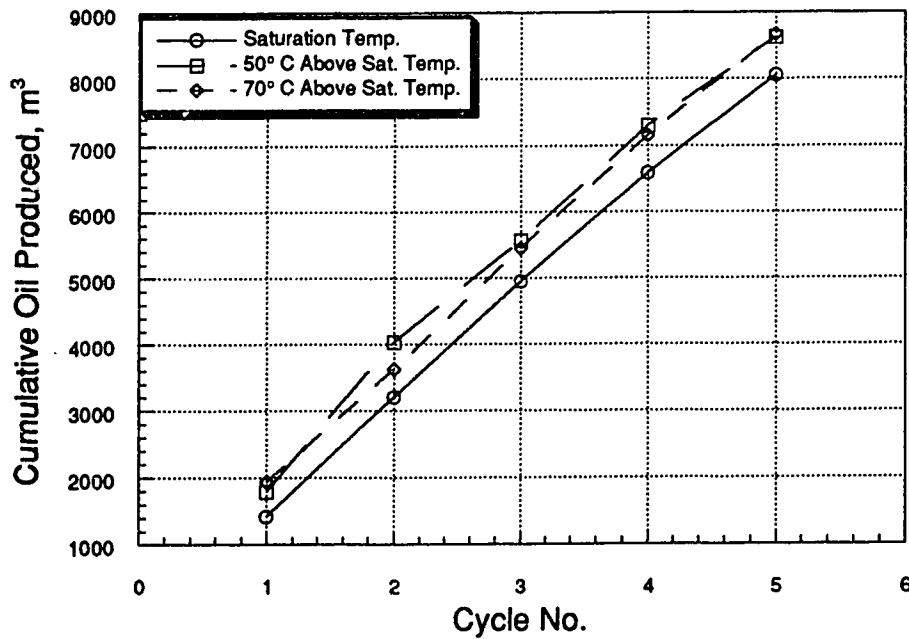


Figure 6.71—Cumulative oil produced for different steam injection temperatures.

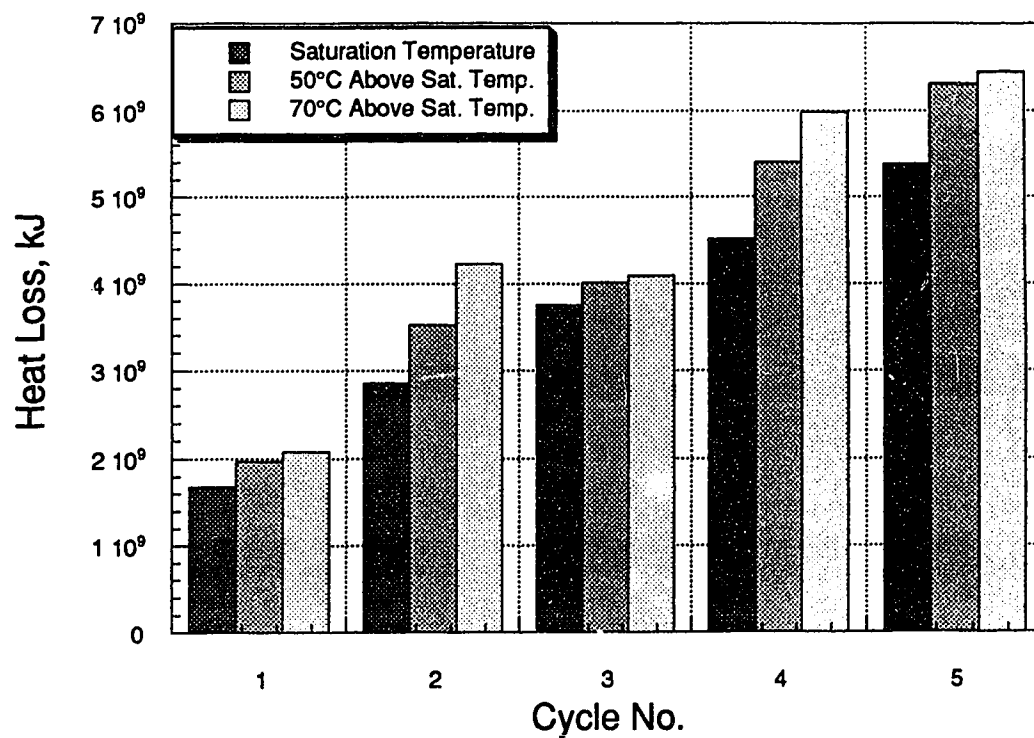


Figure 6.72—Heat lost to fluid production at each cycle for varying steam injection temperatures.

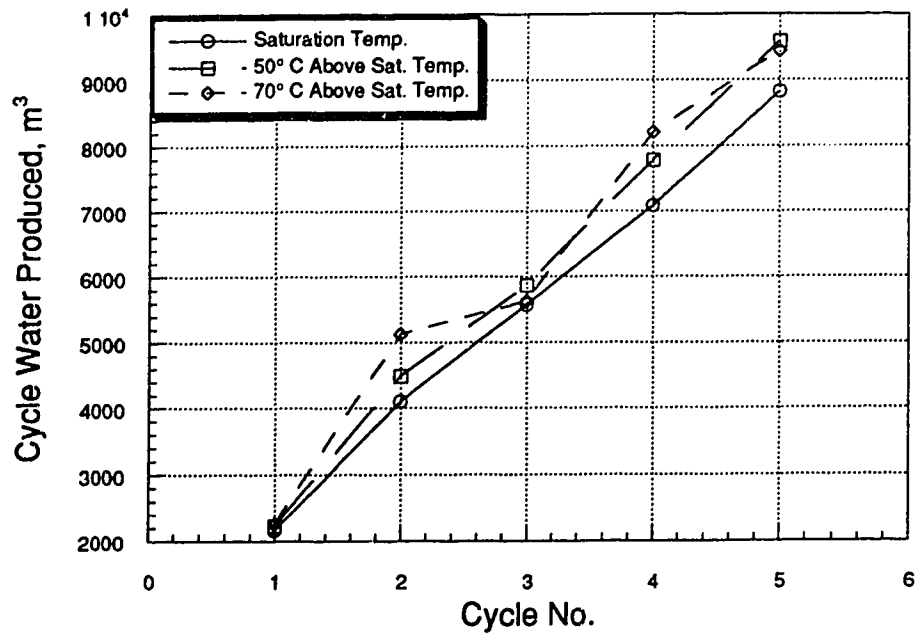


Figure 6.73—Water production at each cycle for various steam injection temperatures.

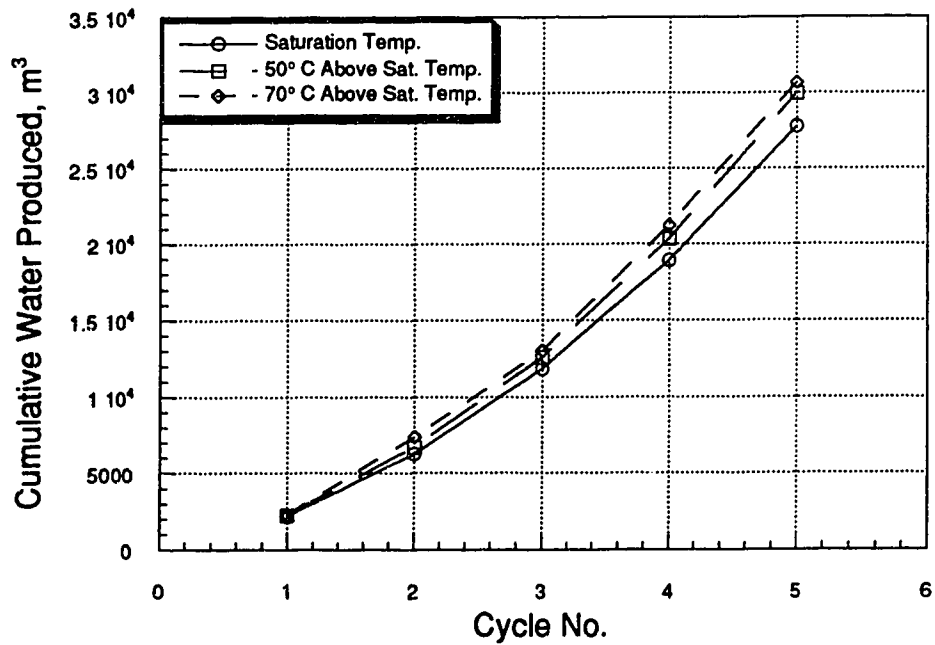


Figure 6.74—Cumulative water produced for different steam injection temperatures.

return. Similar observations were made by other authors (Davidson *et al.*, 1967; Gontijo and Aziz, 1984). Martin (1967) actually got better performance from low pressure steam injection. Moreover, a substantial jump in cost does not justify increasing the steam temperature for such nominal incremental oil. It should be noted that the aforesaid investigators used very different mechanistic models from the one used for the present study.

6.6.7 Steam Quality

The last controlling factors for the heat content of the injecting steam is quality. For an effective steam operation, sufficient quality steam at an optimum rate has to be injected. Better quality increases the heat content and more importantly, it increases the latent heat part of the steam enthalpy. Latent heat plays a significant role in steam zone expansion (Marx and Langenheim, 1959; Wheeler, 1969; Mandl and Volek, 1969). Steam qualities of 0.6, 0.75 and 0.96 were used to see the effects on oil and water production.

Figure 6.75 shows a monotonic increase in cycle oil production with increasing steam quality. The impact of increased heat input is greater with increased slug size. In the first cycle with the smallest slug size, the difference in heat input was not sufficient to change the average hot zone temperature. Cumulative oil production also increased monotonically with increasing steam quality. Figure 6.76 shows a 10% increase in total oil production for an increase in quality from 0.6 to 0.96. This improvement is not as much as in California (Gontijo and Aziz, 1984) or in Venezuela (Trebolle *et al.*, 1993). This is due to the high injection pressure in the Cold Lake area (over 10 MPa). As the pressure increases, the contribution from latent heat decreases and the effect of improved quality diminishes. Cycle water production (Fig 6.77) slightly increased after the 2nd cycle for the increasing steam quality cases. There was no significant difference in the total water production (Fig. 6.78).

All three production performance parameters – OSR (Fig. 6.79), CDOR (Fig. 6.80) and WOR (Fig. 6.81) show favourable results for higher steam quality. This could be somewhat misleading, as none of these parameters considers the cost of improving the steam quality. Performance has to be assessed on the basis of economic factors involved in steam production. Wellhead steam qualities of 0.75 to 0.8 are most widely produced in the field.

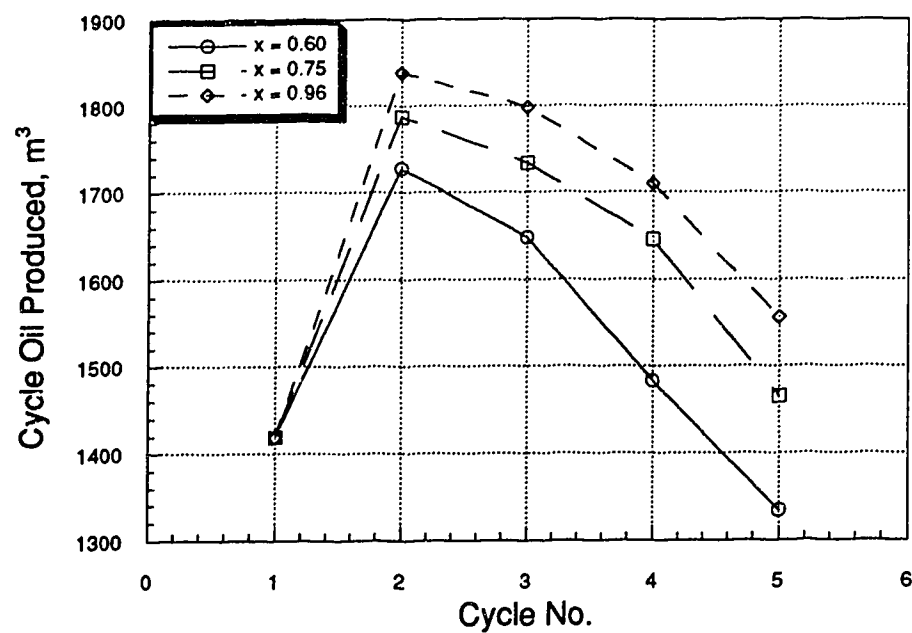


Figure 6.75—Oil production at each cycle for various steam qualities.

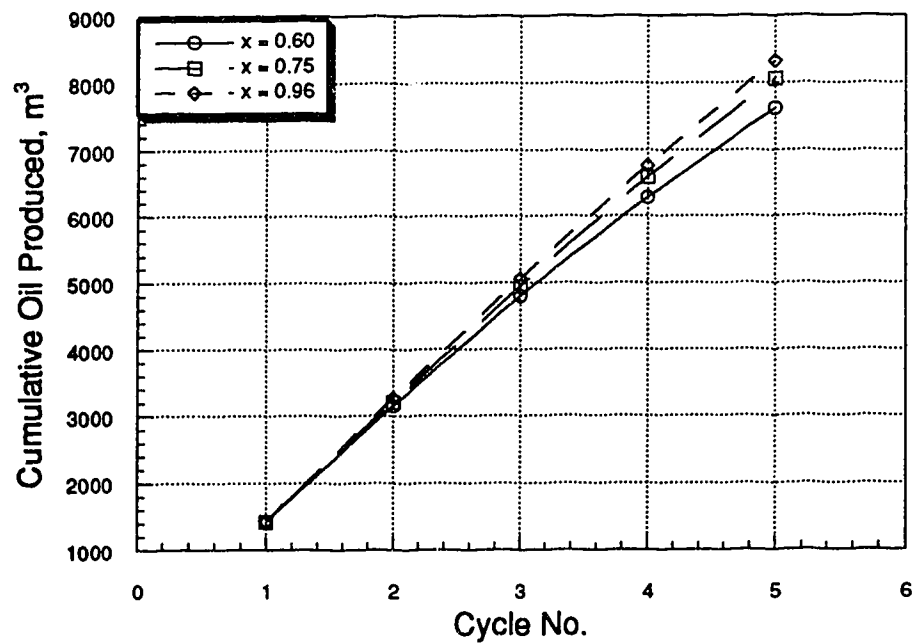


Figure 6.76—Cumulative oil production for various steam qualities.

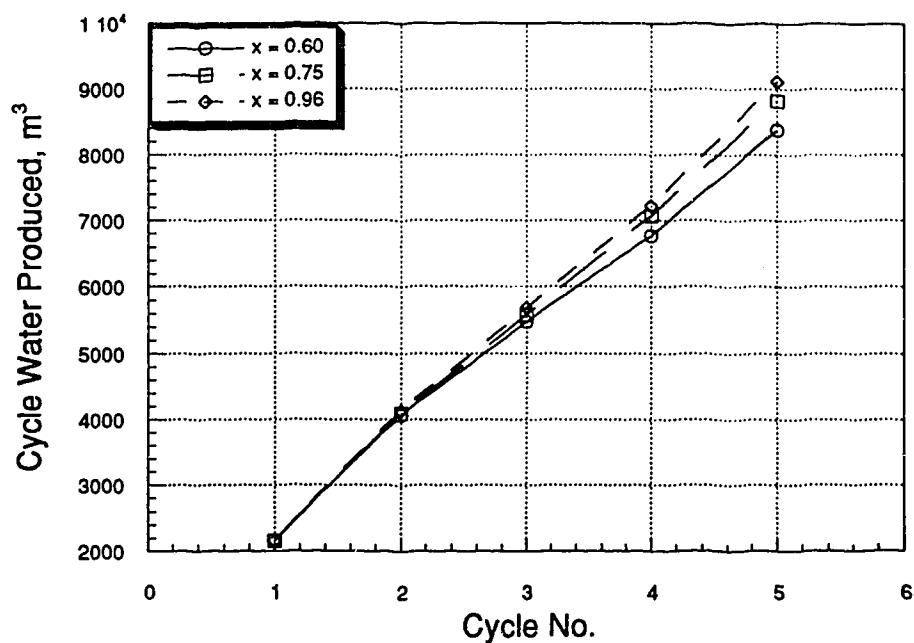


Figure 6.77—Water production at each cycle for various steam qualities.

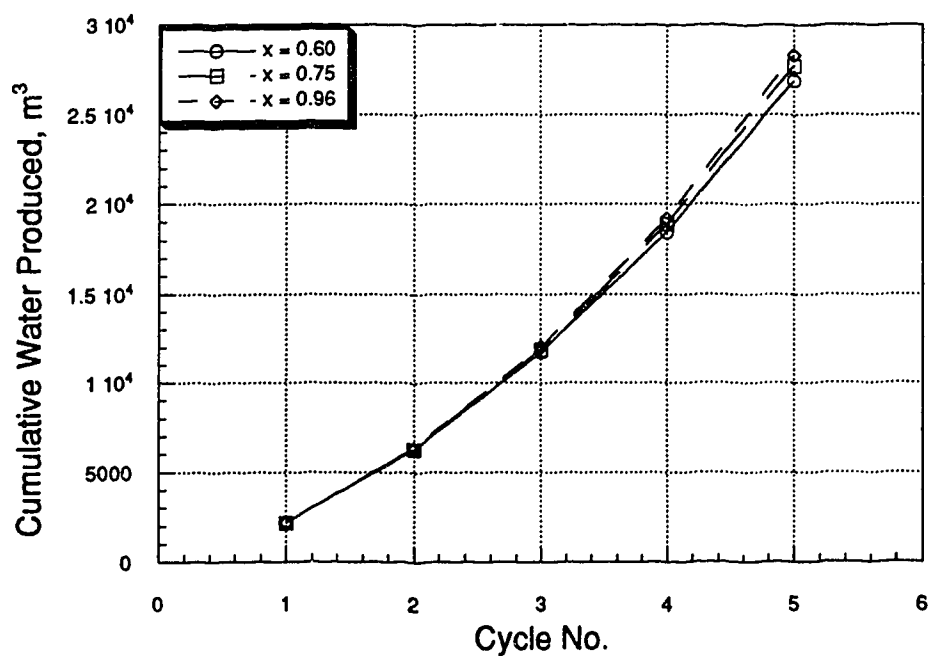


Figure 6.78—Cumulative water production for various steam qualities.

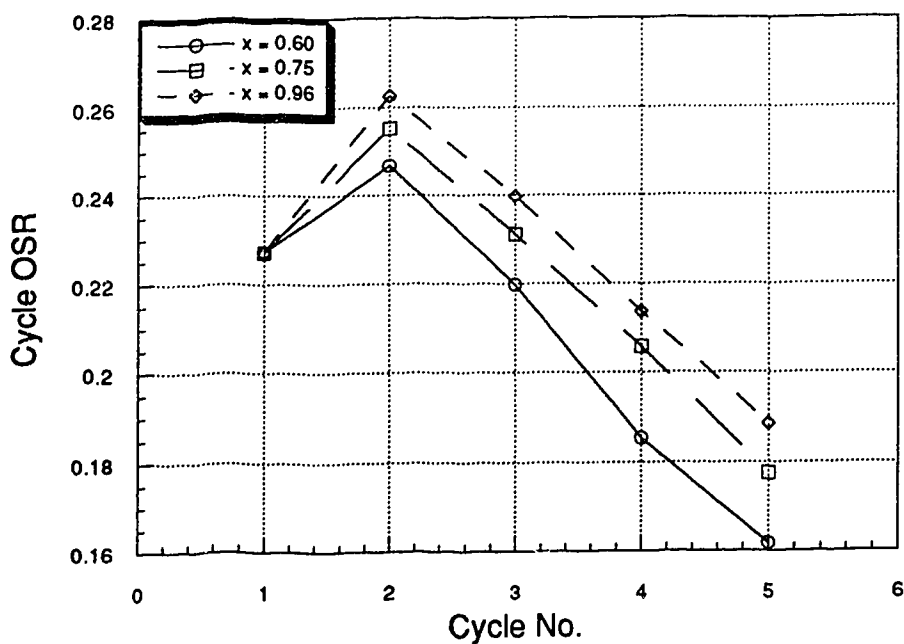


Figure 6.79—Oil-steam ratios at each cycle for various steam qualities.

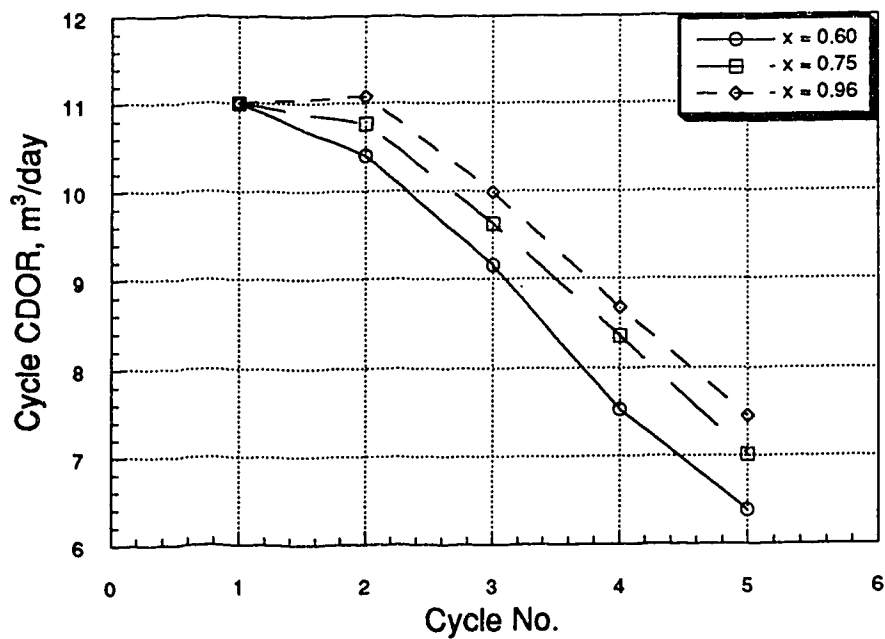


Figure 6.80—Calendar day oil rate at each cycle for various steam qualities.

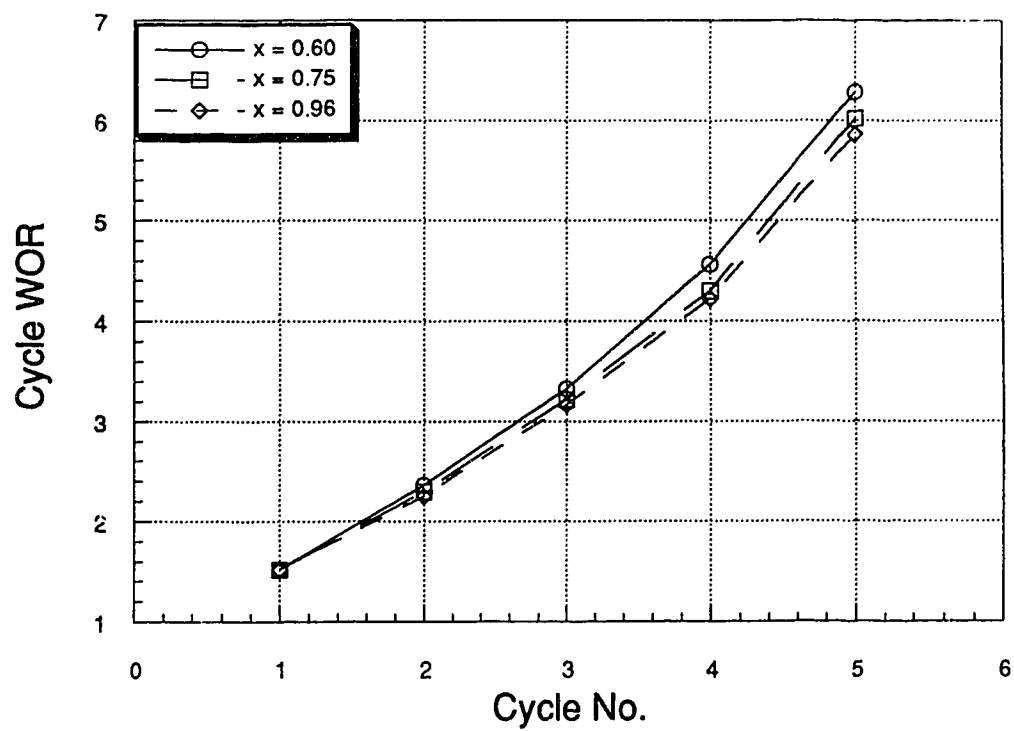


Figure 6.81—Water-oil ratios at each cycle for various steam qualities.

6.6.8 Initial Reservoir Temperature

To a considerable extent, the effectiveness of steam processes depends on the initial reservoir temperature. While the average reservoir temperature in California varies between 30 to 40°C, Alberta heavy oil fields have formation temperatures between 10 to 20°C. For many Venezuelan reservoirs this value exceeds 50°C. In the present study, the same viscosity-temperature relationship was used for all the runs. This relationship actually varies from reservoir to reservoir and should be considered for a true comparison between reservoirs.

Initial reservoir temperature determines the amount of net heat input into the reservoir. With a high initial temperature, the available enthalpy would be less as the sensible heat transfer from the steam decreases. The effectiveness of steam injection varies directly with the available enthalpy to the reservoir. Figure 6.82 shows the net heat injected into the reservoir for different initial reservoir temperatures. As a consequence of greater heat input, lower initial temperatures would have a higher hot zone average temperature. This would allow more production. Figure 6.83 shows the effect of initial reservoir temperature on cycle oil production. Up to the 20°C case the cycle oil production response shows little change. Faster growth of the hot zone in the early cycles for higher initial reservoir temperatures (40°C and 60°C) produced saturation values quite different than the lower temperature cases (10°, 16° and 20°C). Because of these saturation values and lower production rates, the cycle oil production curves for 40°C and 60°C follow different trends than the lower temperature cases. Figure 6.84 shows a reduction in cumulative oil production when the initial reservoir temperature is increased beyond 40°C. For the 10°, 16° and 20°C cases the values are almost identical. One advantage of a higher initial temperature is quicker early growth of the hot zone. Figure 6.85 shows the progression of the 100°C isotherm. At $T_R=60^\circ\text{C}$, the 100°C isotherm moves 0.6 m more beyond the fracture face after 5 cycles. This gain was not sufficient to offset the effect of a lower average zone temperature. Water production for the higher temperature cases (40°C and 60°C) was also less due to the lower average temperature. Figure 6.86 displays the cumulative water production up to the 5th cycle. It is clear from these results that due to more available enthalpy, steam injection is more effective for colder reservoirs.

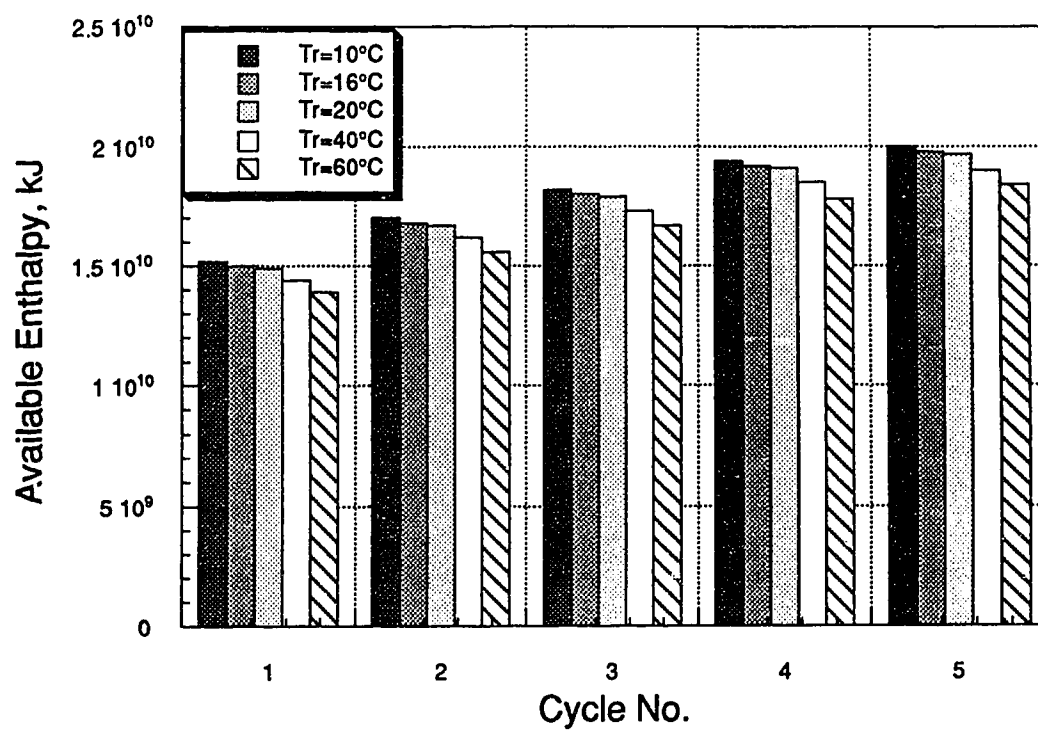


Figure 6.82—Effect of initial reservoir temperature on net heat injection.

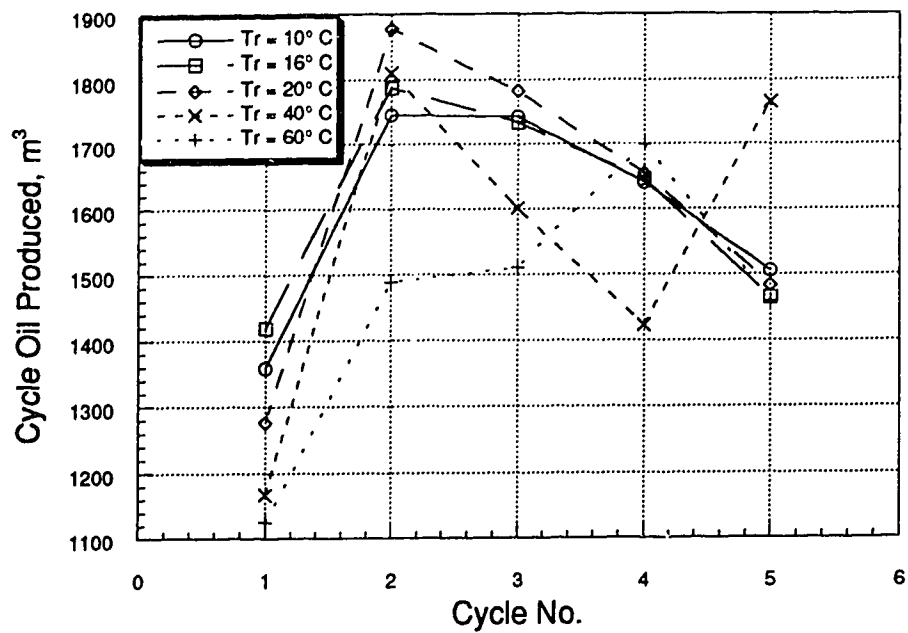


Figure 6.83—Oil production at each cycle for different initial reservoir temperatures.

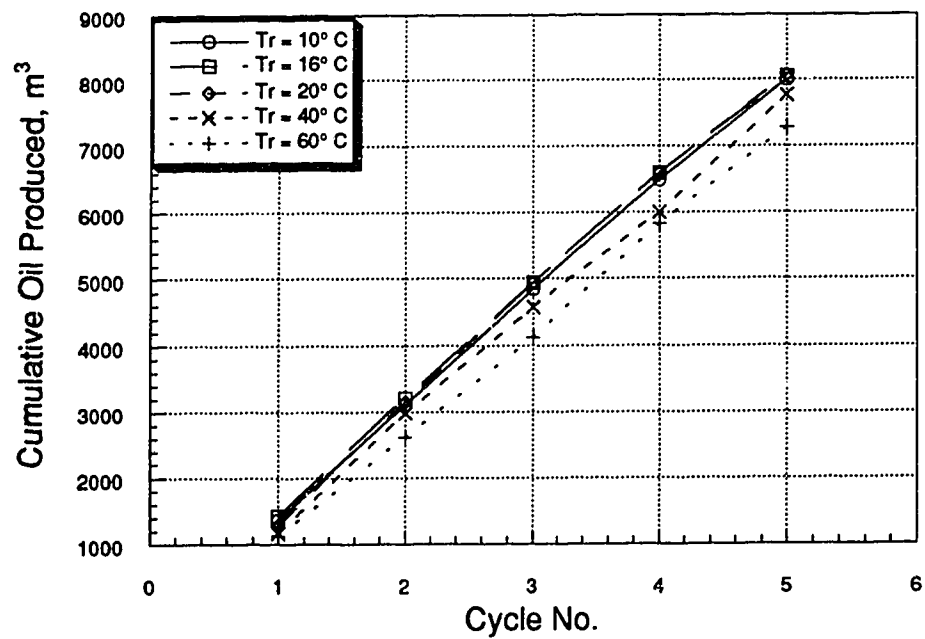


Figure 6.84—Effect of initial reservoir temperature on total oil production.

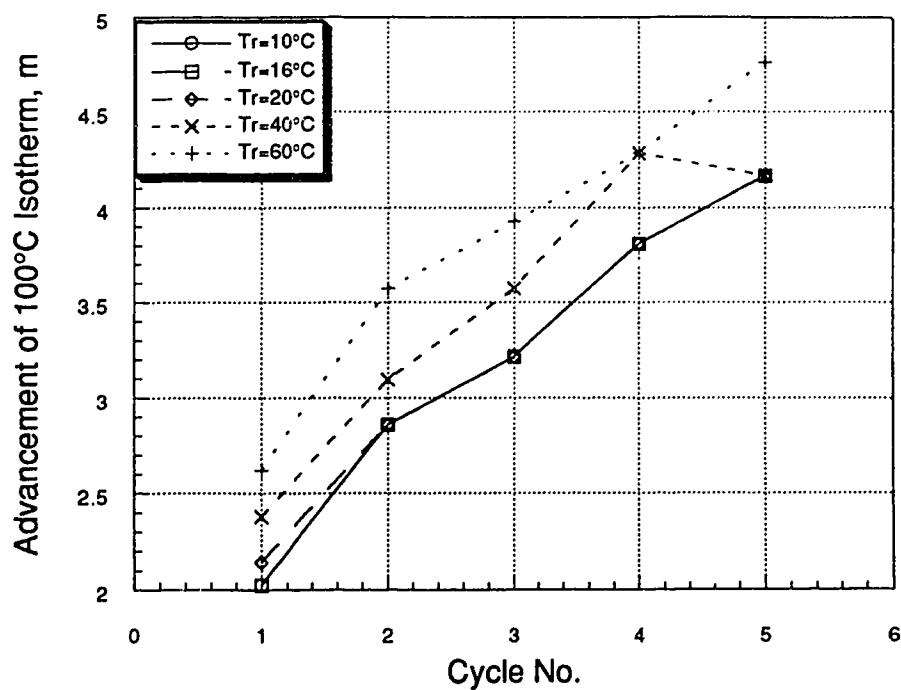


Figure 6.85—Effect of initial reservoir temperature on hot zone propagation.

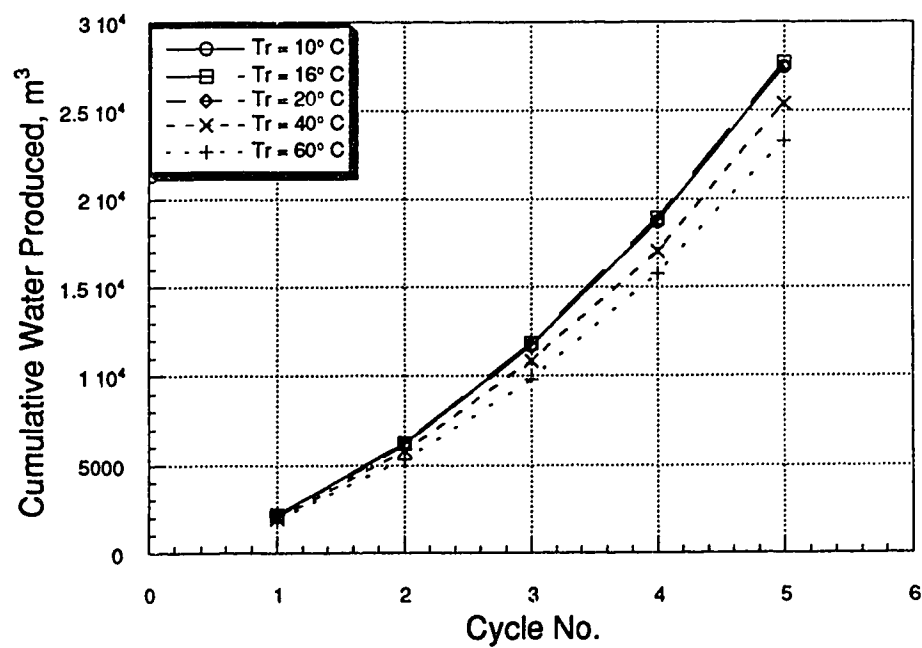


Figure 6.86—Effect of initial reservoir temperature on total water production.

6.6.9 Formation Thickness

Oil recovery from steam stimulation is affected by the pay thickness. The effect would be more prominent due to gravity drainage. The capability of the model to predict this effect was investigated. Reservoir height for the base case was 23.8 m. Two more runs with pay thicknesses of 30 m and 45 m were simulated.

Cycle oil productions are presented in Figure 6.87. As expected, a greater pay thickness produced a larger amount of oil. Interestingly, increasing the thickness from 30 to 45 m did not produce any significant amount of incremental oil over the 5 cycle period. Results are shown in Figure 6.88. This can be explained due to the fact that the injected steam volume was kept constant for all three cases. For the initial increase in thickness a reduction in injection rate per meter of pay was outweighed by the lower heat loss. Although heat loss to the over- and underburden reduced further with the increase of thickness, the same amount of heat was not sufficient to heat up the entire formation to a higher temperature level. As a result the oil production did not improve. Heat losses to the adjacent strata for the 45 m thickness was 45% to 50% less than for 23.8 m. Heat losses for all three cases are shown in Figure 6.89. Apart from a lower heat losses in the thicker formations, gravity flow was also more effective. Water production for thicker formations was much higher too. Results are shown in Figures 6.90 and 6.91.

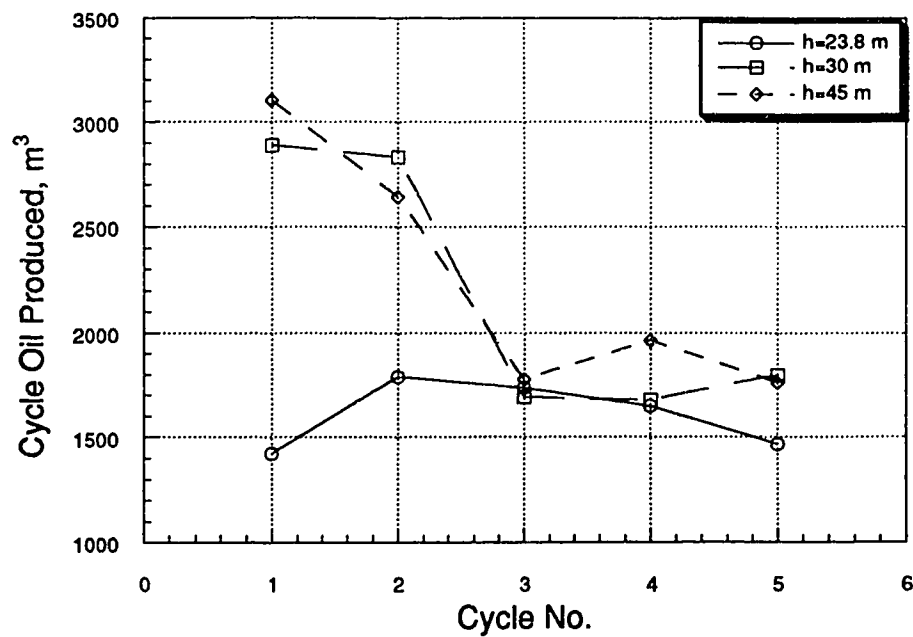


Figure 6.87—Oil produced at each cycle for different pay thicknesses.

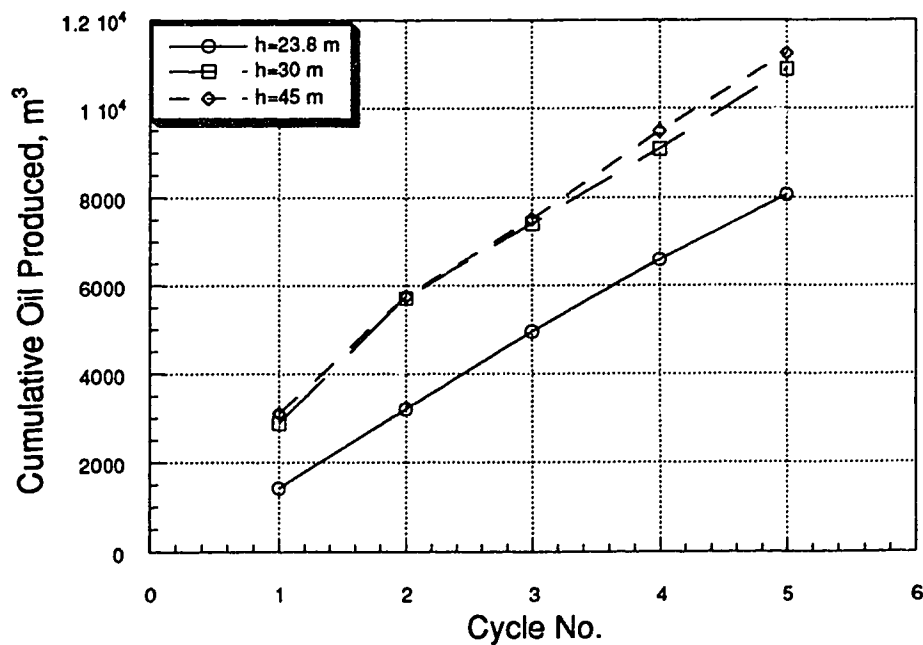


Figure 6.88—Cumulative oil production for different pay thicknesses.

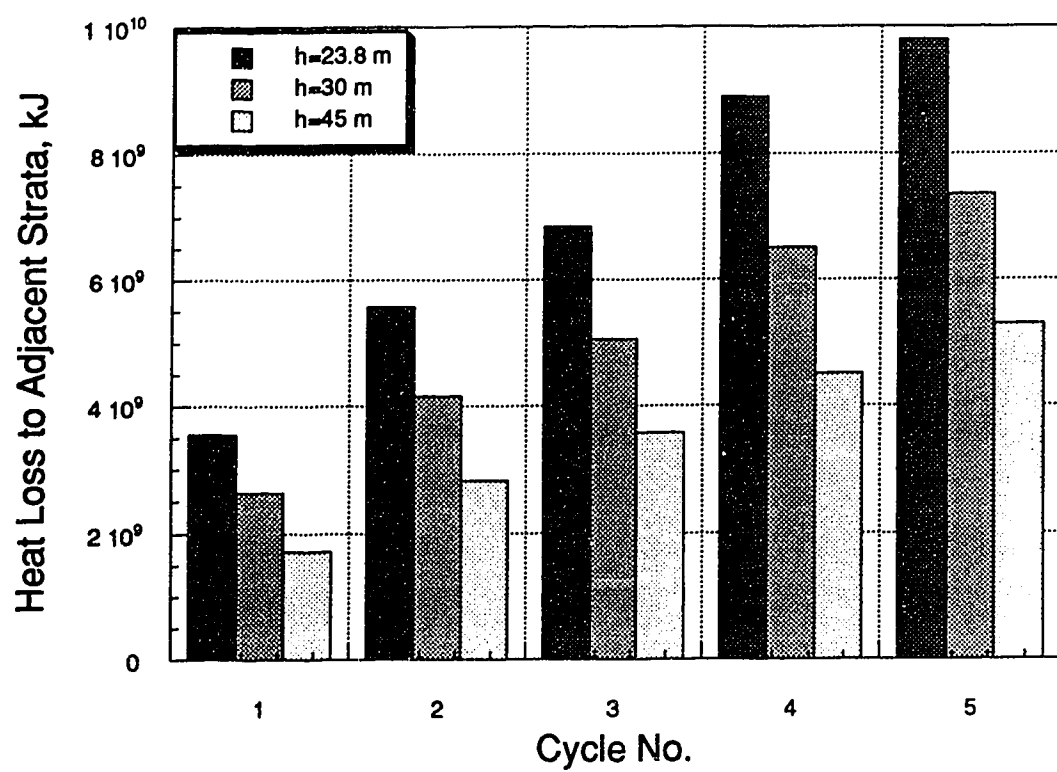


Figure 6.89—Effect of formation thickness on heat loss to over- and underburden.

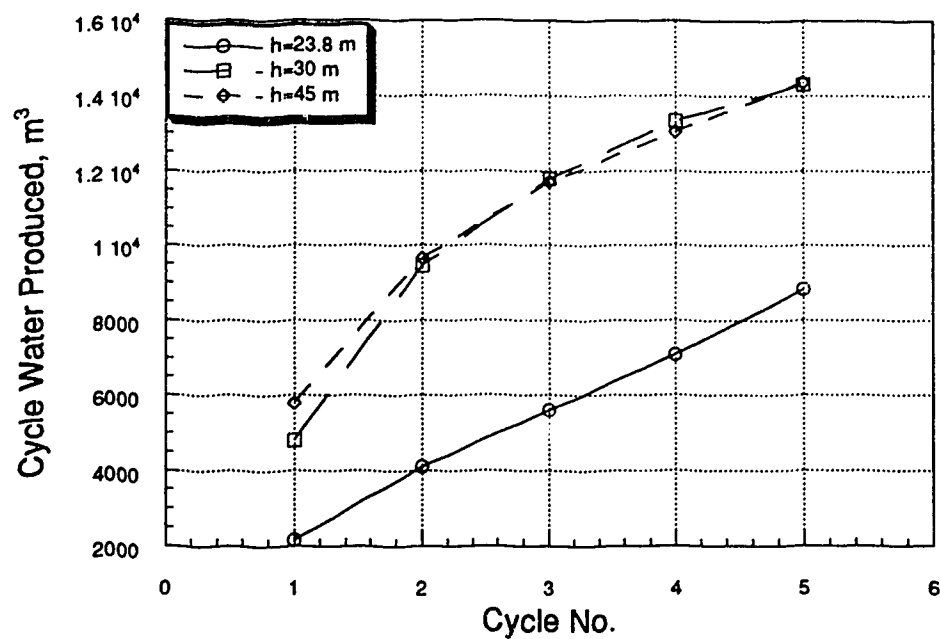


Figure 6.90—Water produced at each cycle for different pay thicknesses.

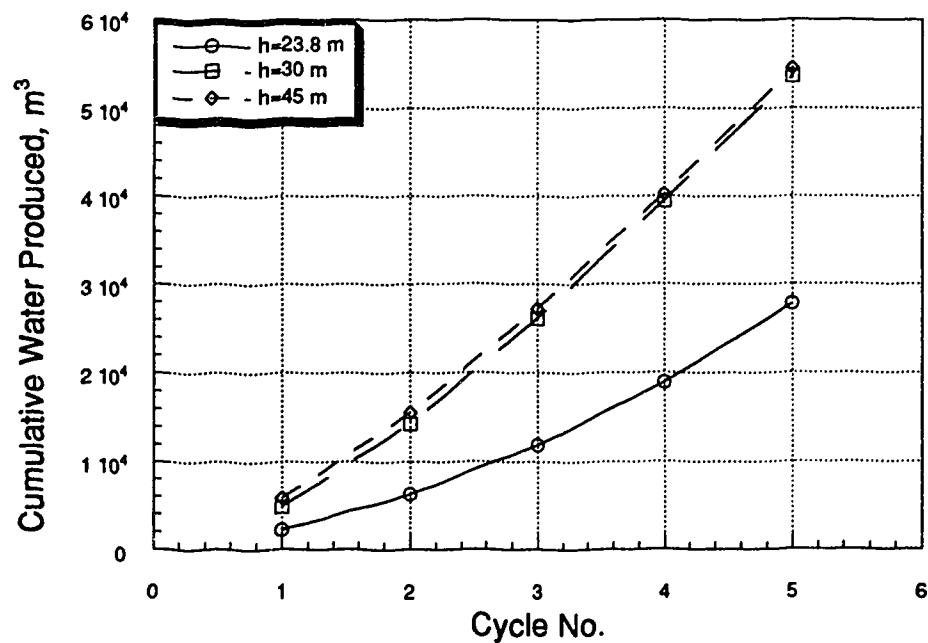


Figure 6.91—Cumulative water production for different pay thicknesses.

Chapter VII

CONCLUSIONS

An analytical predictive model was developed with the objective of defining heat and fluid flow in heavy oil CSS operations more accurately. Contributions made by this study and the conclusions reached are as follows:

1. For the first time a comprehensive analytical study of the elliptical shaped steam zone with a wellbore at the centre has been made. Flow into a circular wellbore in the centre of an elliptical flow geometry does not represent the flow pattern in the field (heavy oil). It underestimates production.
2. This is the first analytical model which considers gravity flow into a partially open fracture. It has been compared with a simulation study and yields satisfactory results.
3. An area weighted true average oil and water viscosity evaluation technique has been developed for the first time. It has been shown that the conventional method of calculating viscosity may produce rates as five times too high.
4. The importance of horizontal heat conduction in a two-zone heat balance has been established. Inclusion of the conduction term provides improved average hot and warm zone temperatures.
5. The model shows plausible response to variations of a wide variety of physical and operational parameters: steam volume, slug size, steam temperature, steam quality, formation thickness, hot zone boundary temperature, initial reservoir temperature, soak time and production time step.
6. This study provides a quick means of assessing CSS operations and optimization and providing a sensitivity study.

7.1 Suggestions for Future Studies

Several ideas were explored for further studies in the process of developing this model. The more important ones are:

1. To investigate the effect of a horizontal fracture.
2. To accommodate the concept of dilation and compaction, especially in the closed fracture case.
3. To implement the average temperature calculation method in a horizontal well steam injection process.
4. To apply the model to more field data.

REFERENCES

- Adams, R.H. and Khan, A.M. (1969): "Cyclic Steam Injection Project Performance Analysis and Some Results of a Continuous Steam Displacement Pilot," *JCPT* (January) 95-100.
- Arthur, J.E., Best, D.A., Jha, K.N. and Mourits, F.M. (1991): "An Analytical Composite Model for Cyclic Steam Stimulation in Elliptical Flow Geometry," presented at the 5th UNITAR Conference on Heavy Crude and Tarsands, Caracas, Venezuela, Aug. 4-9.
- Bang, H.W. (1984): "Simulation Study Shows Hysteresis Effect on Oil Recovery During a Cyclic Steam Process," *Oil and Gas J.* (Feb. 27) 83-86.
- Beattie, C.I., Boberg, T.C. and McNab, G.S. (1991): "Reservoir Simulation of Cyclic Steam Stimulation in the Cold Lake Oil Sands," *SPE* (May) 200-206.
- Ben-Naceur, K. and Stephenson, P. (1985): "Models of Heat Transfer in Hydraulic Fracturing," *SPE/DOE* 13865, presented at the Low Permeability Gas Reservoir Symposium of SPE/DOE, Denver, May 19-22.
- Bentsen, R.G. and Donahue, D.A. (1969): "A Dynamic Programming Model of the Cyclic Steam Injection Process," *JPT* (December) 1582-1596.
- Bidner, M.S., Horclo, M.K. and Vampa, V.C. (1990): "Analysis of the Transient Production of a Thermally Stimulated Well," *SPE* (November) 539-543.
- Biot, M.A., Massé, L. and Medlin, W.L. (1987): "Temperature Analysis in Hydraulic Fracturing," *JPT*, (November) 1389-1397.
- Boberg, T.C. and Lantz, R.B. (1966): "Calculation of the Production Rate of a Thermally Stimulated Well," *JPT* (December) 1613-1623.
- Boone, T.J., Gallant, R.J. and Kry, P.R. (1993): "Exploiting High-Rate Injection and Fracturing To Improve Areal Thermal Conformance in Cyclic Steam Stimulation," *SPE*

25796, presented at the International Thermal Operations Symposium, Bakersfield, CA, Feb. 8-10.

Boone, T.J. and Bharatha, S. (1993): "Temperature distribution Along Propagating Leakoff-Dominated Hot Water or Steam-Induced Fractures," SPE 25791, presented at the International Thermal Symposium, Bakersfield, CA, Feb. 8-10.

Buckles, R.S. (1979): "Steam Stimulation Heavy Oil Recovery at Cold Lake, Alberta," SPE 7994, presented at the California Regional Meeting of SPE, Ventura, CA, April 18-20.

Butler, R.M., McNab, G.S. and Lo, H.Y. (1979): "Theoretical Studies on the Gravity Drainage of Heavy Oil During In-Situ Steam Heating," presented at the 29th Canadian Chemical Engineering Conference, Sarina, ON, Oct. 1-3.

Carslaw, H.S. and Jaeger, T.C. (1959): *Conduction of Heat in Solids*, Oxford Press, London, 58-61.

Carter, R.D. (1957): "Derivation of the General Equation for Estimating the Extent of Fracture Area," Appendix to: "Optimum Fluid Characteristics for Fracture Extension," by Howard, G.C. and Fast, C.R., *Drill. and Prod. Prac.*, API, 261-270.

Chan, M.Y.S. and Sarioglu, G. (1992): "Numerical Modelling of Cyclically Steamed and Fractured Oil-Sand Reservoirs," SPE 22369, presented at the SPE international Meeting on Petroleum Engineering, Beijing, China, March 24-27.

Chase, C.A. and O'Dell, P.M. (1973): "Application of Variational Principles to Cap and Base Rock Heat Losses," *Trans. AIME*, **225**, II, 200-210.

Chen, H-L. (1987): "Analytical Modeling of Thermal Oil Recovery by Steam Stimulation and Steamflooding," Ph. D. dissertation, The University of Tulsa.

Chen, H-L. and Sylvester, N.D. (1990): "Appraisal of Analytical Steamflood Models," SPE 20023, presented at the 60th California Regional Meeting of the SPE, Ventura, CA, April 4-6.

Chen, H-L. (1993): *Personal Communication*, August 17.

Closmann, P.J. (1967): "Steam Zone Growth During Multiple-Layer Steam Injection," *SPEJ* (March) 1-10.

Closmann, P.J. (1968): "Steam Zone Growth in a Preheated Reservoir," *SPEJ* (September) 313-320.

Closmann, P.J., Ratliff, N.W. and Truitt, N.E. (1970): "A Steam-Soak Model for Depletion Type Reservoirs," *JPT* (June) 757-770.

Coats, K.H., Tek, M.R. and Katz, D.L. (1959): "Unsteady-State Liquid Flow Through Porous Media Having Elliptic Boundaries," *Trans. AIME*, **216**, 460-464.

Davidson, L.B., Miller, F.G. and Mueller, T.D. (1967): "A Mathematical Model of Reservoir Response During the Cyclic Injection of Steam," *SPEJ* (June) 174-188.

Denbina, E.S., Boberg, T.C. Rotter, M.B. (1991): "Evaluation of Key Reservoir Drive Mechanisms in the Early Cycles of Steam Stimulation at Cold Lake," *SPERE* (May) 207-211.

De Haan, H.J. and van Lookeren, J. (1969): "Early Results of Large-Scale Steam Soak Project in the Tia Juana Field, Western Venezuela," *JPT* (January) 101-110.

De Swaan, O.A. (1972): "Improved Numerical Model of Steam-Soak Process," *The Oil and Gas J.* (Jan. 3) 58-62.

Dietrich, J.K. (1981): "Relative Permeability During Cyclic Steam Stimulation of Heavy-Oil," *JPT* (October) 1987-1989.

Dietrich, J.K. (1986): "Cyclic Steaming of Tar Sands Through Hydraulically Induced Fractures," *SPERE* (May) 217-229.

Doscher, T.M. (1966): "Factors that Spell Success in Steaming Viscous Crude," *Oil and Gas J.* (July 11) 95-100.

- Duerksen, J.W., Cruikshank, G.W. and Wasserman, M.L. (1984): "Performance and Simulation of a Cold Lake Tar Sand Steam-Injection Pilot," *JPT* (October) 1781-1790.
- Dysart, G.R. and Whittsit, N.F. (1967): "Fluid Temperatures in Fractures," SPE 1902, presented at the 42nd Annual Fall Meeting of SPE, Houston, TX, Oct. 1-4.
- Ershaghi, I., Al-Adawiya, M.S. and Kogawan, V.D. (1983): "A Graphical Method Estimation of Production Response from Cyclic Steam Stimulation Using Past Performance Data," SPE11954, presented at the 58th Annual Fall Technical Conference and Exhibition of SPE, San Francisco, CA, Oct. 5-8.
- Farouq Ali, S.M. (1982): "Steam Injection Theories—A Unified Approach," SPE 10746, presented at the California Regional Meeting of the SPE, San Fransisco, CA, March 24-26.
- Farouq Ali, S.M. (1994): "CSS—Canada's Super Strategy for Oil Sands," *JCPT* (November) 16-19.
- Ferrer, J. and Farouq Aii, S.M. (1977): "A Three-Phase, Two-Dimensional Compositional Thermal Simulator for Steam Injection Processes," *JCPT* (Jan.-March) 78-90.
- Fialka, B.N., McClanahan, R.K., Robb, G.A. and Longstaffe, F.J. (1993): "The Evaluation of Cyclic Steam Stimulation in an Oil Sand Reservoir Using Post-steam Core Analysis," *JCPT* (February) 56-62.
- Forchheimer, Ph. (1930): *Hydraulik*, 3rd Ed., Chapt. III.
- Frizzell, D.F. (1990): "Analysis of 15 Years of Thermal Laboratory Data: Relative Permeability Saturation Endpoint Correlations for Heavy Oils," SPE 20528, presented at the 65th Annual Fall Technical Conference and Exhibition of SPE, New Orleans, LA, Sept. 23-26.
- Gajdica, R.J., Brigham, W.E. and Aziz, K. (1990): "A Semianalytical Thermal Model for Linear Steam Drive," SPE/DOE 20198, presented at the Seventh Symposium on Enhanced Oil Recovery of SPE/DOE, Tulsa, April 22-25.

- Gallant, R.J., Stark, S.D. and Taylor, M.D. (1993): "Steaming and Operating Strategies at a Midlife Cyclic Steam Stimulation Operation," SPE 25794, presented at the International thermal Operations Symposium, Bakersfield, CA, Feb. 8-10.
- Gomma, E.E. (1980): "Simplified Method for Predicting Oil Recovery by Steamflood," *JPT* (February) 325-332.
- Gontijo, J.E. (1983): "A Simple Cyclic Steam Analytical Model for Heavy Oil, Pressure Depleted Reservoirs," M.Sc. dissertation, Stanford University.
- Gontijo, J.E. and Aziz, K. (1984): "A Simple Analytical Model for Simulating Heavy Oil Recovery by Cyclic Steam in Pressure Depleted Reservoirs," SPE 13037, presented at the 59th Annual Technical Conference and Exhibition, Houston, TX, September 16-19.
- Gozde, S., Chhina, H.S. and Best, D.A. (1989): "An Analytical Cyclic Steam Stimulation Model for Heavy Oil Reservoirs," SPE 4757, presented at the California Regional Meeting of SPE, Bakersfield, CA, April 5-7.
- Gringarten, A.C., Ramey, JR., H.J. and Raghavan, R. (1974): "Unsteady-State Pressure Distributions Created by a Well With a Single Infinite-Conductivity Vertical Fracture," *SPEJ* (August) 347-360.
- Gros, R.P., Pope, G.A. and Lake, L.W. (1985): "Steam Soak Predictive Model." SPE 14240, presented at the 60th Annual Fall Technical Conference and Exhibition of SPE, Las Vegas, NV, Sept. 22-25.
- Hale, B.W. and Evers, J.F. (1981): "Elliptical Flow Equations for Vertically Fractured Gas Wells," *JPT* (December) 2489-2497.
- Hearn, C.L. (1969): "Effect of Latent Heat Content of Injected Steam in a Steam Drive," *JPT* (April) 374-375.
- Hong, K.C. (1994): "Effects of Steam Quality and Injection Rate on Steamflood Performance," *SPERE* (September) 53-64.

- Jones, J. (1977): "Cyclic Steam Reservoir Model for Viscous Oil, Pressure Depleted, Gravity Drainage Reservoirs," SPE 6544, presented at the California Regional Meeting of SPE, Bakerfield, April 13-15.
- Jones, J. and Cawthon, G.J. (1990): "Sequential Steam: An Engineered Cyclic Steaming Method," *JPT* (July) 898-901.
- Jones, J. (1992): "Why Cyclic Steam Predictive Models Get No Respect," *SPEE* (February) 67-74.
- Karyampudi, R.S. (1995): "Evaluation of Cyclic Steam Performance and Mechanisms in a Mobile Heavy Oil Reservoir at Elk Point Thermal Pilot," *JCPT* (March) 48-56.
- Kucuk, F. and Brigham, W.E. (1979): "Transient Flow in Elliptical System," *SPEJ* (December) 401-410.
- Kucuk, F. and Brigham, W.E. (1981): "Unsteady-State Water Influx in Elliptic and Anisotropic Reservoir/Aquifer Systems," *SPEJ* (June) 309-314.
- Kuo, C.H., Shain, S.A. and Pochas, D.M. (1970): "A Gravity Drainage Model for the Steam Soak Process," *SPEJ* (June) 119-126.
- Lauwerier, H.A. (1955): "The Transport of Heat in an Oil Layer Caused by the Injection of Hot Fluid," *Appl. Sci. Res., Sec. A*, **5**, 145.
- Leshchyshyn, T.H., Seyer, W.G. and Langdon, I. (1991): "Hall Plot and Fracture Growth Analysis as Applied to the PCEJ Cyclic Steam Process in the McMurry Oil Sands," presented at the 8th Annual Heavy Oil and Oil Sands Technical Symposium, U of Calgary/CHOA, Calgary, AB, March.
- Leshchyshyn, T.H., Farouq Ali, S.M., Settari, A. and Chan, M.Y. (1994): "Estimation of Dilation from Fall-off Data in a Hydraulically Fractured McMurry Oil Sands Well," presented at the 45th Annual Technical Meeting of CIM/AOSTRA, Calgary, AB, June 12-15.

Leshchyshyn, T.H. and Kennedy, W. (1994): "Post Core Analysis to Determine the Steam Flow Path in the McMurry Oil Sands," *JCPT* (September) 53-64.

Leshchyshyn, T.H. (1995): *Personal Communication*, January.

Lowe, K. and Donovan, T (1989): "Thermal Zone Monitoring in an Athabasca Oil Sand Pilot," presented at the 64th Annual Technical Meeting of SPE, San Antonio, TX.

Mandl, G. and Volek, C.W. (1969): "Heat and Mass Transport in Steam Drive Processes," *SPEJ* (March) 59-79; *Trans.*, AIME, **246**.

Martin, J.C. (1967): "A Theoretical Analysis of Steam Stimulation," *JPT* (March) 411-418.

Marx, J.W. and Langenheim, R.H. (1959): "Reservoir Heating by Hot Fluid Injection," *Trans.*, AIME, **216**, 312-315.

Matthews, C.S. and Lefkovits, H.C. (1956): "Gravity Drainage Performance of Depletion-Type Reservoirs in the Stripper stage," *Trans.*, AIME, **207**, 265-272.

McGee, B.C.W., Arthur, J.E. and Best, D.A. (1987): "Analytical Analysis of Cyclic Steam Stimulation Through Vertical Fractures," presented at the 38th Annual Technical Meeting of CIM, Calgary, AB, June 7-10.

Meyer, B.R. (1987): "Heat Transfer in Hydraulic Fracturing," SPE 17041, Eastern Regional Meeting of SPE, Pittsburgh, Oct. 21-23.

Muskat, M. (1937): *Flow of Homogeneous Fluids*, McGraw-Hill Book Company Inc., New York, 191, 389.

Myhill, N.A. and Stegemeier, G.L. (1978): "Steam-Drive Correlation and Prediction," *JCPT* (February) 173-182.

Nakornthap, K. and Evans, R.D. (1986): "Temperature Dependent Relative Permeability and Its Effects on Thermal Methods," *SPEE* (May) 230-242.

- Neuman, C.H. (1975): "A Mathematical Model of the Steam Drive Model," SPE 4757, presented at the California Regional Meeting of SPE, Ventura, April 2-4.
- Neuman, C.H. (1985): "A Gravity Override Model of Steam Drive," *JPT* (January) 163-169.
- Niko, H. and Troost, P.J.P.M. (1971): "Experimental Investigation of Steam Soaking in a Depletion Type Reservoir," *JCPT* (August) 1006-1014.
- Nzekwu, B.I., Hallam, R.J. and Williams, G.J.J. (1990): "Interpretation of Temperature Observations From a Cyclic-Steam/In-Situ-Combustion Project," *SPEFE* (May) 163-169.
- Obut, S.T. and Ertekin, T. (1987): "A Composite System Solution in Elliptic Flow Geometry," *SPEFE* (September) 227-238.
- Okoye, C.U., Matese, J.J., Hayatdavoudi, A. and Ghalambor, A. (1988): "Application of Laplace Transformation in Naturally Fractured Reservoirs: Part I - Theoretical Treatment," SPE 17643, presented at the Permian Basin Oil and Gas Recovery Conference, Texas, March 10-11.
- Owens, W.D. and Suter, V.E. (1965): "Steam Stimulation for Secondary Recovery," *JCPT* (Oct.-December) 227-235.
- Perkins, T.K. and Gonzalez, J.A. (1985): "The Effect of Thermoelastic Stresses on Injection Well Fracturing," *SPEJ* (February) 78-88.
- Pethrick, W.D., Sennhauser, E.S. and Harding, T.G. (1988): "Numerical Modelling of Cyclic Steam Stimulation in Cold Lake," *JCPT* (Nov.-Dec.) 89-97.
- Powers, W.L., Kirkham, D. and Snowden, G. (1967): "Orthonormal Function Tables and the Seepage of Steady Rain Through Soil Bedding," *J. GeoPhys. Res.*, 72(24) 6225-6237.
- Prats, M. (1961): "Effect of Vertical Fractures on Reservoir Behavior - Incompressible Fluid Case," *SPEJ* (June) 105-118; *Trans.*, AIME, 224.

Prats, M., Hazebroek, P. and Strickler, W.R. (1962): "Effect of Vertical Fractures on Reservoir Behavior - Compressible Fluid Case," *SPEJ* (June) 87-94; *Trans.*, AIME, **225**.

Prats, M. (1986): *Thermal Recovery*, SPE Monograph Series.

Ramey, H.J., Jr. (1959): "Discussion on Reservoir Heating by Hot Fluid Injection," *Trans.*, AIME, **216**, 364-365.

Ramey, H.J., Jr. (1970): "Approximate Solutions for Unsteady Liquid Flow in Composite Reservoirs," *JCPT* (Jan.-March) 32-37.

Reis, J.C. (1990): "Studies of Fractures Induced During Cyclic Steam Injection," presented at the 60th California Regional Meeting of the SPE, Ventura, CA, April 4-6.

Seba, R.D., Jr. and Perry, G.E. (1969): "A Mathematical Model of Repeated Steam Soaks of Thick Gravity Drainage Reservoirs," *JPT* (January) 87-94.

Shepherd, D.W. (1979): "Predicting Bitumen Recovery from Steam Stimulation," *World Oil* (September) 68-72.

Sinclair, A.R. (1971): "Heat Transfer Effects in Deep Well Fracturing," *JPT* (December) 1484-1492.

Smith-Magowan, D., Brauge, A. and Hepler, L.G. (1982): "Specific Heat of Athabasca Oil Sands and Components," *JCPT* (May-June) 28-32.

Souza, A.L.S., Pedrosa Jr., O.A. and Marchesin, D. (1987): "A New Approach for Calculating Formation heat Loss," presented at the 2nd International Symposium on Enhanced Oil Recovery, Maracaibo, Venezuela, Feb. 24-27.

Stanislav, J.F., Easwaran, C.V. and Kokal, S.L. (1987): "Analytical Solutions for Vertical Fractures in a Composite System," *JCPT* (Sept.-Oct.) 51-56.

- Sylvester, N.B. and Chen, H-L. (1988): "An Improved Cyclic Steam Stimulation Model for Pressure-Depleted Reservoirs," SPE 17420, presented at the California Regional Meeting of SPE, Long Beach, March 23-25.
- Svrcek, W.Y. and Mehrotra, A.K. (1988): "One Parameter Correlation for Bitumen Viscosity," *Chem. Eng. Res. Des.*, Vol. 66, July, 323-326.
- Tamim, M. and Farouq Ali, S.M. (1995): "A New Analytical Cyclic Steam Stimulation Model Including Formation Fracturing," presented at the 46th Annual Technical Meeting of CIM, Calgary, AB, May 14-17.
- Tortike, W.S. and Farouq Ali, S.M. (1989): "Saturated Steam -Property Functional Correlations for Fully Implicit Thermal Reservoir Simulation," *SPE* (November) 471-474.
- Towson, D.E. and Boberg, T.C. (1967): "Gravity Drainage in Thermally Stimulated Wells," *JCPT* (Oct.-Dec.) 130-135.
- Trebolle, R.L., De Paz, M.C. and Martinez, D.E. (1993): "Parametric Studies of the Design Factors for Cyclic Steam Injection in Lake Maracaibo Oil Fields," SPE 25810, presented at the International Thermal Operations Symposium, Bakersfield, CA, Feb. 8-10.
- Van Everdingen, A.F. and Hurst, W. (1949): "The Application of Laplace Transformation to Flow Problems in Reservoirs," *Trans., AIME*, **186**, 305-324.
- Van der Ploeg, R.R., Kirkham, D. and Boast, C.W. (1971): "Steady State Well Flow Theory for a Confined Elliptical Aquifer," *Water Resource Research* (August) 942-954.
- Van Lookeren, J. (1983): "Calculation Methods for Linear and Radial Steam Flow in Oil Reservoirs," *SPEJ* (June) 427-439.
- Vinsome, P.K.W. and Westerveld, J. (1980): "A Simplified Method for Predicting Cap and Base Rock Heat Losses in Thermal Reservoir Simulators," *JCPT* (July-Sept.) 87-90.

- Vittoratos, E. (1990): "Interpretation of Production Data From Cyclic Steam Stimulation at Cold Lake," SPE 20527, presented at the 65th Annual Fall Technical Conference and exhibition of SPE, New Orleans, LA, Sept 23-26.
- Vittoratos, E. (1991): "Flow Regimes During Cyclic Steam Stimulation at Cold Lake," *JCPT* (Jan.-Feb.) 82-86.
- Vogel, J.V. (1984): "Simplified Heat Calculations for Steam Drive," *JPT* (July) 1127-1136.
- Weinstein, H. G. (1972): "Semi-Analytic Method for Thermal Coupling of Reservoir and Overburden," *SPEJ* (October) 439-447.
- Weinstein, H. G. (1974): "Extended Semi-Analytical Method for Increasing and Decreasing Boundary Temperature," *SPEJ* (April) 152-164.
- Wheeler, J.A. (1969): "Analytical Calculations for Heat Transfer from Fractures," SPE 2494, Improved Oil Recovery Symposium of SPE, Tulsa, April 13-15.
- Whittsitt, N.F. and Dysart, G.R. (1970): "The Effect of Temperature on Stimulation Design," *JPT* (April) 493-502.
- Williamson, A.S., Dake, L.P. and Chappelle, J.E. (1976): "A Steam-Soak Model for an Isothermal Reservoir Simulator," SPE 5739, presented at the 4th Symposium of Numerical Simulation of Reservoir Performance of SPE, Los Angeles, CA, Feb. 19-20.
- Yortsos, Y.C. and Gavalas, G.R. (1981a): "Analytical Modeling of Oil Recovery by Steam Injection: Part I - Upper Bounds," *SPEJ* (April) 162-178.
- Yortsos, Y.C. and Gavalas, G.R. (1981b): "Analytical Modeling of Oil Recovery by Steam Injection: Part II - Asymptotic and Approximate Solutions," *SPEJ* (April) 179-190.

Appendix A

CORRECTION OF SYLVESTER AND CHEN (1988) EQUATION

Sylvester and Chen (1988) developed a steam soak model for a homogeneous gravity drained pressure-depleted reservoir. They argued that the proposed gravity drainage model by Towson and Boberg (1967) had several uncertain terms. One has to calculate fluid heights at the wellbore, heated radius and the average fluid height in the heated zone. Chen (1987) in his Ph.D. dissertation derived an equation which eliminated all of these parameters and was replaced with one parameter. This flow equation was derived based on Equation A7 of Towson and Boberg (1967) which is Equation III-19 in Chen's thesis. There is a serious error in the derivation of this equation. Chen's Equation III-19 is Equation A.1 below. Starting with this equation, Chen's error will be shown:

$$\bar{h} = h_h - \frac{h_h^2 - h_w^2}{(R_h^2 - r_w^2)\bar{h}\left(\ln \frac{R_h}{r_w} - 0.5\right)} \left(\frac{R_h^2 - r_w^2}{8}\right). \quad (\text{A.1})$$

If $B = \left(\ln \frac{R_h}{r_w} - 0.5\right)$, then Equation A.1 can be written as

$$\bar{h} = h_h - \frac{h_h^2 - h_w^2}{8\bar{h}B}. \quad (\text{A.2})$$

After rearranging,

$$h_h^2 - 8\bar{h}Bh_h + 8\bar{h}^2B - h_w^2 = 0. \quad (\text{A.3})$$

This is a quadratic equation in h_h , so the solution is

$$h_h = \frac{8\bar{h}B \pm \sqrt{64\bar{h}^2B^2 - 32\bar{h}^2B + 4h_w^2}}{2}, \quad (\text{A.4})$$

$$h_h = 4\bar{h}B \pm \sqrt{16\bar{h}^2B^2 + h_w^2 - 8\bar{h}^2B}. \quad (\text{A.5})$$

Instead of the (+) sign in front of h_w^2 , Chen proceeded with a (-) sign and derived a relationship between h_w and h_h in terms of B which is (using his relationship $\bar{h} = (h_w + h_h) / 2$):

$$h_h^2 = \frac{2B+1}{2B-1} h_w^2. \quad (\text{A.6})$$

If one proceeds with the right sign, the above relationship cannot be reached. Taking squares of both sides of Equation A.5 and assuming that $\bar{h} = (h_w + h_h) / 2$, as Chen did, it can be written

$$h_h^2 - h_w^2 = B \left[8h_h \left(\frac{h_h + h_w}{2} \right) - 8 \left(\frac{h_w^2 + 2h_w h_h + h_h^2}{4} \right) \right], \quad (\text{A.7})$$

$$h_h^2 - h_w^2 = 2B(h_h^2 - h_w^2). \quad (\text{A.8})$$

This gives us $B=0.5$ or with rearrangement $h_w = h_h$, neither of which gives us any meaningful correlation. Chen (1993) was apprised of this error and recognized the mistake.

Appendix B

FLOW INTO A WELL LOCATED AT THE CENTRE OF AN ELLIPTICAL DRAINAGE BOUNDARY

The standard procedure to solve this problem is to employ elliptical coordinates. Van der Ploeg, Kirkham and Boast (1971) presented a closed-form solution for steady-state saturated flow into a finite circular wellbore in an elliptical confined aquifer. They solved the flow problem for a number of well locations in an isotropic and homogeneous aquifer.

B.1 Well at the Centre of an Ellipse

The equation of ellipse in a rectangular coordinate is

$$\frac{x^2}{a^2} + \frac{y^2}{b^2} = 1. \quad (\text{B.1})$$

Using polar coordinates (R, θ) , x and y may be written as

$$x = R \cos \theta, \quad (\text{B.2})$$

$$y = R \sin \theta, \quad (\text{B.3})$$

and the equation of ellipse for a point $P(R, \theta)$ at the boundary is

$$R^2 \left(\frac{\cos^2 \theta}{a^2} + \frac{\sin^2 \theta}{b^2} \right) = 1. \quad (\text{B.4})$$

B.1.1 Boundary Conditions

$$\text{a. } \Phi = 0 \quad \text{for } r = r_w \quad 0 \leq \theta \leq \pi/2 \quad (\text{B.5})$$

$$\text{b. } \Phi = 1 \quad \text{for } r = R \quad 0 \leq \theta \leq \pi/2 \quad (\text{B.6})$$

$$\text{c. } \partial \Phi / \partial \theta = 0 \quad \text{for } \theta = 0 \quad r_w < r < a \quad (\text{B.7})$$

$$\text{d. } \partial \Phi / \partial \theta = 0 \quad \text{for } \theta = \pi/2 \quad r_w < r < b \quad (\text{B.8})$$

Laplace's equation in polar coordinates is

$$\frac{\partial^2 \Phi}{\partial r^2} + \frac{1}{r} \frac{\partial \Phi}{\partial r} + \frac{1}{r^2} \frac{\partial^2 \Phi}{\partial \theta^2} = 0. \quad (\text{B.9})$$

The solution of this problem should give an expression of ϕ which would satisfy the boundary conditions and Laplace's equation.

B.1.2 Solution

The authors used the Gram-Schmidt method as modified by Powers, Kirkham and Snowden (1967) to determine the solution as

$$\Phi = \sum_{m=0}^N A_{Nm} u_m(r, \theta), \quad (\text{B.10})$$

where

$$m = 0, 1, 2, \dots, N;$$

$$N = 0, 1, 2, \dots, \infty;$$

$$u_m(r, \theta) = \frac{\left(\frac{r}{a}\right)^{2m} - \left[\frac{r_w^2}{(ar)}\right]^{2m}}{1 - \left(\frac{r_w^2}{a^2}\right)^{2m}} \cos 2m\theta. \quad (\text{B.11})$$

Replacing r with R at the boundary and using Equation B.4 to express R in term of θ , $u(r, \theta)$ may be written as

$$u_m(\theta) = \frac{\left(\frac{R^2}{a^2}\right)^m - \left[\frac{r_w^2}{a^2} \frac{r_w^2}{R^2}\right]^m}{1 - \left(\frac{r_w^2}{a^2}\right)^{2m}} \cos 2m\theta, \quad (\text{B.12})$$

where

$$R^2 = \left(\frac{\cos^2 \theta}{a^2} + \frac{\sin^2 \theta}{b^2} \right)^{-1}. \quad (\text{B.13})$$

The hydraulic head may be written as

$$\Phi_{r=R} = \sum_{m=0}^N A_{Nm} u_m(\theta). \quad 0 \leq \theta \leq \pi/2 \quad (\text{B.14})$$

Applying boundary condition (b) the hydraulic head may be written as

$$\Phi_{r=R} = 1 = \sum_{m=0}^N A_{Nm} u_m(\theta). \quad 0 \leq \theta \leq \pi/2 \quad (\text{B.15})$$

Powers *et al.* (1967) derived a table of orthonormal functions to solve potential flow problems like seepage of steady rain through soil bedding. In accordance with Powers *et al.*, the two constants to determine A_{Nm} in this problem are

$$w_m = \int_0^{\pi/2} (1) u_m(\theta) d\theta, \quad m = 0, 1, 2, \dots, N \quad (\text{B.16})$$

and

$$u_{mn} = \int_0^{\pi/2} u_m(\theta) u_n(\theta) d\theta. \quad m = 0, 1, 2, \dots, N \quad n \leq m \quad (\text{B.17})$$

The parameters $u_m(\theta)$ and $u_n(\theta)$ may be determined from Equation B.12. When $N \rightarrow \infty$, boundary condition (b) is satisfied exactly. It is difficult to calculate the above integrations analytically. A more accurate Gaussian quadrature numerical integration method was used to evaluate the functions w_m and u_{mn} , instead of the Simpson's rule suggested by the authors. It can be seen that terms with zero subscripts produce indeterminants. Using l'Hôpital's rule u_0 would be

$$u_0(\theta) = \frac{\ln \frac{r}{r_w}}{\ln \frac{a}{r_w}}. \quad (\text{B.18})$$

Therefore, the hydraulic head may be written as

$$\Phi = A_{N0} \frac{\ln \frac{r}{r_w}}{\ln \frac{a}{r_w}} + \sum_{m=1}^N A_{Nm} \frac{\left(\frac{r}{a}\right)^{2m} - \left[\frac{r_w^2}{(ar)}\right]^{2m}}{1 - \left(\frac{r_w^2}{a^2}\right)^{2m}} \cos 2m\theta. \quad (\text{B.19})$$

After the values of w_m and u_{mn} are determined, all A_{Nm} values can be calculated by using Table 2 of Powers *et al.* (1967).

B.2 Sequential Formulas Presented by Powers et al.

$$A_{Nm} = E_m - \sum_{p=m+1}^N E_p J_{pm} \quad (\text{B.20})$$

$$E_m = G_m / D_m \quad m = 0, 1, 2, \dots, N \quad (\text{B.21})$$

$$G_m = w_m - \sum_{n=0}^{m-1} C_{mn} G_n \quad m = 0, 1, 2, \dots, N \quad (\text{B.22})$$

$$J_{m0} = C_{m0} - \sum_{n=1}^{m-1} C_{mn} J_{n0} \quad n = 1, 2, 3, \dots \quad (\text{B.23})$$

$$J_{mn} = C_{mn} - \sum_{r=n+1}^{m-1} C_{mr} J_{rn} \quad m = 2, 3, 4, \dots \quad (\text{B.24})$$

$$n = 1, 2, 3, \dots, m-1$$

$$C_{mn} = \frac{U_{mn} - \sum_{r=0}^{n-1} J_{nr} U_{mr}}{D_n} \quad m = 1, 2, 3, 4, \dots \quad (\text{B.25})$$

$$n = 0, 1, 2, 3, \dots, m-1$$

$$D_m = U_{mn} - \sum_{n=0}^{m-1} C_{mn}^2 D_n \quad m = 0, 1, 2, 3, 4, \dots \quad (\text{B.26})$$

$$n = 0, 1, 2, 3, 4, \dots$$

B.3 Well Discharge

Using Darcy's equation for potential flow for unit thickness, the flow rate q can be written as

$$q = -K\Delta\Phi \int_0^{2\pi} \left(\frac{d\Phi}{dr} \right)_{r=r_w} r d\theta \quad r_w \rightarrow 0, \quad (\text{B.27})$$

where K is the hydraulic conductivity. Multiplying the above equation with the thickness h , the total flow is

$$q = -Kh\Delta\Phi \int_0^{2\pi} \left(\frac{d\Phi}{dr} \right)_{r=r_w} r d\theta \quad r_w \rightarrow 0. \quad (\text{B.28})$$

The flow rate for a well in the centre of an elliptical drainage system is

$$q = -\frac{2\pi Kh A_{N0} \Delta\Phi}{\ln \frac{a}{r_w}}. \quad (\text{B.29})$$

Appendix C

HEAT LOSS CALCULATION TO THE CAP ROCK

Vinsome and Westerveld (1980) proposed a simple solution to the thermal diffusivity equation in the cap and base rock. A fitting function

$$T(t, z) = (T_0 + pz + qz^2)e^{-z/d}, \quad (C.1)$$

was used to approximate the temperature profile in the cap rock, where T_0 is the interface temperature and d is the diffusivity length. The parameters p and q are to be determined. This is a sensible function to pick to describe the temperature profile. The function automatically satisfies the two boundary conditions ($T=0$ at $z=0$ and $T=0$ at $z=\infty$).

The equation of heat flow into the cap rock is

$$\frac{\partial T}{\partial t} = \alpha_h \frac{\partial^2 T}{\partial z^2}. \quad (C.2)$$

The above equation can be written satisfying the interface condition as

$$\frac{\partial T_0}{\partial t} = \alpha_h \left. \frac{\partial^2 T}{\partial z^2} \right|_{z=0}. \quad (C.3)$$

Inserting Eqn. C.1 into Eqn. C.3, together with a finite-difference discretization they came up with a solution for the heat loss rate and the energy stored in the cap rock. These equations were presented in the main text (Eqns. 4.16, 4.17) and are repeated here for convenience.

$$\dot{q}_L = k_h \left(\frac{T_0}{d} - p \right)$$

$$E_c = \frac{k_h}{\alpha_h} d (T_0 + pd + 2qd^2)$$

Arthur *et al.* (1991) defined the parameters in the following manner,

$$p = \frac{\frac{\alpha_h T_0 \Delta t}{d} + I^n - \frac{d^3(T_0 - T_0^n)}{\alpha_h \Delta t}}{3d^2 + \alpha_h \Delta t}, \quad (\text{C.4})$$

$$q = \frac{2pd - T_0 + \frac{d^2(T_0 - T_0^n)}{\alpha_h \Delta t}}{2d^2}, \quad (\text{C.5})$$

$$d = \frac{\sqrt{\alpha_h \Delta t}}{2}, \quad (\text{C.6})$$

and

$$I^n = T_0^n d^n + p^n (d^n)^2 + 2q^n (d^n)^3. \quad (\text{C.7})$$

The heat loss term was expressed as

$$\dot{q}_L = \alpha_* T_0 - k \alpha_{n2}, \quad (\text{C.8})$$

where $\alpha_* = k \left(\frac{1}{d} - \alpha_{n1} \right)$ and

$$\alpha_{n1} = \frac{\alpha_h \Delta t}{d(3d^2 + \alpha_h \Delta t)} - \frac{d^3}{\alpha_h \Delta t(3d^2 + \alpha_h \Delta t)}, \quad n=1, 2 \quad (\text{C.9})$$

$$\alpha_{n2} = \frac{T_0^n d^3}{\alpha_h \Delta t(3d^2 + \alpha_h \Delta t)} + \frac{I^n}{3d^2 + \alpha_h \Delta t}. \quad (\text{C.10})$$

Appendix D

AVERAGE ZONE TEMPERATURES DURING SOAK AND PRODUCTION

A heat balance is done on two concentric elliptical cylinders (Fig. D.1) to obtain the average temperatures. The parameters A_1 and A_2 are the heat conducting areas of the hot and warm zones adjacent to the cap and base rocks. They are assumed to be same at the top and at the bottom. The parameter A_b is the area between the two zones.

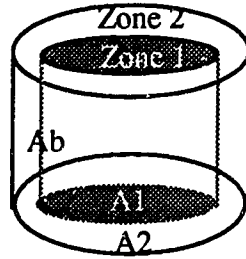


Figure D.1—Physical diagram for the heat balance.

Heat balance in the hot region (zone 1)

$$-\frac{\partial}{\partial t}(A_1 h M_1 T_1) = q_1 \rho_1 C_{p1}(T_1 - T_R) - q_2 \rho_2 C_{p2}(T_1 - T_2) + Q_1(t) + Q_b(t). \quad (D.1)$$

Heat balance in the warm region (zone 2)

$$-\frac{\partial}{\partial t}(A_2 h M_2 T_2) = q_2 \rho_2 C_{p2}(T_1 - T_2) + Q_2(t) - Q_b(t). \quad (D.2)$$

Assuming the flow rates and the fluid and rock properties to be constant during a time step, the above equations can be written in expanded form as

$$-A_1 h M_1 \frac{dT_1}{dt} = q_1 \rho_1 C_{p1}(T_1 - T_R) - q_2 \rho_2 C_{p2}(T_1 - T_2) + (2A_1 + A_b)(\alpha_s T_1 - k \alpha_{21}), \quad (D.3)$$

$$-A_2 h M_2 \frac{dT_2}{dt} = q_2 \rho_2 C_{p2}(T_1 - T_2) + 2A_2(\alpha_s T_2 - k \alpha_{22}) - A_b(\alpha_s T_1 - k \alpha_{21}). \quad (D.4)$$

The hot zone equation can further be expanded into

$$\begin{aligned}\frac{dT_1}{dt} &= -\frac{q_1 \rho_1 C_{p1}}{A_1 h M_1} (T_1 - T_R) + \frac{q_2 \rho_2 C_{p2}}{A_1 h M_1} (T_1 - T_2) - \frac{\alpha_s (2A_1 + A_b)}{A_1 h M_1} T_1 + \frac{k_h \alpha_{21} (2A_1 + A_b)}{A_1 h M_1}, \\ \frac{dT_1}{dt} &= -\beta_1 (T_1 - T_R) + \beta_2 (T_1 - T_2) - \beta_3 T_1 + \beta_4, \\ \frac{dT_1}{dt} &= (\beta_2 - \beta_1 - \beta_3) T_1 + \beta_1 T_R - \beta_2 T_2 + \beta_4, \\ \frac{dT_1}{dt} &= \beta_5 T_1 - \beta_2 T_2 + \beta_1 T_R + \beta_4, \\ \frac{dT_1}{dt} &= \beta_5 T_1 - \beta_2 T_2 + \beta_6.\end{aligned}\tag{D.5}$$

Using the operator D for d/dt, the equation may be written as

$$(D - \beta_5) T_1 + \beta_2 T_2 - \beta_6 = 0.\tag{D.6}$$

Similarly for zone 2,

$$\begin{aligned}\frac{dT_2}{dt} &= (\beta_7 - \beta_8) T_2 - (\beta_7 - \beta_{11}) T_1 + \beta_9 - \beta_{12}, \\ \frac{dT_2}{dt} &= \beta_{10} T_2 - \beta_{13} T_1 + \beta_{14}.\end{aligned}\tag{D.7}$$

Using the operator D

$$\beta_{13} T_1 + (D - \beta_{10}) T_2 - \beta_{14} = 0.\tag{D.8}$$

The constants are defined as

$$\beta_1 = \frac{q_1 \rho_1 C_{p1}}{A_1 h M_1},\tag{D.9}$$

$$\beta_2 = \frac{q_2 \rho_2 C_{p2}}{A_1 h M_1},\tag{D.10}$$

$$\beta_3 = \frac{\alpha_s (2A_1 + A_b)}{A_1 h M_1},\tag{D.11}$$

$$\beta_4 = \frac{k_h \alpha_{21} (2A_1 + A_b)}{A_1 h M_1}, \quad (D.12)$$

$$\beta_5 = \beta_2 - \beta_1 - \beta_3, \quad (D.13)$$

$$\beta_6 = \beta_1 T_R + \beta_4, \quad (D.14)$$

$$\beta_7 = \frac{q_2 \rho_2 C_{p2}}{A_2 h M_2}, \quad (D.15)$$

$$\beta_8 = \frac{2\alpha_*}{h M_2}, \quad (D.16)$$

$$\beta_9 = \frac{2k_h \alpha_{22}}{h M_2}, \quad (D.17)$$

$$\beta_{10} = \beta_7 - \beta_8, \quad (D.18)$$

$$\beta_{11} = \frac{A_b \alpha_*}{A_2 h M_2}, \quad (D.19)$$

$$\beta_{12} = \frac{A_b k_h \alpha_{21}}{A_2 h M_2}, \quad (D.20)$$

$$\beta_{13} = \beta_7 - \beta_{11}, \quad (D.21)$$

$$\beta_{14} = \beta_9 - \beta_{12}. \quad (D.22)$$

The following differential equations have to be solved simultaneously.

$$(D - \beta_5)T_1 + \beta_2 T_2 = \beta_6 \quad (D.23)$$

$$\beta_{13}T_1 + (D - \beta_{10})T_2 = \beta_{14} \quad (D.24)$$

The determinant of the matrix

$$\begin{vmatrix} (D - \beta_5) & \beta_2 \\ \beta_{13} & (D - \beta_{10}) \end{vmatrix} \quad (D.25)$$

is $D^2 - DA - B$, where, $A = \beta_5 + \beta_{10}$ and $B = \beta_{13}\beta_2 - \beta_{10}\beta_5$. Now it can be written

$$\Delta T_1 = \begin{vmatrix} \beta_6 & \beta_2 \\ \beta_{14} & (D - \beta_{10}) \end{vmatrix} = D\beta_6 - P, \quad (\text{D.26})$$

and

$$\Delta T_2 = \begin{vmatrix} (D - \beta_5) & \beta_6 \\ \beta_{13} & \beta_{14} \end{vmatrix} = D\beta_{14} - Q, \quad (\text{D.27})$$

where, $P = \beta_6\beta_{10} + \beta_2\beta_{14}$ and $Q = \beta_5\beta_{14} + \beta_6\beta_{13}$. The characteristic equations for T_1 and T_2 are found to be,

$$T_1 = C_1 e^{\lambda_1 t} + C_2 e^{\lambda_2 t} + \frac{P}{B}, \quad (\text{D.28})$$

$$T_2 = C_3 e^{\lambda_1 t} + C_4 e^{\lambda_2 t} + \frac{Q}{B}, \quad (\text{D.29})$$

where,

$$\lambda_1 = \frac{A + \sqrt{A^2 + 4B}}{2}, \quad (\text{D.30})$$

$$\lambda_2 = \frac{A - \sqrt{A^2 + 4B}}{2}, \quad (\text{D.31})$$

$$A = \beta_5 + \beta_{10}, \quad (\text{D.32})$$

$$B = \beta_{13}\beta_2 - \beta_5\beta_{10}, \quad (\text{D.33})$$

$$P = \beta_6\beta_{10} + \beta_2\beta_{14}, \quad (\text{D.34})$$

and

$$Q = \beta_5\beta_{14} + \beta_6\beta_{13}. \quad (\text{D.35})$$

After applying the initial condition and simplifying, the two average temperatures can be expressed as

$$T_1 = C_1 e^{\lambda_1 t} + C_2 e^{\lambda_2 t} + \frac{P}{B}, \quad (\text{D.36})$$

$$T_2 = \frac{\beta_5 - \lambda_1}{\beta_2} C_1 e^{\lambda_1 t} + \frac{\beta_5 - \lambda_2}{\beta_2} C_2 e^{\lambda_2 t} + \frac{\beta_5 P}{\beta_2 B} + \frac{\beta_6}{\beta_2}, \quad (\text{D.37})$$

where,

$$C_1 = \frac{\beta_2 T_2^0 - T_1^0 (\beta_5 - \lambda_2) - \beta_6 - \lambda_2 \frac{P}{B}}{\lambda_2 - \lambda_1}, \quad (\text{D.38})$$

$$C_2 = T_1^0 - C_1 - \frac{P}{B}. \quad (\text{D.39})$$

Appendix E

SATURATIONS

The mobile oil/water saturations (Arthur *et al.*, 1991) at any time $n+1$ in the hot and warm zones are given by

$$S_{omh,w}^{n+1} = S_{omh,w}^n \exp^{-x_1(t^{n+1}-t^n)} + \frac{x_2}{x_1} \left(1 - \exp^{-x_1(t^{n+1}-t^n)} \right), \quad (E.1)$$

$$S_{wmh,w}^{n+1} = S_{wmh,w}^n \exp^{-x_1(t^{n+1}-t^n)} + \frac{x_3}{x_1} \left(1 - \exp^{-x_1(t^{n+1}-t^n)} \right), \quad (E.2)$$

where for hot zone,

$$x_1 = \frac{-q_{o1} - q_{w1} + q_{o2} + q_{w2}}{V_{hot}}, \quad (E.3)$$

$$x_2 = \frac{-q_{o1}\rho_{o1} + q_{o2}\rho_{o2}}{\rho_{o1}V_{hot}}, \quad (E.4)$$

$$x_3 = \frac{-q_{w1}\rho_{w1} + q_{w2}\rho_{w2}}{\rho_{w1}V_{hot}}. \quad (E.5)$$

For the warm zone, these variables are

$$x_1 = \frac{q_{o1} + q_{w1} - q_{o2} - q_{w2}}{V_{warm}}, \quad (E.6)$$

$$x_2 = \frac{-q_{o2}}{V_{warm}}, \quad (E.7)$$

$$x_3 = \frac{-q_{w2}}{V_{warm}}. \quad (E.8)$$

Saturations are computed from the following equations

$$S_{wh,w} = S_{wmh,w} + S_{wc}, \quad (E.9)$$

$$S_{oh,w} = 1 - S_{wmh,w}. \quad (E.10)$$

Appendix F

FLUID PROPERTIES**F.1 Steam Properties**

Steam properties are one of the more essential parts of any thermal calculation in reservoir engineering. Interpolating data from the steam table needs the entire steam table to be included as an input file. Interpolation polynomials have been widely used to avoid this. Tortike and Farouq Ali (1989) presented a set of polynomials which were continuous and covered almost the full saturation envelope. This set of polynomials was used for the present work.

F.1.1 Steam Condensate*Viscosity*

$$\mu_{sc} = -0.0123274 + \frac{27.1038}{T} - \frac{23525.5}{T^2} + \frac{1.01425 \times 10^7}{T^3} - \frac{2.17342 \times 10^9}{T^4} + \frac{1.86935 \times 10^{11}}{T^5}$$

$$273.15 \leq T \leq 645 \text{ K} \quad (\text{F.1})$$

Density

$$\rho_{sc} = 3786.31 - 37.2177T + 0.196246T^2 - 5.04708 \times 10^{-4}T^3 + 6.29368 \times 10^{-7}T^4 - 3.0848 \times 10^{-10}T^5$$

$$273.15 \leq T \leq 640 \text{ K} \quad (\text{F.2})$$

F.1.2 Steam Vapour*Viscosity*

$$\mu_{sv} = -5.46807 \times 10^{-4} + 6.89490 \times 10^{-6}T - 3.39999 \times 10^{-8}T^2 + 8.29842 \times 10^{-11}T^3 - 9.97060 \times 10^{-14}T^4 + 4.71914 \times 10^{-17}T^5$$

$$273.15 \leq T \leq 645 \text{ K} \quad (\text{F.3})$$

Density

$$\ln \rho_{st} = -93.7072 + 0.833941T - 0.003208T^2 + 6.57652 \times 10^{-6}T^3 - 6.92747 \times 10^{-9}T^4 + 2.97203 \times 10^{-12}T^5$$

$$273.15 \leq T \leq 645 \text{ K} \quad (\text{F.4})$$

F.1.3 Latent Heat of Vaporization

$$L_v = \left(7184500 + 11048.6T - 88.4050T^2 + 0.162561T^3 - 1.21377 \times 10^{-4}T^4 \right)^{\frac{1}{2}}$$

$$273.15 \leq T \leq 645 \text{ K} \quad (\text{F.5})$$

F.1.4 Saturation Temperature

$$T_s = 280.034 + 14.0856 \ln p + 1.38075(\ln p)^2 - 0.101806(\ln p)^3 + 0.019017(\ln p)^4$$

$$.611 \text{ kPa} \leq p \leq 22.12 \text{ MPa} \quad (\text{F.6})$$

F.1.5 Saturation Pressure

$$p_s = \left(-175.776 + 2.292727T - .011395T^2 + 2.6278 \times 10^{-5}T^3 - 2.73726 \times 10^{-8}T^4 + 1.13816 \times 10^{-11}T^5 \right)^2$$

$$80 \leq T \leq 647.3 \text{ K} \quad (\text{F.7})$$

All the units in the above equations are in derived SI metric. Viscosity in Pa.S., pressure in kPa, density in kg/m³, latent heat of vaporization in kJ/kg and temperature in K.

F.2 Oil Properties

Viscosity

Svrcek and Mehrotra (1988) used an ASTM viscosity-temperature chart D341 for seven different high viscosity petroleum samples to come up with a one parameter correlation. Although this is an adequate way to estimate viscosity of different bitumen,

their temperature range was limited to a maximum value of 130°C or y. A good approximate method was suggested by Farouq Ali (1982), in terms of dynamic viscosity, in SI unit

$$\mu_o = ae^{b/(T+273.15)} \quad (F.8)$$

If two points are known a and b can be easily found out. For the present study, two sets of a and b were found from the given values,

$$\begin{aligned} a &= 6.54053 \text{ E-15,} & \text{for } T \leq 373.15 \text{ K} \\ b &= 11380.31 \end{aligned} \quad (F.9)$$

and

$$\begin{aligned} a &= 1.77632 \text{ E-7,} & \text{for } T > 373.15 \text{ K} \\ b &= 4993.018 \end{aligned} \quad (F.10)$$

Density

A simple correlation was used to calculate the oil density using a thermal expansion factor,

$$\rho_o = \rho_{oR} \{1 - \beta_o (T - T_{oR})\} \quad (F.11)$$

The subscript R represents a reference point (standard condition).

Specific Heat

Smith-Magowan *et al.* (1982) developed a correlation for the specific heat of bitumen from several samples of low, medium and high grade Athabasca oil sands. These were tested over a temperature range of 50 to 300°C, along with specific heats of components. Their equation gave an acceptable estimate of oil sands specific heat in J/°C g,

$$c_p = 1.557 + 5.219 \times 10^{-3} T - 8.686 \times 10^{-6} T^2 \quad (F.12)$$

©1995 Mohammad Tamim.
All rights reserved.

A good word is as a good tree-
its roots are firm,
and its branches are in heaven;
it gives its produce every season
by the leave of its Lord.

—**Qur'an.** *Ibrahim 14:24-25*